UNIVERSITY OF CALIFORNIA
RIVERSIDE

Genetically Engineered Protein Modules: Development and Applications in Anti-Viral Agent Screening and Cancer Marker Detection

A Dissertation submitted in partial satisfaction
of the requirements for the degree of

Doctor of Philosophy

in

Cell, Molecular, and Developmental Biology

by

Payal Biswas

August 2010

Dissertation Committee:
Dr. Wilfred Chen, Chairperson
Dr. Ashok Mulchandani
Dr. Marylynn V. Yates

The Dissertation of Payal Biswas is approved:

_____

_____

_____

Committee CHAIRPERSON

University of California, Riverside

Acknowledgement

I owe my gratitude to all those people who have made this dissertation possible and because of whom my graduate experience has been one that I will cherish forever.

My deepest gratitude is to my advisor, Dr. Wilfred Chen. I have been very fortunate to have an advisor who gave me the freedom to explore on my own and at the same time the guidance to recover when my steps faltered. Dr. Chen taught me how to critically analyze the datas and pinpoint the problems. His passion for science and enthusiasm was highly motivating. I am deeply grateful to him for the long discussions that helped me sort out the technical details of my work. His patience and support helped me overcome many situations and finish this dissertation. I would like to thank him for everything.

I would like to acknowledge my dissertation committee members Dr. Ashok Mulchandani and Dr. Marylynn V. Yates. Dr. Mulchandani's insightful comments and constructive criticisms at different stages of my research were thought-provoking and they helped me focus my ideas. I am grateful to him for holding me to a high research standard and enforcing strict validations for each research result. Dr. Yates has been always there to listen and give advice. Her pleasing personality was a sigh of relief in the wearisome days of graduate life. I am also thankful to her for encouraging the use of correct grammar and consistent notation in my writings and for carefully reading and commenting on the manuscripts.

During my stay at UCR I made numerous friends, who have helped me stay sane through these difficult years and have made my journey joyful. Their support and care

helped me overcome setbacks and stay focused on my graduate study. I greatly value the friendship of Subhas, Arinder and Piyush and I deeply appreciate their belief in me. I was fortunate to have amazing roommates like Karthi and Bhawna. I would cherish the friendship of Sandeep, Yusuf, Melissa and Maneet. I was lucky to have great labmates like Divya, Miso, Lakshmi, Garima and Shen long.

Most importantly, none of this would have been possible without the love and support of my family. My dad, grandmom, aunt-Dipa, and sister- Nilanjana has been a constant source of love, concern, support and strength all these years. I would like to express my heart-felt gratitude to my family. A special thanks goes to my then boyfriend and now husband Shailendra, without whose support this would not have been possible. His never ending enthusiasm and encouragement were undeniably the bedrock upon which the past six years of my life have been built. My extended family has aided and encouraged me throughout this endeavor. I warmly appreciate the generosity and understanding of my extended family.

Dedication

This dissertation is dedicated to my grandmother Late Mrs Kanchan Prava Biswas who shared with me the risks and sacrifices required to complete it. Her love, concern, encouragement, support and blessings have helped me throughout this endeavor.

ABSTRACT OF THE DISSERTATION

Genetically Engineered Protein Modules: Development and Applications in Anti-Viral Agent Screening and Cancer Marker Detection

by

Payal Biswas

Doctor of Philosophy
Cell Molecular and Developmental Biology Graduate Program
University of California, Riverside, August 2010
Dr. Wilfred Chen, Chairperson

One of the most critical aspects in drug discovery is the bioactivity screening assay, by which compounds that most effectively inhibit the target are identified. During the past decade, the antiviral marketplace had experienced tremendous growth and is expected to grow further as new viral targets are identified. The persistent problem of viral resistance requires developing new-generation drugs to replace the existing ones. The pharmaceutical industry faces huge cost due to the failure of promising drug candidates to pass the test of potency and safety in humans. The quest for successful antiviral drugs is further hampered by the fact that successful drugs must often enter an infected cell and neutralize the replicating virus without causing harm to the host cell. To meet these challenges, the screening assays should be representative of the *in vivo* setting so that the results can be interpreted, with sufficient confidence, from the viewpoint of clinical efficacy. To this end, cell-based high-throughput screening (HTS) assays are preferred since they can provide additional information on the adverse effects of the drug and transport efficiency to the target cells.

The overall objective of this thesis is to develop a genetically programmable module that is easily adaptable for screening inhibitors for a wide range of proteases. Proteases are proteolytic enzymes that catalyze the cleavage of peptide bonds. They play important role in many essential intracellular and extracellular processes such as viral infection, blood coagulation, caner development, fibrinolysis, hormone maturation, and apoptosis. These properties make proteases a prime target for detailed investigation in order for better understanding the disease development process and to identify targets for drug treatment.

The approach was to generate a quantum dot (QD)-modified, protease-specific protein module that can be used as a Fluorescence Resonance Energy Transfer (FRET) based nanoprobe for probing protease activity. The site-specific incorporation of an acceptor fluorescent dye was accomplished using the thiol group of cysteine. While conjugation to QDs was facilitated by the presence of a hexa-histidine tag, due to its affinity for the Zn shell of QDs. Presence of an elastin domain within the module enabled the simple purification of the QD-modified FRET substrate. The modular nature of the design allowed easy alteration of the recognition sequence without significantly modifying other domains. Moreover, the FRET efficiency within the nanoassemblies was easily controlled by changing the QD- peptide dye ratios. The flexibility of the approach was demonstrated by generating nanoprobes for rapid and sensitive detection of the cancer-specific matrix metalloprotease (MMP-7) and the West Nile virus protease (NS3). Intracellular delivery of the substrates was facilitated by the use of a flanking TAT peptide. The effectiveness of the FRET substrate was investigated by monitoring the

whole-cell fluorescence ratio between the QD and the acceptor fluorescence dye when introduced into a HeLa cell line. The utility of the assay system was validated for the HTS of HIV protease inhibitors.

This modular QD based FRET assay provides a future platform useful for general HTS of a wide range of protease activities relating to viral infection, blood coagulation, fibrinolysis, hormone maturation, and apoptosis. The ease of using this genetic approach also significantly reduced the cost associated with peptide synthesis. This could ultimately result in a low-cost screening drug platform for a wide range of protease targets important for human health.

The integration of the development of tunable biomolecules with FRET-based HTS screening represents a unique effort that expands the fundamental development of protein engineering with the implementation of drug discovery. Through this research an integrated perspective of the important interfaces and synergies connecting biochemistry, modern genetics, and HTS was gained.

Table of Contents

List of Figures

Chapter 1

Introduction

Introduction

Development of robust, sensitive and convenient bio-assay systems is a strong current scientific priority. As such, recognition based bioassays capable of specifically detecting chemicals, toxins and bio-agents in their native environment are under active development in many laboratories. The development of sound bioanalytical methods is of paramount importance during the process of drug discovery and development culminating in a marketing approval. Recent advance in combinatorial chemistry have opened up new avenues in the synthesis of large libraries of molecules as potential therapeutic agents (Geysen et al., 2003). This has revolutionized the field of drug discovery and necessitated the development of rapid and reliable assays for enzyme inhibition. One of the most critical aspects in drug discovery is the bioactivity screening assay, by which compounds that most effectively inhibit the enzyme target are identified. The screening assay should be representative of the *in vivo* setting so that the results can be interpreted, with sufficient confidence, from the viewpoint of clinical efficacy. To this end, high-throughput screening (HTS) methods to assay the activity of a formidable number of proteases have become indispensable to search through this vast library of targets.

Importance of proteases as pharmaceutics targets

Proteases are proteolytic enzymes that catalyze the cleavage of peptide bonds. There are an estimated 561 proteases in the human genome (Puente et al., 2003). Proteases perform essential functions in all living organisms. They play important role in

many essential intracellular and extracellular processes such as blood coagulation, fibrinolysis, hormone maturation, and apoptosis (Neurath, 1999; Vihinen et al., 2005). In addition, proteolytic processing events are fundamental in ovulation, fertilization, embryonic development, bone formation, control of homeostatic tissue remodelling, neuronal outgrowth, antigen presentation, cell-cycle regulation, immune and inflammatory cell migration and activation, wound healing, angiogenesis and apoptosis (Barrett et al., 1998; Hooper N.M. 2002). Accordingly, alterations in the structure and expression patterns of proteases underlie many human pathological processes including cancer, arthritis, osteoporosis, neurodegenerative disorders and cardiovascular diseases (Egeblad, M. & Werb, Z. 2002; Krane, S. M. 2003; Esler, W. P. & Wolfe, M. S. 2001; Luttun et al., 2000). Besides, many infectious microorganisms such as bacteria, viruses, and parasites use proteases as the key virulence factors for infection (Shao et al., 2002; Anand et al., 2003). These properties make proteases a prime target for detailed investigation to better understand the disease development process and to identify targets for drug treatment. Cysteine peptidases of the papain family, for example, have been used as putative drug targets for the treatment of musculoskeletal diseases and parasite infection (Steverding et al., 2006). Caspases are another class of drug targets involved in programmed cell death and inflammation (Wolf and Green, 1999). Other important proteases that have been examined as pharmaceutical drug targets include different viral proteases, botulinium neurotoxin, human renin for blood pressure, and plasmepsin for Malaria (Mittl and Grutter, 2006).

Role of proteases in virus life-cycles

Rapid detection of viral infections and understanding viral pathogenesis are crucial for the prevention of infectious disease outbreaks, development of anti-viral drugs and biodefense. During antiviral drug development, any essential stage of the viral life cycle can serve as a potential drug target. Viral proteases are essential in the life cycle of many viruses, including picornviruses such as poliovirus (PV), retroviruses such as human immunodeficiency virus (HIV), and caliciviruses such norovirus (Byrd and Hruby, 2006). Proteases cleave viral protein precursors to form functional units or to release structural components. Viral protease has therefore been proposed as a main target for antiviral agents (Patick and Potts, 1998). Saquinavir, ritonavir, indinavir, and nelfinavir are FDA-approved antiviral agents against HIV that act by inhibiting the viral protease activity (Andre et al., 1998). Similarly, research on the treatment of severe acute respiratory syndrome (SARS) coronavirus has targeted protease inhibitors as the main focus since the epidemic of SARS occurred in southeastern Asia (Kuo et al., 2004; Toney *et al.*, 2004). It has also been proposed to screen effective inhibitors against poliovirus 3C protease (Hata *et al.*, 2000). Compound AG7088, a potent inhibitor of human rhinovirus (HRV) 3C protease, has proceeded into clinical trails (Patick et al., 1999). With vast progresses in development of viral protease inhibitors, methods providing quick and accurate screening processes at low cost are greatly desirable.

Bio-assays for high-throughput anti-protease drug screening

Over the past decade, the HTS strategy has been bolstered by technological advances on several fronts: automation of liquid handling and dispensing for multi-well plates, creation of novel platforms such as microarrays, and development of better analytical tools to handle massive quantities of data (Fox et al., 2004). These advances in HTS have resulted in a paradigm shift in all stages of drug discovery, from target identification to toxicity assessment (Kumar and Clark, 2006). Although a wide range of *in vitro* HTS activity methods have been developed for proteases, they require the use of cell extracts or purified proteases and do not provide any information on cytotoxicity of the potential drug targets (Steinkuhler et al., 1996; Chen et al., 2003; Gosallia et al., 2005; Sudo et al., 1996). In recent years, several cell-based platforms have been proposed for the HTS of protease inhibitors (Zhang, 2004; Lee et al., 2005).

One of the most promising reporters for probing protease activity is based on the use of protease-targeted fluorogenic substrates in which fluorescence of the reporter molecule increases or changes following cleavage within the peptide scaffold of the probe (Mitra et al., 1996; Pennington and Thornberry, 1994). In most cases, the principle of fluorescence resonance energy (FRET) containing two organic fluorophores located less than 100Å apart were used for the probe design. Cleavage of the linker peptide separates the two fluorophores, resulting in an increase in the emission intensity of the donor and a reduction of the acceptor emission (Figure 1.1). This change in fluorescence intensity can be correlated with the target protease activity. This approach, unfortunately, is suitable only for detecting extracellular proteases in the absence of a cell-permeable

partner. Moreover, *in vitro* studies pose a major drawback because they are not able to address questions regarding the adverse effects due to addition of the drug and the transport efficiency of the drug to the target cells. Efforts to alleviate this problem have been made by using genetically engineered green fluorescence protein (GFP) pairs as the FRET donors and acceptors (Zhang, 2004). GFP variants have been generated that harbor improved fluorescence properties and possess two different absorbance and emission spectra suitable for FRET applications (Nguyen and Daugherty, 2005). The most commonly used FRET reagents are based on the cyan fluorescent protein (CFP) and yellow fluorescent protein (YFP) pair (Heim and Tsien, 1996). The most distinct advantage of GFP FRET pairs is the ability to produce these substrates intracellularly in the desired location via genetic engineering. Recently the use of this approach has been demonstrated for intracellular monitoring of poliovirus 2A protease activity (Hwang et al., 2006). Cleavage of the FRET substrate by cells infected with polio viruses changes the emission to CFP rather than YFP. However, the use of stable, genetically engineered cell lines expressing different protease FRET substrates of interest is a formidable task, requiring the cloning of different vectors and the establishment of many different cell lines. One feasible alternative is to develop a simple platform to introduce FRET-probes inside living cells in a benign and robust manner with minimal cytotoxic effects.

Delivery of peptide-conjugates

Different strategies have been employed in the past for cargo delivery to living cells including microinjection (Sokol et al., 1998), liposomal delivery (Matsuo, 1998), and electroporation (Chen and Gerion, 2004). Microinjection and electroporation are very invasive and may cause severe cell damage; liposome delivery often results in significant aggregation of signal in the endosomes. Recent research has identified several protein transduction domains (PTDs) and cell penetrating peptides (CPPs), such as the TAT peptide derived from HIV, that confer the ability of a conjugated cargo to enter living cells without permeabilization (Zorko and Langel, 2005). Peptide-mediated delivery has quickly become one of the more attractive methods due to the ease of use and the ability to target a range of cell types. A large number of cargoes such as DNA (Eguchi et al., 2001), antibodies (Stein et al., 1999), PNA (Kaushik et al., 2002), and proteins (Pooga et al., 2001), have been successfully delivered inside living cells with minimal acute toxicity. Even nanoparticles such as quantum dots have been selectively delivered into the endosomes while maintaining the fluorescence property (Delehanty et al., 2006). This novel delivery method, when combined with protease-specific FRET pairs, could provide a powerful means for rapid, real-time detection of protease activity in living cells with high specificity and sensitivity.

Quantum dot-peptide conjugates as protease FRET pairs

One major limitation of conventional FRET substrates is the use of organic fluorophores as the label. These organic fluorophores have characteristics that limit their effectiveness, including narrow excitation bands and broad emission bands, which can

make simultaneous evaluation of several light-emitting probes problematic due to spectral overlap (Goldman et al., 2002). Also, many organic dyes exhibit low resistance to photodegradation, rendering them ineffective for long-term monitoring (Hermanson, 1996).

Luminescent colloidal semiconductor nanocrystals (quantum dots, QDs) are inorganic fluorophores that have the potential to circumvent some of the functional limitations encountered by organic dyes. In particular, CdSe-ZnS core-shell QDs exhibit size-dependent tunable photoluminescence (PL) with narrow emission bandwidths that span the visible spectrum and broad absorption spectra that allow simultaneous excitation of several particle sizes at a single wavelength (Chan and Nie, 1998). These nanoparticles also exhibit a high quantum yield (20 times more than organic fluorophores) and a high resistance to photodegradation (100 times better than organic fluorophores) (Goldman et al., 2002). Even individual QDs are easily observable by confocal microscopy. Recently, FRET-based bioassays have been successfully demonstrated using QDs as the energy donor (Medintz et al., 2006). QD emission can be size tuned to optimize the spectral overlap with a particular acceptor and a broad range of wavelength can be used for excitation. Successful replacement of organic fluorophores with CdSe-ZnS QDs as the fluorescence donor and Cy3 as the acceptor has recently been demonstrated, resulting in increased fluorescent stability suitable for long-term analysis (Medintz et al., 2006). A multifunctional modular peptide (Figure 1.2) was rationally designed to have several functional domains in a linear N to- C-terminal configuration including: (i) an N-terminal hexahistidine (His6) to facilitate self assembly onto ZnS shell of the QDs, (ii) a helix-

linker spacer region to provide rigidity, (iii) an exposed protease recognition/cleavage sequence, and (iv) a C-terminal site-specific location (cysteine thiol) for fluorescent dye attachment. Cleavage of the linker peptide by the protease thrombin resulted in an increase in QD emission and quantitative data including enzyme kinetic parameter could be obtained and analyzed. However, the use of synthetic peptides as FRET substrates is expensive and lacks precise controllability of the FRET distance. Potentially, a simple method that will enable easy production, purification and conjugation of the fluorescent dye and QD can be employed to provide a low-cost and tunable approach for protease inhibitor discovery. A simple approach has been recently reported for bioconjugation and purification of QDs with IgGs using a tripartite elastin (ELP) fusion protein (Lao et al., 2006). The tripartite fusion protein (His-ELP-PL) (Figure 1.3A) consisted of 1) a N-terminus histidine tag (His) used for QD conjugation via strong metal-affinity coordination with Zn^{2+} on the core-shell, 2) an elastin (ELP) mid-block comprised of 78 VPGVG repeating units for thermally-responsive purification, and 3) a C terminus Protein L (PL) that has high affinity towards immunoglobulin (Ig) κ-light chain of a wider range of species. For efficient purification, the unique phase transition behavior of elastin-like protein (ELP) was adopted. ELP is temperature-responsive protein consisting of repeating unit VPGXG. In higher temperature than transition temperature (T_t), phase transition of ELP occurs from soluble forms into aggregates and the precipitates can be resolubilized by lowering the temperature below T_t (Urry 1997). Due to its ability to undergo a reversible phase transition, ELP offers a convenient and efficient purification

method. Simple separation of the QD- His-ELP-PL-IgG complex was achieved by thermally-triggered precipitation without any interference of the QD functionality.

Development of novel QD-based FRET assay system

It is easy to envision that a direct extension of the approach is to create a genetically engineered protein module that is designed with 1) a QD binding moiety containing poly-histidine, 2) a C-terminal site-specific location (cysteine thiol) for fluorescent dye attachment, 3) a protease cleavage site, 5) a flanking TAT peptide sequence for cell penetration and 6) an ELP domain for thermal purification (Figure 1.3B). The most important feature of the approach is that the modular design is intended to obviate the need for major redesign when targeting a new protease. Peptide specificity can be varied by altering only the recognition sequence without significantly modifying other modules. In addition, different cell-penetration peptides can be employed for optimal delivery efficiency and dye-QD spacing can be easily modulated by changing the encoding DNA sequences.

The overall objective of this thesis is to develop a genetically programmable module that is easily adaptable for detecting a wide range of proteases and further to screen their inhibitors in a high throughput format. The approach is to generate a QD-modified, protease-specific protein module that can be used as a FRET substrate for probing protease activity. Intracellular delivery of the substrates will be facilitated by the use of a flanking TAT peptide and the site-specific incorporation of an acceptor

fluorescent dye will be accomplished using a cysteine site by thiol modification of the cysteine residue. Presence of an elastin domain within the module would enable the simple purification of the QD-modified FRET substrate. The effectiveness of the FRET substrate will be investigated by monitoring the whole-cell fluorescence ratio between the QD and the acceptor fluorescence dye when introduced into a mammalian cell line expressing a protease under study. The overall goal was realized by research directed towards the following:

1. Generated genetically engineered protein modules that can be used as TAT-modified QD FRET substrates.

2. Investigated the FRET efficiency in response to proteases by varying the dye/QD ratio.

3. Generated nanoprobes using the engineered protein module for detecting wide range of proteases

4. Investigated the QD FRET assay system for detecting protease activity in-vivo.

5. Investigated utility of the FRET substrates for inhibitor screening using known protease inhibitors.

6. Determined the utility of the system for probing different cleavage sites simultaneously.

References

Anand, K., Ziebuhr, J., Wadhwani, P., Mesters, J.R., Hilgenfeld, R. 2003. Coronavirus main proteinase (3CL(pro)) structure: Basis for design of anti-SARS drugs. Science. **300**; 1763-1767.

Andre, P., M. Groettrup, P. Klenerman, R. DeGiuli, B. Booth, V. Cerundolo, M. Bonneville, F. Jotereau, R. Zinkernagel, and V. Lotteau. 1998. An inhibitor of human immunodeficiency virus-1protease modulates proteasome activity, antigen presentation, and T-cell response. Proc. Natl.Acad. Sci. USA. **95**:13120-13124.

Barrett, A. J., Rawlings, N. D. & Woessner, J. F. Handbook of Proteolytic Enzymes Academic Press: San Diego, 1998.

Byrd, C.M., Hruby, D.E. 2006. Viral Proteinases: Targets of opportunity. Drug. Develop. Res. **67**: 501-510.

Chan, W. and Shuming, J. 1998. Quantum dot bioconjugates for ultrasensitive nonisotopic detection, Science **281**: 2016–2018.

Chen, F.Q., Gerion, D. 2004. Fluorescent CdSe/ZnS nanocrystal-peptide conjugates for longterm,nontoxic imaging and nuclear targeting in living cells, Nano Lett., **4**:1827-1832.

Chen, G.Y.J., Uttamchandani, M., Zhu, Q., Wang, G., Yao, S.Q. 2003. Developing a strategy for activity-based detection of enzymes in a protein microarray. ChemBioChem. **4**:336-339.

Delehanty, J.B., Medintz, I., Pons, T., Brunel, F.M., Dawson, P.E., Mattoussi, H. 2006. Self assembled quantum-dot-peptide bioconjugates for selective intracellular delivery, Bioconjug. Chem., **17**:920-927.

Egeblad, M. & Werb, Z. 2002.New functions for the matrix metalloproteinases in cancer progression. Nature Rev.Cancer **2**:161–174

Eguchi, A., T. Akuta, H. Okuyama, T. Senda, H. Yokoi, H. Inokuchi, S. Fujita, T. Hayakawa, K.Takeda, M. Hasegawa, M. Nakanishi. 2001. Protein transduction domain of HIV-1 Tat proteinpromotes efficient delivery of DNA into mammalian cells, J. Biol. Chem., **276**: 26204–26210.

Esler, W. P. & Wolfe, M. S. 2001. A portrait of Alzheimer secretases— new features and familiar faces. Science **293**:1449–1454

Fox, S., Farr-Jones, S., Sopchak, L., Boggs, A., Comley, J. 2004. High-throughput screening: searching for higher productivity. J. Biomol. Screen. **9**:354-358.

Geysen, H.M., Schoenen, F., Wagner, D., Wagner, R. 2003. Combinatorial compound libraries for drug discovery; an ongoing challenge. Nat. Rev. Drug Discov.2:222-230.

Goldman, E.R., Anderson, G.P., Tran, P.T., Mattoussi, H., Charles, P.T., and Mauro, J.M. 2002. Conjugation of luminescent quantum dots with antibodies using an engineered adaptor protein to provide new reagents for fluoroimmunoassays. Anal. Chem. 74:841-847.

Gosalia, D.N., Salisbury, C.M., Maly, D.J., Ellman, J.A., Diamond, S.L. 2005. Profiling serine protease substrate specificity with solution phase fluorogenic peptide microarrays. Proteomics.**5**:1292-1298.

Hata, S., T. Sato, H. Sorimachi, S. Ishiura, and K. Suzuki. 2000. A simple purification and fluorescent assay method of the poliovirus 3C protease searching for specific inhibitors. J. Virol. Methods. **84**:117-126.

Heim, R., Tsien, R.Y. 1996. Engineering green fluorescent protein for improved brightness, longer wavelengths and fluorescence resonance energy transfer. Curr. Biol. **6**: 178-182.

Hermanson, G. T. *Bioconjugate Techniques*; Academic Press: London, 1996; Chapter 8.

Hooper, N. M. Proteases in Biology and Medicine; Portland Press: London, 2002

Hwang, T.-C., Chen, W., Yates, M.V. 2006. Using Fluorescence Resonance Energy Transfer for Rapid Detection of Enteroviral Infection *In Vivo*. Appl. Environ. Microbiol., **72**, 3710-3715.

Kaushik, N., A. Basu, P. Palumbo, R.L. Myers, V.N. Pandey. 2002. Anti-TAR polyamide nucleotide analog conjugated with a membrane-permeating peptide inhibits human immunodeficiency virus type 1 production. J. Virol. **76**: 3881–3891.

Krane, S. M. 2003. Elucidation of the potential roles of matrix metalloproteinases in skeletal biology. Arthritis Res. Ther. **5**:2–4

Kumar, R.A., Clark, D.S. 2006. High-throughput screening of biocatalytic activity; applications in drug discovery. Curr. Opin. Chem. Biol. **10**:162-168.

Kuo, C., Y. Chi, J. Hsu, and P. Liang. 2004. Characterization of SARA main protease and inhibitor assay using a fluorogenic substrate. Biochem. and Biophy. Res. Com. **318**:862-867.

Lao, UL, Mulchandani, A., and Chen, W. 2006. Simple Conjugation and Purification of Quantum Dot-Antibody Complexes Using A Thermally Responsive Elastin-Protein L Scaffold As Immunofluorescent Agents, J. Am. Chem. Soc., **128**:14756-14757.

Lee, J-C., Yu, M-C, Lien, T-W, Chang, C-F., Hsu, J. T-A. 2005. High-throughput cell-based screening for hepatitis C virus NS3/4A protease inhibitors. Assay and Drug Development Technologies, **3**:385-392.

Luttun, A., Dewerchin, M., Collen, D. & Carmeliet, P. 2000. The role of proteinases in angiogenesis, heart development,restenosis, atherosclerosis, myocardial ischemia, and stroke:insights from genetic studies. Curr. Atheroscler. Rep. **2**:407–416

Matsuo, T. 1998. In situ visualization of messenger RNA for basic fibroblast growth factor in living cells. *Biochimica et Biophysica Acta* **1379**:178-184.

Mitra, R.D., Silva, C.M., Touvan, D.C. 1996. Fluorescence resonance energy transfer between blue-emitting and red-shifted excitation derivatives of the green fluorescent protein. Gene. **173**:13-17.

Mittl, P.R.E., Grutter, M.G. 2006 Opportunities for structure-based design of protease-directed Drugs. Curr. Opin. Struct. Biol. **16**:769-775.

Neurath, H. 1999. Proteolytic enzymes, past and future. Proc Natl Acad Sci USA.**96**:10962-10963.

Nguyen, A.L. and Daugherty, P.A. 2005. Evolution optimization of fluorescent proteins for intracellular FRET. Nat. Biotechnol. **23**:355-360.

Patick, A., and K. Potts. 1998. Protease inhibitors as antiviral agents. Clin. Microbiol. Rev. **11**:614-627.

Patick, A., S. Binford, M. Brothers, R. Jackson, C. Ford, M. Diem, F. Maldonado, P. Dragovich, R. Zhou, T. Prins, S. Fuhrman, J. Meador, L. Zalman, D. Matthews, and S. Worland. 1999. In vitro antiviral activity of AG7088, a potent inhibitor of human rhinovirus 3C protease. Antimicrob. Agents Chemother. **43**:2444-2450.

Pennington, M.W., Thornberry, N.A. 1994. Synthesis of a fluorogenic interleukin-1-beta converting enzyme substrate based on resonance energy transfer. Pept. Res. **7**:72-76.

Pooga, U., C. Kut, M. Kihlmark, M. H7llbrink, S. Fernaeus, R. Raid, T. Land, E. Hallberg, T. Bartfai, U, Langel. 2001. Cellular translocation of proteins by transportan. FASEB J. **15**: U304–U316.

Puente, X. S., Sanchez, L. M., Overall, C. M. & Lopez-Otin, C. 2003. Human and mouse proteases: A comparative genomic approach. *Nature Rev. Genet.* **4:**544–558

Shao, F., Merritt, P.M., Bao, Z.Q., Innes, R.W., Dixon, J.E. 2002. A Tersinia effector and a pseudomonas a virulence protein define a family of cysteine proteases functioning in bacterial pathogenesis. Cell.**109**:575-588.

Sokol, D.L., Zhang, X., Lu, P. and Gewirtz, A.M. 1998. Real time detection of DNA-RNA hyvridization in living cells. *Proc. Natl. Acad. Sci. USA* **95:**11538-11543.

Stein, S., A. Weiss, K. Adermann, P. Lazarovici, J. Hocman, H. Wellhoner. 1999. A disulfide conjugate between anti-tetanus antibodies and HIV (37-72) Tat neutralizes tetanus toxin inside cromaffin cells, FEBS Lett. **458**:383– 386.

Steinkuhler, C., Urbani, A., Tomei, L., Viasiol, G., Sardana, M., Bianchi, E., Pessi, A., De Francesco, R. 1996. Activity of purified hepatitis C virus protease NS3 on peptide substrates. J. Virol. **70**:6694-6700.

Steverding, D., Caffrey C.R.,, Sajid, M. 2006. Cysteine protein inhibitors as therapy for parasitic diseases: advances in inhibitor design, Mini-reviews in medicinal chemistry. **6**:1025-1032.

Toney, J., S. Navas-Martin, S. Weiss, and A. Koeller. 2004. Sabadinine: a potential non-peptide anti-severe acute-respiratory-syndrome agent identified using structure-aided design. J. Med.Chem. **47**:1079-80.

Urry, D.W. 1997. Physical Chemistry of biological free energy transduction as demonstrated by elastic protein-based polymers. Journal of Physical Chemistry B**. 101:**11007-11028

Vihinen, P., Ala-Aho,R, Kahari, V.M .2005. Matrix metalloproteinases as therapeutic targets in Cancer. Curr. Cancer Drug Targets. **5**:203-220.

Wolf, B.B., Grenn, D.R. 1999. Suicidal tendencies: apoptotic cell death by caspase family Proteinases. J.Biol. Chem. **274**:20049-20052.

Zhang, B. 2004. Design of FRET-based GFP probes for detection of protease inhibitors. Biochem. Biophys. Res. Commun. **323**:674-678.

Zorko, M., Langel, U. 2005. Cell-penetrating peptides: mechanism and kinetics of cargo Delivery. Adv. Drug Delivery Rev. **57**:529-545.

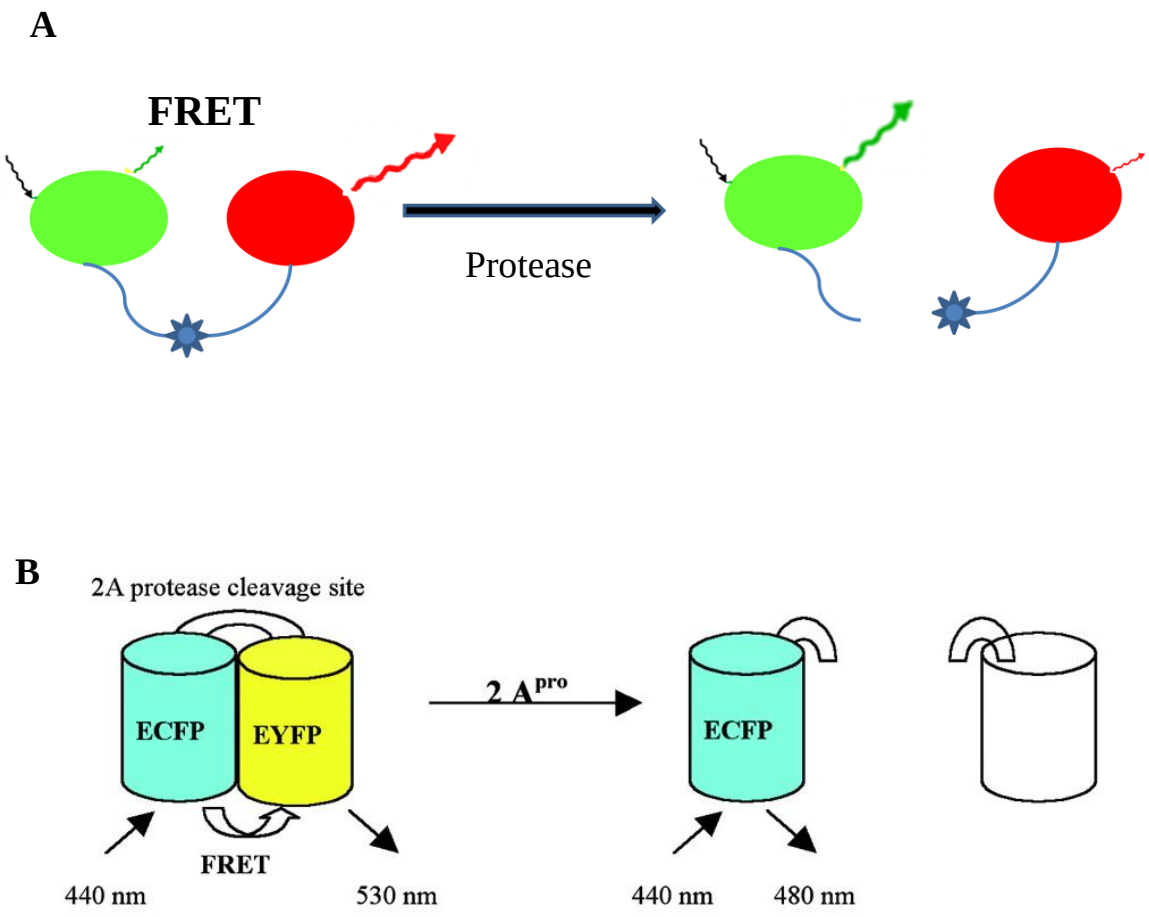

Figure 1.1. (A) Fluorescence resonance energy transfer (FRET)-based probes for protease activity by incorporating donor and acceptor fluorochromes in proximity to each other. Proteolytic cleavage of the linker releases FRET.

(B) Schematic representation of the fluorescent substrate of the 2Apro. In the presence of 2Apro, the linker peptide is cleaved via the protease and resulting in the increased ECFP signal (adapted from Hwang et al., 2006)

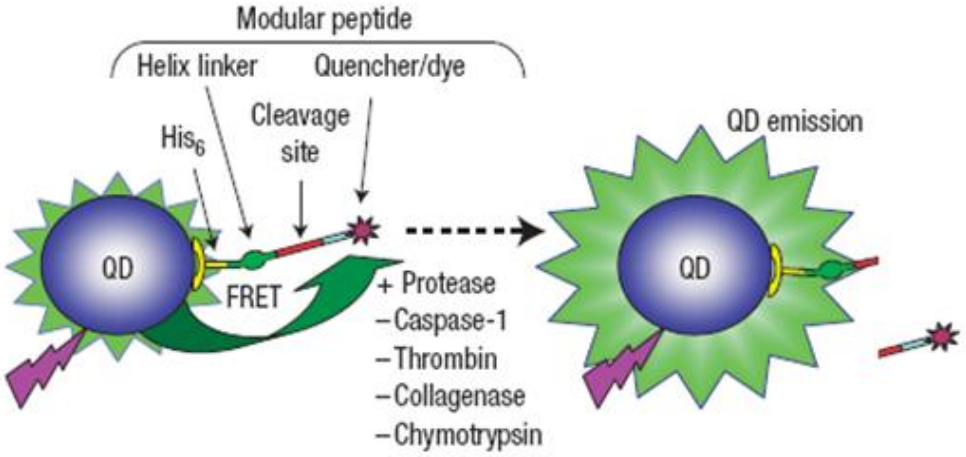

Figure 1.2: Schematic diagram of the self-assembled QD–peptide nanoprobes. Dye-labeled modular peptides containing appropriate cleavage sequences are self-assembled onto the QD. Specific protease cleaves the peptide and alters FRET signature (adapted from Menintz et al, 2006).

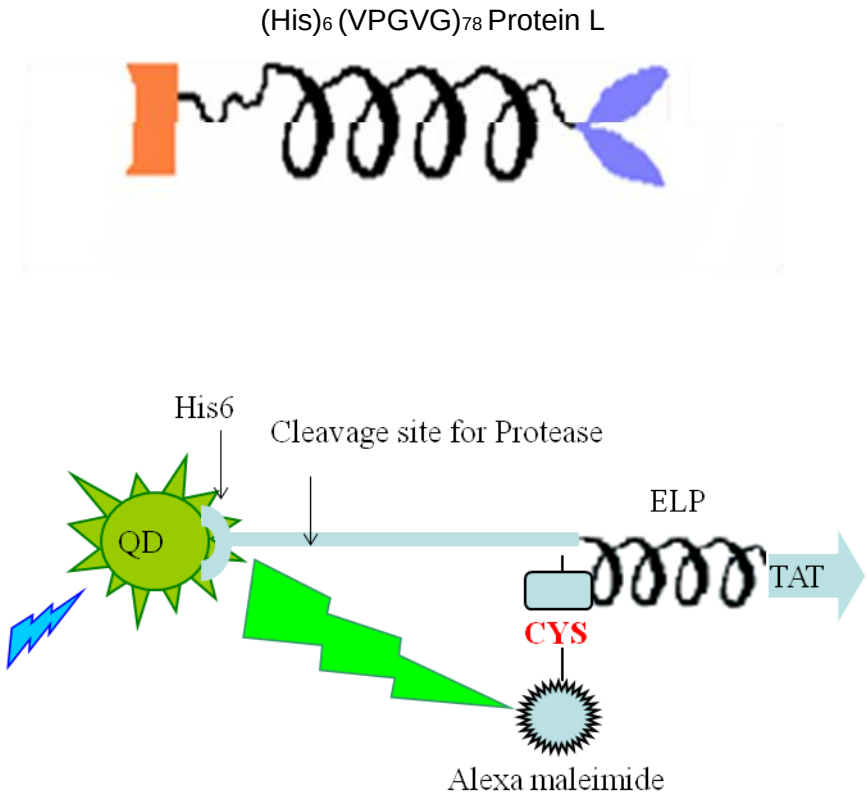

Figure 1.3: (A) Elastin like protein was flanked by an N-terminus hexa-histidine tag and a C-terminus protein L. (B) A genetically engineered protein module for intracellular delivery of QD-based protease FRET substrate

Chapter 2

Development of a QD-based nanoprobe using a novel genetically programmable multifunctional protein module for sensing protease activity

Abstract

The important role of proteases in normal cellular processes, in disease progression and in viral infection calls for the development of sensors for monitoring protease activity and screening their inhibitors in a high throughput manner. Here, we demonstrate the development of a quantum dot (QD) based nanoprobe for probing protease activity. The nanoprobe consists of a genetically engineered protein module that is designed with: 1) a QD binding moiety containing poly-histidine, 2) a cysteine site for fluorescent dye incorporation based on cysteine-thiol interaction, 3) a protease cleavage site, and 4) an ELP domain for thermal purification. In this design, the QD photoluminescence (PL) is quenched by the fluorescent dye due to fluorescence resonance energy transfer (FRET). Presence of active proteases disrupts FRET resulting in an increased QD PL thus enabling a simple activity assay. The modular nature of the genetically programmable protein module can be exploited for a wide range of proteases and significant reduction of cost on peptide synthesis. The flexibility of the approach was demonstrated by generating nanoprobes for rapid and sensitive detection of the cancer-specific matrix metalloproteases (MMPs) and the West Nile virus protease (NS3). The FRET efficiency within the nanoassemblies was easily controlled and the sensors were able to detect protease activity with the sensitivity to a few nanograms per milliliter. The assays provided quantitative information on enzyme kinetics and were utilized for screening protease inhibitors. Our system is anticipated to find applications in the diagnostic and pharmaceutical fields for the diagnosis of protease related diseases and screening of potential drugs with high sensitivity in a high throughput manner.

Introduction

Proteases play an important role in many human disease progression such as cancer and inflammation (Edwards et al., 2008), and in viral infection such as AIDS and Hepatitis (Anand et al., 2003). As a result, many of these proteases have been employed as a main target for drug development and disease diagnostics. With the increasing number of synthetic molecules that can be used as potential therapeutic agents (Geysen et al., 2003), a rapid and sensitive method to assay proteases and their corresponding inhibitors in a high throughput setting is needed. One of the most promising methods for probing protease activity is based on the principle of fluorescence resonance energy transfer (FRET) (Mitra et al., 1996; Pennington and Thornberry, 1994). Typically, two organic fluorophores located less than 100 Å apart are linked by a protease cleavage sequence thereby enabling the transfer of energy from the donor to the acceptor. Activity of the protease can be assessed by an increase in the emission intensity of the donor and a reduction of the acceptor emission due to cleavage of the linker peptide. However, one of the major drawbacks of using organic fluorophores is their low resistance to photodegradation, rendering them ineffective for long-term monitoring (Hermanson et al., 1996).

To circumvent some of the functional limitations encountered by organic dyes, quantum dots (QDs) have been exploited as the energy donor (Bruchez et al., 1998; Michalet et al., 2005; Medintz et al., 2003 and 2005). QDs are luminescent semiconductor nanocrystals that exhibit excellent optical properties including narrow emission, broad excitation, high quantum yield and high resistance to photodegradation.

These unique spectral properties enable the use of QD for simultaneous multiplex labeling and detection using a broad range of excitation wavelength (Xia et al., 2008; Kim et al., 2008). Recently, FRET-based protease bioassays have been successfully demonstrated using QDs as the energy donor (Medintz et al., 2006). A chemically synthesized peptide was designed to contain an N-terminal hexahistidine (His6) for QD conjugation and a C-terminal cysteine for Cy3 attachment. Cleavage of the linker peptide by the protease thrombin resulted in increase in QD emission and quantitative data of proteolysis can be determined. However, the use of synthetic peptides as the FRET substrate is expensive. Moreover, purification of the protein-dye conjugates require tedious washing and elution steps making it difficult to be configured in a high-throughput manner. Ideally, a method that offers easy production, purification and conjugation of the peptide substrate to both fluorescent dyes and QDs is of great significance for high throughput screening of protease inhibitors.

In this paper, we introduce a new generation of genetically programmable protein module that can be used as a QD-modified, protease-specific FRET nanoprobes for probing protease activity. The protein modules are designed with: 1) a QD binding moiety containing a hexa-histidine (his6) tag, 2) a protease cleavage site, 3) a unique cysteine site for fluorescent dye incorporation based on thiol-maleimide interaction, and 4) an ELP domain for thermally triggered purification based on ELP's ability to undergo a reversible phase transition from water-soluble forms into aggregates. Since the protein module can be produced in large quantities by fermentation, this approach offers a significant reduction in the cost of substrate. Moreover, the modular nature of the

different domains simplifies the redesign of the protein module when targeting a new protease. To demonstrate the modular nature of the approach, two QD-based FRET nanoprobes were generated for rapid and sensitive detection of two proteases - the cancer-specific matrix-metalloprotease (MMP-7) and the West Nile virus protease (NS3) - with therapeutic applications.

Materials and Methods

Materials

TOPO capped QDs (QD 545) were purchased from Evident Tech. Inc. Dihydro-Lipoic acid was from Sigma. Tris-(2-carboxyethyl) phosphine (TCEP) and Alexa 568 maleimide were from Invitrogen. Matrix metalloproteinase-7 (MMP-7) and its inhibitor were purchased from Calbiochem. West Nile Virus protease (NS3) and its inhibitor undeca- D-Arg- NH_2 were from Anaspec. All other chemicals were purchased from Sigma. Fluorescence emission spectra were collected using a fluorometer (Synergy^{TM} 4, BIOTEK® Instruments)

Design of constructs

To construct an expression vector for His6-MMP-7-Cys-ELP105K-TAT (pET-H-MMP-7-ET), plasmid p08-ELP105K-EC20 described by Lao et al (Lao 2007) was digested with *Sma*I and *Hin*dIII and a DNA fragment encoding TAT peptide (amino acid sequence: GGTKTGRRRQRRKKRGY) was inserted between the same restriction sites. The resulting plasmid p08-ELP105K-TAT was cut with *Bam*HI and *Nde*I and 1.7 kb fragment was ligated to plasmid pET14 (Novagen, Madison, WI) treated with same enzymes to generate pET-ELP105K-TAT. An artificial gene carrying hexa-histidines and the MMP-7 cleavage sequence containing peptide with cysteine was prepared by heating and annealing two oligonucleotides, CATGGGCCATCATCATCATCATCATGTGCCTCTGTCACTGACTATGGGTTGCC A and TATGGCAACCCATAGTCAGTGACAGAGGCACATGATGATGATGATG

ATGGCC and ligated to the 6.3kb fragment obtained from pET-ELP105KTAT by digesting with *Nco*I and *Nde*I to create pET-H-MMP-7-ET. The expression vector for His6-NS2B/NS3-Cys-ELP105KTAT (pET-H- NS2B/NS3-ET) was prepared the same way by using the oligonucleotides CATGGGCCATCATCATCAT CATCATCTTCAATATACAAAGAGAGGGGGCGTGCTTTGGGACTGCCA and TATGGCAGTCCCAAAGCACGCCCCCTCTCTTTGTATATTGAAGATGATGATGA TGATGATGGCC.

Expression and purification of peptides

For protein expression, *E. coli* BL-21 (DE3) (Novagen) transformed with plasmid pET-H-MMP-7-ET and pET-NS2B/NS3-ET was grown in terrific broth media containing 100 μg/ml ampicillin at 37^{o}C until optical density (O.D.) at 600 nm reached 0.5. The flasks were then transferred to 30^{o}C for expression. When the O.D. at 600nm reached 5, cells were harvested by centrifugation, resuspended in 50mM Tris/HCl (pH 8.0) with 0.1M NaCl and 1 mg/ml of lysozyme, and lysed by sonication. Cell debris was removed by centrifugation at 16,000 g for 30 min. Proteins were purified by repeated temperature transition cycles as described previously (Kim et al 2005). Briefly, for each cycle, NaCl was added to the sample at a final concentration of 2M and the sample was heated to 37^{o}C and centrifuged at 16,000 g at 30^{o}C for 15 min. The pellet containing the proteins were resuspended in ice-cold 50mM Tris/HCl (pH 8.0) with 0.1M NaCl and centrifuged at 16,000 g at 4^{o}C for 15 min to remove undissolved proteins. This temperature transition cycle was repeated once more, and the pellet containing either H-

MMP-7-ET or H-NS2B/NS3-ET was finally resuspended in ice cold 50mM Tris/HCl (pH 8.0) with 0.1M NaCl. The purity of the protein was determined by SDS-PAGE electrophoresis.

Conjugation of peptides with fluorescent dye

The labeling of the proteins with thiol reactive dye was performed by modifying the procedure of Massodi *et al*. (Massodi 2005). Purified proteins were resuspended in 50mM potassium phosphate buffer (pH 7) at a final concentration of 40 uM. Tris-(2-carboxyethyl) phosphine (TCEP) and Alexa 568 maleimide, thiol reactive dye, were added to a 10-fold and 2-fold molar excess, respectively. The mixture was incubated with end-over-end rotation for 2hr at room temperature in the dark. The reaction was stopped and the unreacted dyes were removed by two or three thermal precipitation cycles as described in the protein purification procedure. The degree of labeling of the protein was calculated by using the formula:

$$\frac{A_x}{\epsilon} \times \frac{\text{MW of protein}}{\text{mg protein/mL}} = \frac{\text{moles of dye}}{\text{moles of protein}}$$

Where Ax is the absorbance value of the dye at the absorption maximum wavelength and Ɛ is the molar extinction coefficient of the dye.

Assembly of QD-protein-dye conjugates to a functional nanoprobe

The conjugation of QDs to fluorophore-labeled protein module to complete the FRET pair, was adapted from Clapp *et al* (Clapp 2006). To start with the TOPO-capped

CdSe/ZnS QDs with 540 nm of emission maximum were made water-soluble QDs, by doing a cap exchange with dihydrolipoic acid (DHLA) according to the protocol by Clapp et al (Clapp 2006). 390 nM of DHLA-capped QDs were added to Alexa568-labeled proteins, resuspended in 10mM HEPES buffer (pH 8.2) at 1:1 to 1:20 ratio of QDs to protein module. The samples were mixed thoroughly and incubated at room temperature for overnight. After conjugation, the FRET efficiency was measured using a fluorometer by exciting at 430 nm and the spectrum was recorded from 475 nm to 650 nm.

In-vitro protease assays using the nanoprobes

For the in-vitro MMP-7 assay, 130 nM of QD545-MMP-7-Alexa 568 conjugates in 10 mM HEPES buffer (pH 7.4, 150 mM NaCl, 5 mM $CaCl_2$) was taken in a 96 well plate and MMP-7 was added at a final concentration of 10 ng/ml- 10 µg/ml. The 96- well plate was incubated at 37°C for 1-2 hrs with a tight seal to prevent water evaporation. Following a protease reaction, fluorescence intensity in each well was measured using a microplate reader (Synergy^{TM} 4, BIOTEK® Instruments, Inc., Winooski, VT). For the in-vitro NS3 assay a similar reaction was set up, with 130 nM of QD545–NS2B-NS3-Alexa 568 conjugates in 200mM Tris pH 9.5, 13.5mM NaCl, 30 percent glycerol and NS3 was added at a final concentration of 100 pM- 100 nM. For the inhibition studies, a similar reaction was set up except that the proteases were pre-incubated with the increasing concentration of the respective inhibitors and then the protease-inhibitor complex was incubated with the substrates.

Results

Protein module design and peptide synthesis

To detect MMP-7 activity, a protein module was designed to contain the MMP-7 cleavage sequence (VPLSLTMG) and the ELP domain $[(VPGVG)_2VPGKG(VPGVG)_2]_{21}$. This particular ELP domain was chosen based on its transition temperature of ~50^oC under physiological conditions, which enables the potential usage of the module for *in vivo* studies (scheme 2.1). By taking advantage of the modular nature of the design, a similar protein module was designed for the WNV NS3 protease by replacing the MMP-7 cleavage sequence with that for NS3 sequence (LQYTKRGGVLWD). Unlike other probes designed for WNV NS3, which employed only a quadrapeptide sequence, the entire NS2B-NS3 cleavage sequence was used in this module to mimic the natural WNV NS3 cleavage site. Both protein modules were produced in *E. coli* BL-21 Gold (DE3) and purified by taking advantage of the temperature-responsive properties of ELP. After two rounds of temperature triggered precipitation and resolubilization, purified proteins of the expected molecular weight of 48 kDa (Figure 2.1 A and 2.1C) were detected by SDS-PAGE.

Assembly and characterization of the nanoprobes

Dihydrolipoic acid (DHLA) capped QDs with an emission maximum at 545 nm (QD545) was selected for the nanoprobes assembly. A thiol-reactive Alexa 568 maleimide dye was chosen as the fluorescent acceptor because of the favorable spectral

overlap with the DHLA-capped QD545. Conjugation of Alexa 568 to the proteins was mediated through the formation of a thioether bond with a unique cysteine residue after the protease cleavage sequence (Kim et al., 2005; Scheme 2.1). Presence of the ELP domain enabled the separation of unreacted dyes using thermally triggered precipitation in place of more tedious and expensive methods such as desalting column or dialysis. The conjugation of the dye to the two different protein modules was evaluated using SDS-PAGE (Figure 2.1 B and 2.1 D). A strong fluorescent band corresponding to each of the two protein modules was detected under UV light, confirming the successful conjugation to Alexa 568.

To generate the functional nanoprobes, Alexa-labeled MMP-7 modules were assembled onto DHLA-capped QDs via metal affinity interaction between the His6 tag and the ZnS shell of the QD. As expected, binding of Alexa-labeled MMP-7 modules to QD 545 resulted in FRET with a corresponding quenching of the QD signal and an increase in the Alexa intensity (Figure 2.2 A). The FRET ratio expressed as Alexa (568 nm)/QD (545 nm) emission increased with an increasing amount of MMP-7 module added (Figure 2.2 B). A conjugation ratio of 3 Alexa-labeled MMP-7 modules per QD was chosen for further study as there was over 85% loss in the QD photoluminescence and cleavage of even a small number of target protease sequences should result in a large, detectable change in the FRET ratio as indicated by previous reports (Medintz et al., 2006). A similar increase in the FRET ratio was obtained with the Alexa-labeled NS3 module, although the maximum FRET ratio obtained was 11, which is lower than that of the MMP-7 module (Figure 2.2 C and 2.2 D) even at a module to QD ratio of 20. This

smaller FRET ratio is likely due to the increased distance for the NS3 cleavage sequence and the different orientation of the assembled modules. Subsequent investigations with the NS3 module were conducted using the assembly ratio of 10.

Detection of MMP-7 proteolytic activity using the nanoprobe

After demonstrating the successful assembly of the MMP-7 nanoprobes, their applicability for MMP-7 detection was evaluated. In principle, the nanoprobes should be cleaved between the serine and leucine residue of the substrate upon addition of MMP-7, leading to a significant change in the FRET ratio (Turk et al., 2001). The nanoprobes were incubated with 10 μg/mL of MMP-7 and the fluorescent signals were recorded for 2 hr. Figure 2.3 shows the temporal profile of the MMP-7 proteolytic reaction. In the absence of MMP-7, the FRET ratio of the nanoprobes was maintained around 12 throughout the 2 h incubation with buffer. In contrast, a sharp decline in the FRET ratio was observed as early as 30 min after MMP-7 addition. This decline in the FRET ratio continued with time, reaching less than 70% (FRET ratio=3.8) of the original value in 2 hr. This notable decrease in the FRET signal is consistent with the MMP-7 mediated cleavage of the nanoprobes which led to the expected release of Alexa dyes from the QDs.

To investigate the sensitivity of the MMP-7 nanoprobes, similar proteolytic reactions were conducted with an increasing concentration of (10 ng/ml-10 μg/ml) MMP-7. As shown in Figure 2.4, the FRET ratio decreased with increasing concentrations of

MMP-7 and as low as 10 ng/ml of MMP-7 could be detected. This result indicates that the FRET ratio change of the MMP-7 nanoprobes can be used to accurately correlate with MMP-7 activity. Moreover, the range of detection is well within the secretion levels in malignant tissues (<600 ng/mL) (Maurel et al., 2007) and in cancer patient sera (< 126 ng/mL) (Watelet et al., 2004), making this a suitable platform for quantitative assessment of MMP-7.

MMP-7 Inhibition Assay

To determine if these MMP-7 nanoprobes could potentially be used in inhibitor screening, we carried out assays with a known broad spectrum MMP-7 inhibitor (MMP Inhibitor III). Figure 2.5 shows the results of assaying an increasing concentration of the inhibitor against a constant concentration of nanoprobes and MMP-7. When compared to samples not treated with MMP-7, 100% inhibition of activity was observed at the highest inhibitor concentration of 10 μM. As expected, the level of inhibition decreased with lowering doses to less than 22% at 0.1 μM. The dose-dependent nature of the inhibition demonstrates the ability of the nanoprobes to provide quantitative assessment of a given inhibitor and can be very useful for screening a wide range of MMP-7 specific inhibitors.

Sensing WNV-Pr (NS3) proteolytic activity using the nanoprobe

The modular nature of our nanoprobe design allowed the easy adaptation to target the WNV NS3 protease. Since the NS3-sensitive cleavage sites in the polyprotein precursor predominantly exhibit arginine at the P1 position, arginine or lysine at the P2 position, and glycine or serine at the P1' position (Shiryaev et al., 2006), a NS3 cleavage site sequence composed of LQYTKRGGVLWD was incorporated in our new nanoprobe design. To detect WNV-Pr activity, the NS3 nanoprobes were incubated with 100 nM of NS3 for 2 h. Similar to the result with MMP-7, a rapid decline in the FRET ratio was observed upon NS3 addition (Figure 2.6). The sensitivity of the NS3 nanoprobes was significantly higher than that for MMP-7 and as low as 0.5 nM can be detected (Figure 2.7). This detection limit is the lowest ever reported in literature when compared with other FRET systems using organic fluorophores and again highlights the benefit of using QD as the donor molecule.

NS3 Inhibition Assay

To further illustrate the utility of the NS3 nanoprobes for screening NS3 inhibitors, a known inhibitor undeca-D-Arg-NH_2 which was found to be effective at the nanomolar range against NS3 was used (Shiryaev et al., 2006). In the undeca-D-Arg-NH_2 treated samples, virtually 100% inhibition of the NS3 activity was observed at 40 nM or higher concentrations, a result consistent with the reported efficacy of undeca-D-Arg-NH_2 (Figure 2.8). The level of inhibition was still 80% even at the lowest concentration

tested of 4 nM, while no inhibition was detected without the addition of undeca-D-Arg-NH_2. These results again highlight the extremely sensitive nature of our QD-based nanoprobes for inhibitor screening. Considering the importance of NS3 in WNV replication, the reported NS3 nanoprobes may find practical applications in developing the next generation of anti-WNV agents.

Discussion

Here we demonstrate the establishment of a nanoscale sensor consisting of QD-peptide conjugates that are capable of specifically detecting the activity of proteolytic enzymes. These sensors are based on the principle of FRET, where the donor fluorophore (QD) is linked to an acceptor fluorophore (Alexa 568 dye) through a protease cleavage sequence. Proteolytic cleavage of the sequence by the protease disrupts FRET and provides rapid and sensitive detection of proteases. The presence of QD offers a central nanoscaffold for assembling multiple dye labeled peptides. The spectral overlap between QD545 and Alexa 568 provides efficient energy transfer making it an ideal FRET pair, however by using QDs of different emission wavelength as the donor several different FRET pairs can be generated.

In preparing these nanoprobes, a genetically programmable protein module harboring different functional domains in a linear N to C terminal has been developed which offers several distinct advantages over the broad array of existing FRET based sensors for detecting protease activity. The in house production of protein modules containing the protease cleavage sequence caused a significant reduction on the cost of peptide synthesis as opposed to use of synthetic peptides for carrying out FRET based assays. Another major advantage of using the programmable protein module is the modular nature of the module which obviates the need for major redesign when targeting a new protease. Peptide specificity can be varied by altering only the recognition sequence without significantly modifying other domains. In addition, the presence of ELP domain at the C terminus allowed rapid and convenient purification of proteins and

helped escaping the conventional and formidable protein purification steps. Moreover the yield of the protein using this purification was significantly higher compared to the other protein purification procedures. ELP domain also enabled the separation of unreacted dyes using thermally triggered precipitation rather than conventional expensive and time consuming methods such as desalting column or dialysis. After three cycles of purification, free dye was no longer detected in the supernatant and fluorescence was only visible in the pellet containing the peptide-Alexa dye conjugates, confirming the efficiency of the thermal precipitation.

The use of histidine driven self assembly of peptides onto the QDs allowed control over peptide to QD ratio, FRET efficiency and enabled quantitative detection of protease activity. It is interesting to note that although the substrate sequence was "sandwiched" between the QD and ELP in the conjugate structure, it was still accessible the enzyme. There are a number of potential applications for this sensor design including high throughput screening of protease inhibitors. It may be further increased by using a 'multiplexed' format for detecting multiple proteases (Clapp et al., 2005). It is reasonable to assume that this assay format may also be applied for monitoring the phophorylation/ dephosphorylation of protein kinases/ phosphatases (Rodems et al., 2002). Further, introducing QD-based FRET sensors into live cells should allow for real –time monitoring of in-vivo enzymatic activity.

References

Anand K, Ziebuhr J, Wadhwani P, Mesters JR, Hilgenfeld R. 2003. Coronavirus Main Proteinase (3CLpro) Structure: Basis for Design of Anti-SARS Drugs. Science **300**: 1763-1767.

Bruchez, M. Jr, Moronne, M., Gin, P.,Weiss, S. & Alivisatos, A. P. 1998. Semiconductor nanocrystals as fluorescent biological labels. Science **281**: 2013–2016.

Clapp AR, Medintz IL, Uyeda HT, Fisher BR, Goldman ER, Bawendi MG, Mattoussi H. 2005. Quantum Dot-Based Multiplexed Fluorescence Resonance Energy Transfer. Journal of the American Chemical Society **127:** 18212-18221.

Clapp, A.R., Goldman, E.R., Mattoussi, H. 2006. Capping of CdSe-ZnS quantum dots with DHLA and subsequent conjugation with proteins. Nature Protocols 1: 1258-1266.

Edwards DR, Hoyer-Hansen G, Blasi F, Sloane BF (eds) (2008) The cancer degradome—proteases and cancer biology. Springer, New York

Geysen, H.M., Schoenen, F., Wagner, D., Wagner, R. 2003. Combinatorial compound libraries for drug discovery; an ongoing challenge. Nat. Rev. Drug Discov., **2**:222-230

Hermanson, G. T. 1996. Bioconjugate Techniques; Academic Press: London; Chapter 8

Kim J.-Y., S. O'Malley, A. Mulchandani and W. Chen. 2005**.** Genetically engineered elastin-protein A fusion as a universal platform for homogeneous, phase-separation immunoassay**.** Analytical Chemistry**.77**:2318-2322

Kim, Y.-P., Young-Hee Oh, Eunkeu Oh, Sungho Ko, Min-Kyu Han, and Hak-Sung Kim. 2008**.** Energy Transfer-Based Multiplexed Assay of Proteases by Using Gold Nanoparticle and Quantum Dot Conjugates on a Surface. Anal. Chem. **80**: 4634 4641

Lao U.L., Chen A., Matsumoto M.R., Mulchandani A., Chen W. 2007. Cadmium removal from contaminated soil by thermally responsive elastin (ELPEC20) biopolymers. Biotechnology and Bioengineering **98:** 349-355.

Massodi, I., Bidwell, G.L. III, Raucher, D. 2005. Evaluation of cell penetrating peptides fused to elastin-like polypeptide for drug delivery. J. Control. Release **108:** 396-408.

Maurel J, Nadal C, Garcia-Albeniz X, Gallego R, Carcereny E, Almendro V, Marmol M, Gallardo E, Maria Auge J, Longaron R, Martínez-Fernandez A, Molina R, Castells A, Gascón P. 2007. Serum matrix metalloproteinase 7 levels identifies poor prognosis advanced colorectal cancer patients. International Journal of Cancer **121:** 1066-1071.

Medintz I.L., Clapp A.R., Mattoussi H., Goldman E.R., Fisher B., Mauro J.M. 2003. Self-assembled nanoscale biosensors based on quantum dot FRET donors. Nat Mater.**2**:630-638

Medintz, I.G., Clapp, A.R., Brunel, F.M., Tiefenbrunn, T., Uyeda, H.T., Chang, E.L., Deschamps, J.R., Dawson, P.E., Mattoussi, H. 2006. Proteolytic activity

monitored by fluorescence resonance energy transfer through quantum-dot–peptide conjugates. Nature Materials **5**: 581-589.

Michalet X, Pinaud FF, Bentolila LA, Tsay JM, Doose S, Li JJ, Sundaresan G, Wu AM, Gambhir SS, Weiss S. 2005. Quantum Dots for Live Cells, in Vivo Imaging, and Diagnostics. Science **307:** 538-544.

Mitra, R.D., Silva, C.M., Touvan, D.C. 1996. Fluorescence resonance energy transfer between blue-emitting and red-shifted excitation derivatives of the green fluorescent protein, Gene. **173**:13-17.

Pennington, M.W., Thornberry, N.A. 1994. Synthesis of a fluorogenic interleukin-1-beta converting enzyme substrate based on resonance energy transfer, Pept. Res., **7**:72-76.

Rodems SM, Hamman BD, Lin C, Zhao J, Shah S, Heidary D, Makings L, Stack JH, Pollok BA. 2002. A FRET-Based Assay Platform for Ultra-High Density Drug Screening of Protein Kinases and Phosphatases. Assay and Drug Development Technologies **1:** 9-19.

Shiryaev, S. A., Ratnikov, B. I., Chekanov, A. V., Sikora, S., Rozanov, D. V., Godzik, A., Wang, J., Smith, J. W., Huang, Z., Lindberg, I., Samuel, M. A., Diamond, M. S., and Strongin, A. Y. 2006**.** Cleavage targets and the D-arginine-based inhibitors of the West Nile virus NS3 processing proteinase. Biochem**.** J **393**:503–511

Turk BE, Huang LL, Piro ET, Cantley LC. 2001. Determination of protease cleavage site motifs using mixture-based oriented peptide libraries. Nat Biotech **19:** 661-667.

Watelet JB, Bachert C, Claeys C, Cauwenberge PV. 2004. Matrix metalloproteinases MMP-7, MMP-9 and their tissue inhibitor TIMP-1: expression in chronic sinusitis and nasal polyposis. Allergy **59:** 54-60.

Xia Z., Y. Xing, M.K. So, A.L. Koh, R. Sinclair and J. Rao. 2008. Multiplex detection of protease activity with nanoprobes prepared by intein-mediated specific bioconjugation.Anal Chem **80:**8649–8655

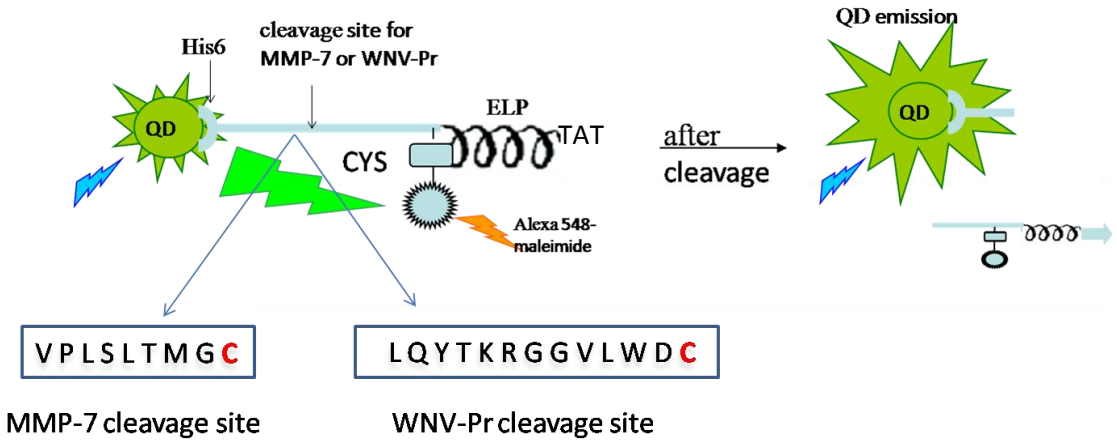

Scheme 2.1: Schematic representation of the self assembled QD-peptide nanoprobes harboring engineered protein modules H-MMP-7-ET or H- NS2B/NS3-ET. H- MMP-7-ET contains hexahistidine, MMP-7 cleavage sequence, cysteine residue (C in bold red) for dye incorporation and ELP for thermal purification. In H- NS2B/NS3-ET only the cleavage sequence is changed to WNV-Pr cleavage sequence NS2B/NS3, keeping the other modules same. Dye labelled modular peptides containing appropriate cleavage sequences are self-assembled onto the QDs. In this design, the QD photoluminescence (PL) is quenched by the fluorescent dye due to fluorescence resonance energy transfer (FRET). Presence of active proteases disrupts FRET resulting in an increased QD PL thus enabling a simple activity assay.

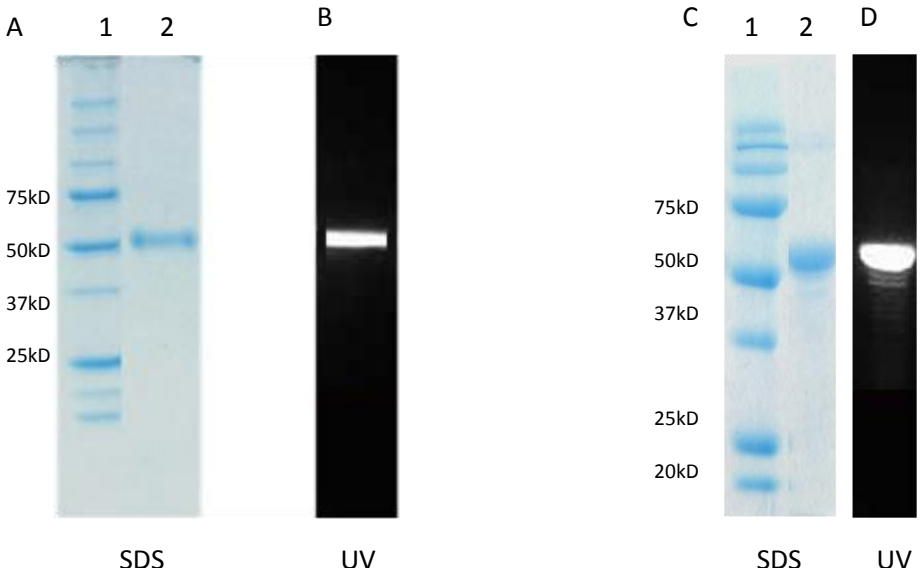

Figure 2.1: **(A)** SDS-PAGE analysis of H-NS2B/NS3-ET. Lane 1: protein size marker, Lane 2: purified protein module. **(B)** Conjugation of H-NS2B/NS3-ET with Alexa 568 maleimide, observed under UV lamp. **(C)** SDS-PAGE analysis of H-MMP-7-ET. Lane 1: protein size marker, Lane 2: purified protein module. **(D)** Conjugation of H-MMP-7-ET with Alexa 568 maleimide, observed under UV lamp.

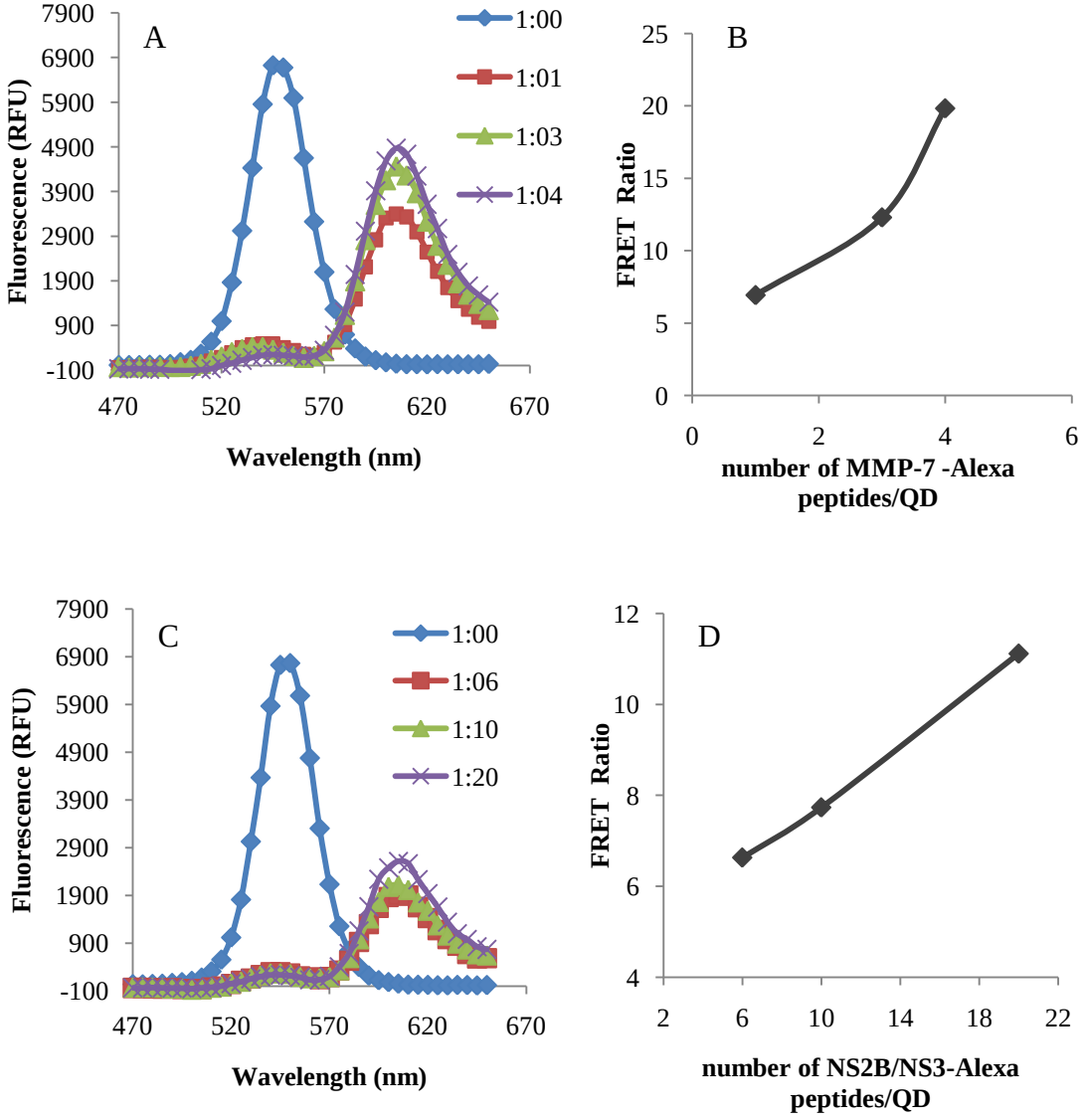

Figure 2.2: FRET efficiency of QD-peptide nanoprobes. **(A)** Emission spectra of QD-MMP-7-Alexa assembly at the various QD: Alexa ratios. Excitation is 435 nm. **(B)** FRET efficiency of the different QD:MMP-7-Alexa ratio conjugates **(C)** Emission spectra of QD-NS2B/NS3-Alexa assembly at the various QD: Alexa ratios. **(D)** FRET efficiency of the different QD:NS2B/NS3-Alexa ratio conjugates

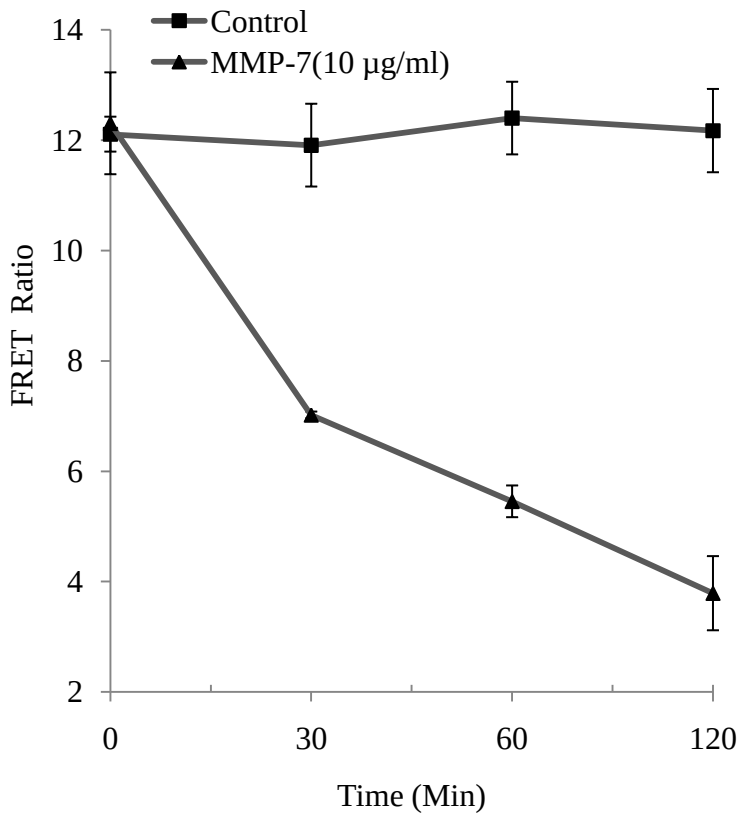

Figure 2.3: Time dependent measurements of the changes in Fa/Fd ratio of QD-MMP-7-Alexa based probes in the presence and absence of 10 µg/ml of MMP-7. The error bars indicate the standard deviation from three independent experiments.

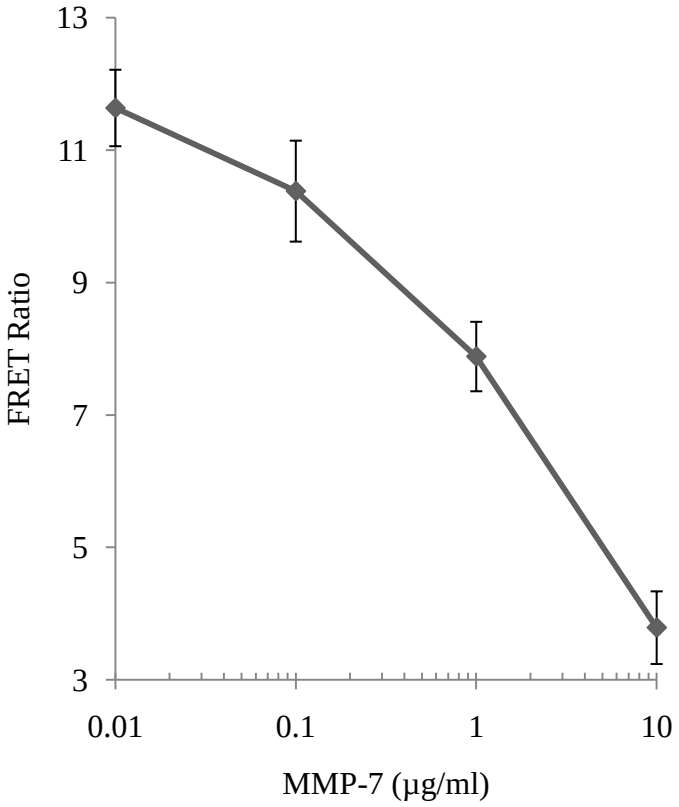

Figure 2.4: MMP-7 proteolytic assay. MMP-7 proteolytic activity was determined by assaying a constant amount of QD-MMP-7-Alexa substrate at an increasing concentration of MMP-7. MMP-7 concentration dependence of Fa/Fd plotted 2 hr following the addition of MMP-7 to solutions of QD-MMP-7-Alexa probes. The error bars indicate the standard deviation from three independent experiments.

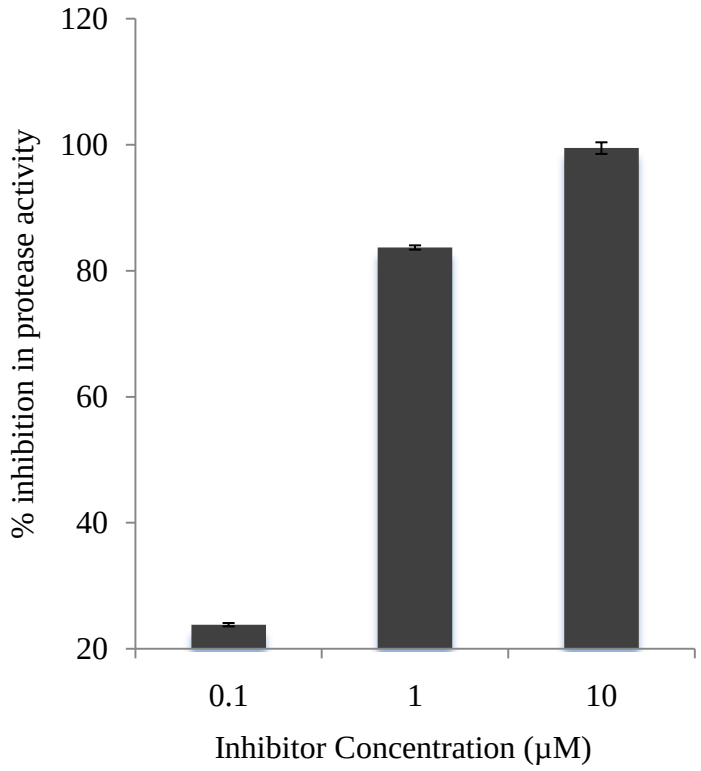

Figure 2.5: MMP-7 inhibition assay. Result of assaying 10 µg/ml of MMP-7 in the presence of an increasing concentration of MMP-7 inhibitor. The error bars indicate the standard deviation from three independent experiments.

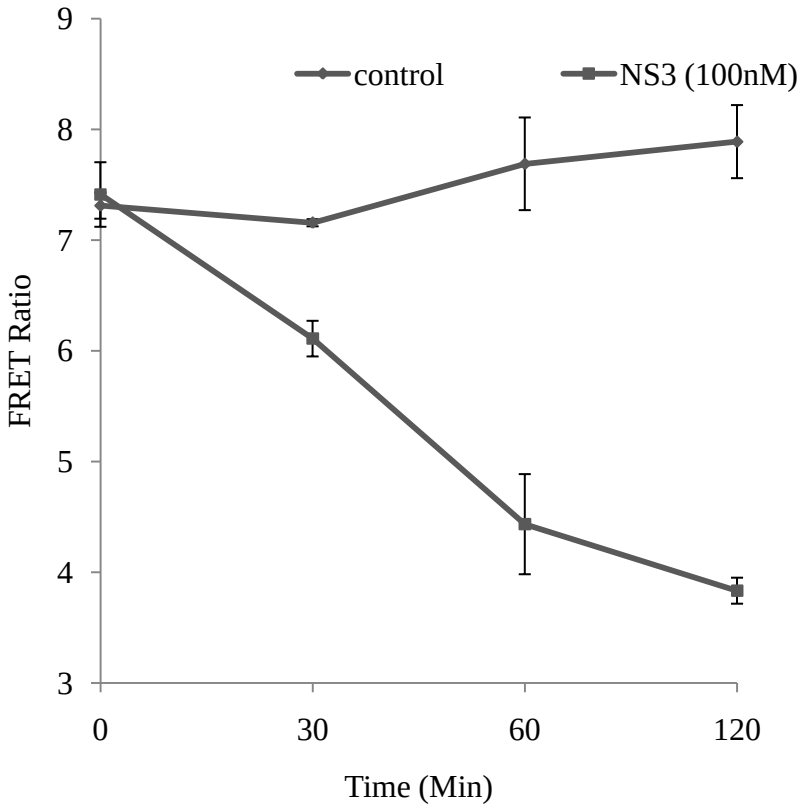

Figure 2.6: Time dependent measurements of the changes in Fa/Fd ratio of QD-NS2B/NS3-Alexa based probes in the presence and absence of 100 nM of WNV-Pr (NS3). The error bars indicate the standard deviation from three independent experiments.

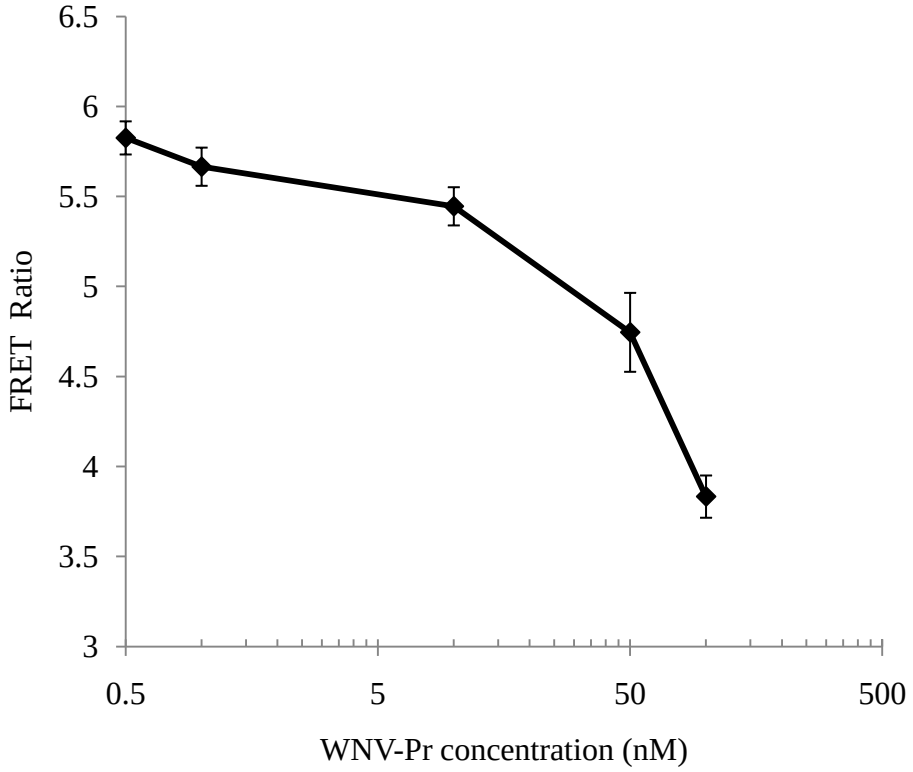

Figure 2.7: WNV-Pr (NS3) proteolytic assay. NS3 proteolytic activity was determined by assaying a constant amount of QD-NS2B/NS3-Alexa substrate at an increasing concentration of NS3. NS3 concentration dependence of Fa/Fd plotted 2 hr following the addition of MMP-7 to solutions of QD-MMP-7-Alexa probes. The error bars indicate the standard deviation from three independent experiments.

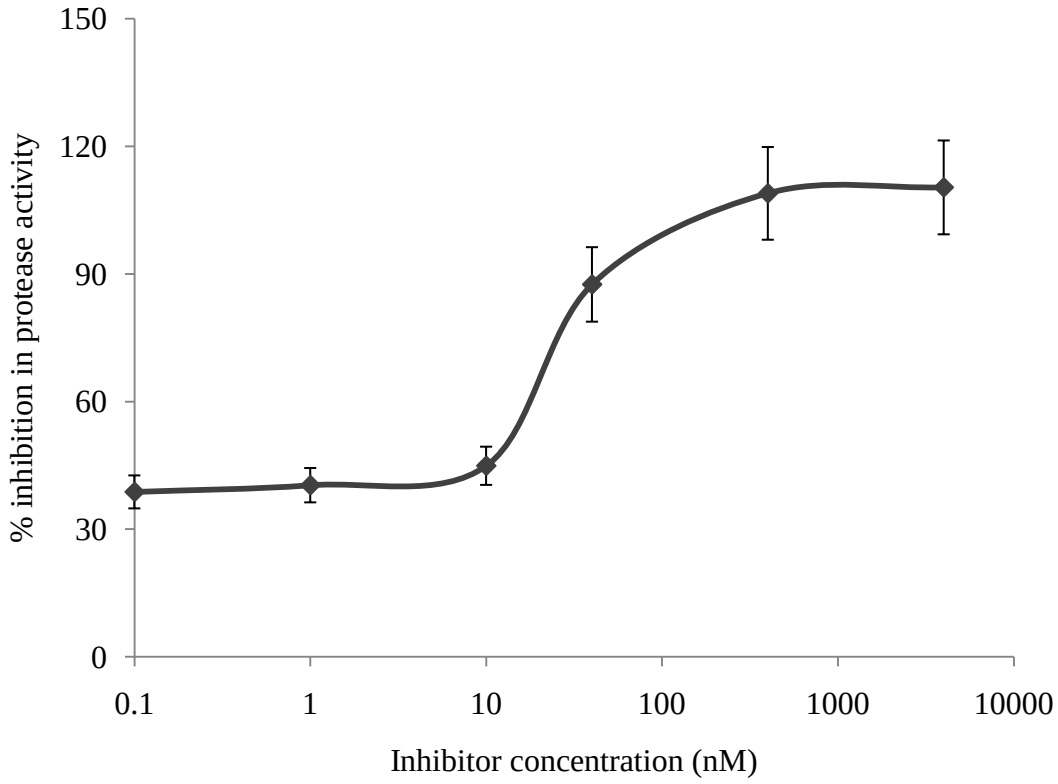

Figure 2.8: NS3 inhibition assay. Result of assaying 100 nM of NS3 in the presence of an increasing concentration of NS3 inhibitor- undeca-D-Arg-NH_2. The error bars represent standard deviations from the mean from triplicate measurements.

Chapter 3

Development of a QD-based FRET bioassay for performing rapid and sensitive screening of HIV-1 protease inhibitors using a genetically programmable protein module

Abstract

Human immunodeficiency virus type 1 protease (HIV-1 PR) is the major target for anti-HIV agents due to its essential role in viral replication. However, one of the emerging problems with antiviral therapy is the emergence of drug resistant variants. Thus, new generation of inhibitors are urgently needed. Here, we demonstrate the development of a Quantum dot (QD) based FRET (fluorescence resonance energy transfer) assay system to detect HIV-1 PR activity in living cells and screen its inhibitors. A genetically programmable protein module was designed to rapidly express, purify and introduce the HIV-1 PR substrate inside living cells. The engineered protein module is designed with: 1) a QD binding moiety containing poly-histidine, 2) a cysteine site for fluorescent dye incorporation based on cysteine-thiol interaction, 3) HIV-1 PR cleavage site (MA/CA), 4) an Elastin Like Protein (ELP) domain for thermal purification and 5) a flanking TAT peptide sequence for cell penetration. In this design, the QD fluorescence (FL) is quenched by the fluorescent dye due to FRET. Cleavage of the MA/CA sequence by HIV-1 PR resulted in separation of the FRET pair with subsequent increase in QD FL, whereas potent protease inhibitors prevented FRET disruption and a reduced QD FL was detected. This assay provides a sensitive and quantitative measure of HIV-1 PR activity and is used to screen HIV-1 PR inhibitors. Thus, by using the genetically programmable protein module a convenient, cost effective and highly efficient system can be developed for high throughput screening of viral protease inhibitors.

Introduction

Proteases are proteolytic enzymes that catalyze the cleavage of peptide bonds. They play important roles in many essential cellular processes such as blood coagulation, fibrinolysis, cancer development, neurodegenerative disorders, and apoptosis (Neurath et al., 1999; Vihinen et al., 2005; Blum et al., 2005). In addition, proteases are used by many infectious microorganisms such as bacteria, viruses, and parasites as the key virulence factors for infection. Due to the essential role of Human Immunodeficiency virus type-1 protease (HIV-1 PR) in conformational rearrangement of the immature virions and production of infectious virus particles, it has become an ideal target for the development of antiviral agents to treat AIDS. Potent HIV-1 protease inhibitors, such as Indinavir, Nelfinavir, Ritonavir, and Saquinavir are widely used in antiretroviral treatment (Patick et al., 1998). Despite the initial antiretroviral activity, the benefit of protease inhibitors is of limited duration due to the constant emergence of drug-resistant viral strains. The emergence of drug-resistant HIV-1 strains thus motivates the continuous development of new anti-HIV-1 PR compounds (Berkhout B., 1999 and Vickrey et al., 2003). In this context, the availability of a sensitive and convenient assay system to detect protease activity is of great importance.

One of the most promising methods for probing protease activity is based on the principle of fluorescence resonance energy transfer (FRET), where a protease-specific sequence is used to link two fluorophores (Zhang et al., 2004). Cleavage of the linker peptide separates the donor and the acceptor, resulting in an increase in the donor emission and a reduction in the acceptor emission. Efforts to adapt this FRET-based

method for probing *in vivo* protease activity have been made by using genetically engineered fluorescence protein (CFP-YFP) pairs as the FRET donors and acceptors (Zhang, 2004; Heim and Tsien, 1996). In vivo protease activity can be easily visualized by detecting the changes in CFP/YFP signal using common imaging modalities.

However, the use of stable, genetically engineered cell lines expressing the protease FRET substrates is a tedious task, more so, in the context of rapidly mutating HIV-1 strains. One feasible alternative is to develop a simple platform to introduce FRET-probes inside living cells in a benign and robust manner with minimal cytotoxic effects. Quantum-dot-based FRET probes are particularly attractive for this purpose because of their high quantum yield, narrow photoemission spectra, and high resistance to photobleaching. Recently, FRET-based protease assays have been successfully demonstrated using QDs as the energy donor and fluorescent dye as the acceptor (Medintz et al., 2006). Cleavage of the protease site results in an increase in QD/dye emission ratio and quantitative data, including enzyme kinetic parameters can be obtained. However, the use of synthetic peptides as the FRET substrates is expensive and these probes lack cell permeability for monitoring protease activity *in vivo*. Ideally, a method that provides easy production, purification and conjugation of the peptide substrate to acceptor dyes and QDs is necessary to provide a low-cost and tunable approach for probing protease activity inside living cells.

In this paper, we present a genetically programmable module that is easily adaptable for *in vivo* monitoring of protease activity and the simultaneous screening of a

wide range of protease inhibitors. The protein module (Scheme 3.1) is composed of 1) a N-terminus histidine tag (His) for QD conjugation via strong metal-affinity coordination with Zn^{2+} on the core-shell, 2) a protease cleavage site, 3) a unique cysteine residue for fluorescent dye incorporation, 4) an elastin-like peptide (ELP) domain, and 5) a flanking TAT peptide sequence for cell penetration (Gupta 2005; Lewin 2000). Presence of the ELP domain enables simple purification of the protein module and the conjugated FRET probe by thermally triggered precipitation (Urry 1997). This modular design is intended to obviate the need for major redesign when targeting a new protease. Peptide specificity can be varied by altering only the recognition sequence without significantly modifying other modules in the overall sequence. Using the HIV-1PR cleavage sequence MA/CA, we demonstrate the new QD based FRET assay system for in-vivo detection of HIV-1Pr activity as well as quantitative assessment of different HIV-1PR inhibitors.

Materials and Methods

Design of constructs

To construct an expression vector for His6-MA/CA-Cys-ELP105K-TAT (H-MA/CA-ET), plasmid p08-ELP105K-EC20 described by Lao et al (Lao 2007) was digested with *Sma*I and *Hin*dIII and a DNA fragment encoding TAT peptide (amino acid sequence: GGTKTGRRRQRRKKRGY) was inserted between the same restriction sites. The resulting plasmid p08-ELP105K-TAT was cut with *Bam*HI and *Nde*I and 1.7 kb fragment was ligated to plasmid pET14 (Novagen, Madison, WI) treated with same enzymes to generate pET-ELP105K-TAT. An artificial gene carrying hexa-histidines and the MA/CA peptide with cysteine was prepared by heating and annealing two oligonucleotides, CATGGGC CAT CAC CAT CAC CAT CAC TCC CAG GTC AGC CAA AAT TAC CCT ATA GTG CAG AAC CTG CAG TTC TGC CA and TATG GCA GAA CTG CAG GTT CTG CAC TAT AGG GTA ATT TTG GCT GAC CTG GGA GTG ATG GTG ATG GTG ATG GC C and ligated to the 6.3kb fragment obtained from pET-ELP105K-TAT by digesting with *Nco*I and *Nde*I to create pET-H-MA/CA-ET.

Expression and purification of peptides

For protein expression, *E.coli* BL-21(DE3) (Novagen, Madison, WI) transformed with plasmid pET-H-MA/CA-ET and was grown in terrific broth media containing 100 μg/ml ampicillin at 37^{o}C until optical density (O.D.) at 600 nm reached 0.5. The flasks were then transferred to 30^{o}C for protein expression. When the O.D. at 600nm reached 5, cells were harvested by centrifugation, resuspended in 50mM Tris/HCl (pH 8.0) with 0.1M

NaCl and 1 mg/ml of lysozyme, and lysed by sonication. Cell debris was removed by centrifugation at 16,000 g for 30 min. Proteins were purified by repeated temperature transition cycle as described previously (Kim et al., 2005). Briefly, for each cycle, NaCl was added to the sample at a final concentration of 2M and the sample was heated to 37^{o}C and centrifuged at 16,000 g at 30^{o}C for 15 min. The pellet containing the proteins were resuspended in ice-cold 50mM Tris/HCl (pH 8.0) with 0.1M NaCl and centrifuged at 16,000 g at 4^{o}C for 15 min to remove undissolved proteins. This temperature transition cycle was repeated once more, and the pellet containing H-MA/CA-ET was finally resuspended in ice cold 50mM Tris/HCl (pH 8.0) with 0.1M NaCl. The purity of the protein was determined by SDS-PAGE electrophoresis.

Conjugation of peptides with fluorescent dye

The labeling of the proteins with thiol reactive dye was performed by modifying the procedure of Massodi *et al*. (Massodi 2005). Purified proteins were resuspended in 50mM potassium phosphate buffer (pH 7) at a final concentration of 40 uM. Tris-(2-carboxyethyl) phosphine (TCEP) and Alexa 568 maleimide (Invitrogen, Carlsbad, CA) (thiol reactive dye) were added to a 10-fold and 2-fold molar excess, respectively. The mixture was incubated with end-over-end rotation for 2 hr at room temperature in the dark. The reaction was stopped and the unreacted dyes were removed by two or three thermal precipitation cycles as described in the protein purification procedure. The degree of labeling of the protein was calculated using the following formula:

$$\frac{A_x}{\epsilon} \times \frac{\text{MW of protein}}{\text{mg protein/mL}} = \frac{\text{moles of dye}}{\text{moles of protein}}$$

Where Ax is the absorbance value of the dye at the absorption maximum wavelength and Ɛ is the molar extinction coefficient of the dye.

Assembly and characterization of QD-protein-dye conjugates

The conjugation of QDs to fluorophore-labeled protein module to complete the FRET pair was adapted from Clapp et al., 2006. To start with, the TOPO-capped CdSe/ZnS QDs with 545 nm of emission maximum (Evident Tech. Inc) were made water-soluble QDs, by doing a cap exchange with dihydrolipoic acid (DHLA) according to the protocol by Clapp et al., 2006. 300 nM of DHLA-capped QDs were added to Alexa568-labeled proteins, resuspended in 10mM HEPES buffer (pH 8.2) at 1:10 ratio of QDs to protein module. The samples were mixed thoroughly and incubated at room temperature for overnight. After conjugation, the FRET efficiency was measured using a fluorometer by exciting at 430 nm and the spectrum was recorded from 475 nm to 650 nm.

In-vitro protease assay

For the in-vitro assay, HIV-1 PR was diluted in 200 mM sodium acetate pH 5.5, 10 % glycerol, 5 % ethylene glycol and 1mM DTT at a concentration of 500 nM. Protease assay was initiated by addition of 45 µL protease solution to micowells containing QD-MA/CA-ALEXA 568 probes. The 96- well plate was incubated at 37°C for 2-3 hrs with a tight seal to prevent water evaporation. Following a protease reaction, fluorescence

intensity in each well was measured using a microplate reader (Synergy^{TM} 4, BIOTEK® Instruments, Inc., Winooski, VT).

Cell culture

HeLa cells obtained from American Type Culture Collection were grown in 400 mL of 1× autoclavable minimum essential medium (AMEM; Irvine Scientific) containing 1% of 7.5% $NaHCO_3$, 2% of 1 M Hepes, 1% of nonessential amino acids (NEAA; HyClone, Thermo Scientific), 100 µg/mL of penicillin and 100 U/mL of streptomycin (HyClone, Thermo Scientific), 1% of 200 mM L-glutamine in 0.85% NaCl (HyClone, Thermo Scientific), and 10% of FBS (Sigma–Aldrich) at 37°C in a 5% CO_2 atmosphere.

Intracellular delivery of probes, Transfection and Titration of HIV-1 PR inhibitors

HeLa cells were seeded into 96 well clear bottom black wall side plates (Nunc Scientific) at 37°C in 5% CO_2 in air and cultured to >90% confluence. After removing the incubation medium, the cell monolayer was washed twice with 1× PBS. Cells were then incubated at 37°C in the dark with 1× Leibovitz L-15 medium (Invitrogen) containing QD- MA/CA- Alexa 568 at QD concentrations of 150 nM. 2 hrs after incubation with the probes, the cells were washed with PBS and observed under Zeiss Axiovert 40 CFL inverted fluorescence microscope. To introduce the HIV-1 PR, HeLa cells containing the probes were transfected using Lipofectamine^{TM} 2000 transfection reagent (Invitrogen) with the plasmid pNL4-3.HSA.R$^-$E$^-$ (Connor et al., 1995; He et al., 1995) expressing the entire HIV-1 genome. After 6 h, the medium was changed to the normal growth medium

and cells were propagated for another 18 hrs and were then observed under fluorescent microscope. In order to test the activity of the HIV-1 PR inhibitors, after removal of the transfection reagent, the cells were incubated with the growth medium containing the different therapeutically used HIV-1 PR inhibitors including Ritonavir, Saquinavir, Nelfinavir, Atazanavir sulfate (AZT) and Amprenavir (NIH) at a concentration of 0.01-10 μM.

Fluorescence Microscopy and image processing

Cell imaging was performed on a Zeiss Axiovert 40 CFL inverted microscope equipped with a 12-V, 35-W halogen lamp (for the phase-contrast images) and an HBO 50 W/AC mercury lamp (for the fluorescence images). The objectives used were a 5×/0.12 A-Plan, a 10×/0.25 A-Plan, a 20×/0.50 EC Plan-NEOFLUAR, and a 40×/0.50 LD A-Plan (Zeiss). Fluorescent probes were detected by using two different filter sets; QD filter consisting of a D436-nm exciter, a D535/50-nm emitter, and a 475 nm-dichroic long pass beam splitter (Chroma Technology) and FRET filter consisting of a D436-nm exciter, a D610/50-nm emitter, and a 475 nm-dichroic long pass beam splitter. Images were acquired by using a ProgRes MFscan Monochrome CCD camera (Jenoptik). Both phase-contrast and fluorescence images were analyzed by using Image-Pro PLUS analysis software (Media Cybernetics). All settings for image processing were kept constant, and the exposure time for image capture was adjusted, if necessary, to maintain output levels similar to those observed under the fluorescence microscope. The intracellular distribution of the QD-based probes were analyzed by merging the bright field images with the fluorescence

images. Composite merged images were produced by superimposing the fluorescence images from the QD filter and from the FRET filter**.**

Quantification of Fluorescent Signals

The QD fluorescence intensity and Alexa fluorescence intensity for each well was quantified by randomly choosing four to five fields within each well of untreated or treated samples using Image-Pro PLUS analysis software.

Results

Protein module design and protein synthesis

To design a protein module for the HIV-1 PR, the matrix/capsid protein (MA/CA) junction in the HIV-1 gag protein was chosen as the target cleavage site. The MA/CA cleavage sequence SQVSQNYPIVQNLQF was inserted between the hexa-histidine tag and the unique cysteine residue as depicted in Scheme 3.1 to generate the protein module H-MA-ET. The protein module was easily produced in *E. coli* BL21-Gold (DE3) cells at a yield of ~500 mg/L. In addition, the multifunctional modular protein provided rapid purification of the protein module by taking advantage of the temperature-responsive nature of ELP. The protein module was easily purified using two cycles of reversible phase transition and the purity was confirmed by SDS-PAGE indicating the expected molecular weight of 48 kDa (Figure 3.1 A).

Assembly and characterization of the QD-peptide-dye conjugates

The peptides were labeled with a thiol-reactive fluorescent dye - Alexa 568 maleimide through the formation of a thioether bond with a unique cysteine residue after the MA/CA cleavage sequence. This particular dye was chosen based on the overlapping optical spectra between the DHLA-capped CdSe/ZnS QD (QD 540) and Alexa-568 (Supplemental information). Successful conjugation of the dye was evaluated using SDS-PAGE (Figure 3.1 B) and a strong fluorescent band corresponding to the size of the protein module was detected under UV light. The fluorescently labeled modules were then assembled on the DHLA capped QD 545 through the metal affinity between the His

tag and the ZnS shell of the QD. Figure 3.2 A shows the spectra for QD 545 self-assembled with different amount of H-MA-ET-Alexa 568. As expected, binding of QDs to protein-Alexa conjugates resulted in a sharp decline in the QD emission and a corresponding increase in the Alexa 568 intensity. As shown in Figure 3.2 B, the FRET ratio expressed as the Alexa (568 nm)/QD (540 nm) emission intensity when excited at 430nm increased from 4 to 20 as the number of H-MA-ET-Alexa dye conjugates assembled onto the QD increased from 5 to 30. This result confirms the correct assembly of H-MA-ET-Alexa conjugates onto QDs based on the His_6 interaction, resulting in the efficient quenching of the QD via donor-quencher FRET. A conjugation ratio of 10 was chosen for subsequent studies since it offers a good FRET ratio and cleavage of even a small number of target sequences would result in a large, detectable change in the FRET ratio.

In vitro sensing of HIV-1 protease activity using the QD-H-MA-ET-Alexa probes

To test the sensitivity, the QD-H-MA-ET-Alexa probes were first used to detect HIV-1 PR activity *in vitro*. The probes were incubated with a HIV-1 PR conc. of 500 nM and the changes in the FRET ratio were recorded from 0 to 3.5 h. Figure 3.3 shows the time-dependent measurements of the FRET ratio. As early as 15 min of incubation, a significant decrease in the FRET ratio was observed which continued to decrease to 5.5 after 3.5 h. This notable increase in the FRET ratio is entirely due to the HIV-1 PR mediated cleavage of the QD-H-MA-ET-Alexa probes as a similar control experiment without the addition of HIV-1 PR showed only a modest decrease in FRET over the same

duration. Addition of other proteases such as the West Nile Virus protease also resulted in similar changes as the control, indicating that the highly specific nature of the newly developed QD-H-MA-ET-Alexa probes toward HIV-1 PR.

Intracellular delivery of QD-MA/CA-alexa probes

To investigate whether presence of the TAT peptide sequence could allow the non-invasive intracellular delivery of the QD-H-MA-ET-Alexa probes, a monolayer of HeLa cells was incubated with the probes for 2 h and washed to remove any unbound materials. Cells were imaged by a fluorescent microscope using a 436/535 filter set for the QD (green) and a 436/610 set for Alexa (red), and the representative merged fluorescent image (left) and merged fluorescent composite image (right) are shown in Figure 3.4. The composite image clearly showed the localization of the probes inside the HeLa cells (as represented by the red spots) with virtually no fluorescence detected in the surrounding medium, indicating the successful translocation of the probes by TAT peptide mediated delivery. In contrast, incubation of QDs alone resulted in no substantial uptake within the same duration (data not shown). Consistent with the *in vitro* fluorescent measurements, the fluorescent signal from Alexa was much higher than the QD signal in nearly 90% of cells containing the probes (red spots), indicating that FRET was preserved even after intracellular delivery. A few green fluorescent spots were detected, probably due to incomplete conjugation. The intracellular fluorescent intensity was constant for up to 48 h, confirming that the probes were retained inside the cells after delivery and were resistant to intracellular degradation.

Detecting HIV-1Pr activity in HeLa cells

To detect HIV-1 PR activity *in vivo,* the plasmid pNL4-3.HSA.R$^-$E$^-$, which is based on the HIV-1 proviral clone pNL4.3, was used to transfect HeLa cells. This plasmid is capable of producing non-infectious HIV viruses that can undergo a single round of replication in transfected cells due to frameshift mutations in the envelope gene and in the vpr region of the genome.

To demonstrate the ability of the QD-H-MA-ET-Alexa probes to monitor HIV-PR activity in individual cells, probes were first delivered into the HeLa cells as described above before an increasing concentration of the proviral plasmid was used for transfection. As shown in Figure 3.5 A, a significantly higher number of green cells (a reflection of the increase in the QD intensity and a corresponding decrease in the Alexa 568 intensity) were observed for transfected cells, while the fluorescent signals were unchanged for control cells without transfection. Moreover, the number of cells showing the increase in QD signal was in agreement with the concentration of the plasmid used in transfection, again confirming that the increase in QD signal was due to cleavage of the target sequence by the intracellular HIV-1 protease. The proteolytic activity of HIV-1 PR was clearly demonstrated by quantifying the QD and Alexa signals using the Image-Pro PLUS software. The total QD fluorescence (Fd) intensity and Alexa fluorescence (Fa) intensity within each well of control (untransfected), transfected and with the different dosages of plasmid was quantified using Image-Pro PLUS analysis software. The Fa/Fd for each set of images were then normalized to $(Fa/Fd)_0$, which is the value of Fa/Fd in

the control cells. As shown in Figure 3.5 B, when the Fa/Fd ratio was plotted, in the untransfected cells the ratio was 1 due to the energy transfer from QD to Alexa 568 dye. In comparison, the Fa/Fd ratio gradually decreased from 1 to 0.34 when the plasmid dose was increased from 0.1 to 0.8 μg. Thus, the QD-based FRET assay system provides a simple, rapid and convenient way of detecting specific protease activity in vivo.

Titration of HIV-1Pr inhibitors using the QD-protein-Alexa assay system

To evaluate usage of the FRET module for screening of HIV-1 Pr inhibitors in a cell based platform, similar *in vivo* assays were repeated in the presence of several known HIV-1 Pr inhibitors (10 nM-10 μM) such as Saquinavir, Nelfinavir, Atazanavir sulfate (AZT), Amprenavir and Ritonavir. As shown in Figure 3.6 A, Saquinavir induced a dose-dependent decrease in the number of cells showing an increase in the QD signal. At the highest inhibitor dosage of 10 μM, which has been shown to completely inhibit HIV-1 Pr activity, the resulting merged image was virtually the same to that obtained with untransfected cells. It is clear that proteolysis was inhibited by Saquinavir and the disruption in FRET was ascribable to the intracllular HIV-1 protease activity. The inhibition effect of Saquinavir can be much more clearly demonstrated by quantifying the QD and Alexa signals using the Image-Pro PLUS software. The total QD fluorescence (Fd) intensity and Alexa fluorescence (Fa) intensity within each well of control (untransfected), transfected and with the different dosages of Saquinavir was quantified using Image-Pro PLUS analysis software. The Fa/Fd for each set of images were then normalized to $(Fa/Fd)_0$, which is the value of Fa/Fd in the control cells. As shown in

Figure 3.6 B, when the Fa/Fd ratio was plotted, in the untransfected cells the ratio was 1 due to the energy transfer from QD to Alexa 568 dye. A similar Fa/Fd ratio was detected for cells treated with 10 μM Saquinavir. In comparison, the Fa/Fd ratio gradually decreased from 1 to 0.65 when the Saquinavir dose was reduced from 10 to 0 μM. Taken together these results clearly indicate that the newly reported in vivo FRET screening assay based on the protein module can detect a large dynamic range of inhibition and offer excellent sensitivity. Similar inhibitory effects were found with other inhibitors (Figures 3.7- 3.10 A and B). In case of Nelfinavir and AZT, the highest dosage used was 1μM, as it became toxic beyond that dosage.

The Fa/Fd ratio of each inhibitor was used to calculate the percent inhibition by using the equation: (Inhibitor treated- Untreated)/ (Untransfected- Untreated)*100. As shown in Figure 3.11, the dose response curve of the different inhibitors had a similar trend and the IC-50 of each inhibitor was determined. Except for Saquinavir, the IC-50 of the different inhibitors was 10 nM. More interestingly, the QD based assay was able to detect the differences in the inhibition efficiencies at the lower dosages of the inhibitors (Figure 3.12) and thus can be used to screen novel inhibitors of different efficiency. Thus, we can conclude that our QD based probes can be used for rapid and sensitive screening of new HIV-1 protease inhibitors.

Discussion

A QD based FRET assay system for screening HIV-1 PR inhibitors in a cell based platform was established in this study. The cornerstone of this method was the use of a genetically programmable protein module harboring different functional domains for rapid expression, purification, conjugation and delivery of the protein containing the protease cleavage sequence into the mammalian cells. In this assay system protease cleavage sequence was used as the linker between QD545 and Alexa 568 maleimide to enable the energy transfer (FRET) from QD to the dye. The use of QDs is particularly useful in vivo studies as it is resistant to photodegradation and thus can be used to take microscopic images with prolonged exposure times. Moreover, the QDs provide a platform for assembling several peptide molecules and thus enable a sensitive detection of protease activity in-vivo, as cleavage of a small number of peptides causes a large detectable change in FRET efficiency. Moreover, the ratiometric changes of the two fluorophores provide a more reliable signal. Our FRET based assay provides specificity, as the disruption in FRET signals occur only in presence of the specific active protease in the cells while in the absence of the protease FRET is being maintained in the cells. Thus, quantification of the changes in FRET signal can be directly correlated to the amount of protease present in the cells.

The QD based FRET assay system offers several distinct advantages over the broad array of existing screening assays for HIV-1 protease activity. Most commonly, assays to detect HIV-1 PR activity and its inhibitor screening are done in an in-vitro

setting which is not suitable to monitor the cytotoxicity or transport efficiency of the inhibitors. Furthermore, the activity of the protease is tested under non-physiologic conditions that may modify the catalytic properties of the enzyme. Most in-vivo assays are based on the introduction of the protease cleavage sites into selectable markers such as β-galactosidase (Baum et al., 1990), tetracycline resistance protein (Block, T. M., and R. H. Grafstrom 1990), thymidylate synthase (Kupiec et al., 1996), galactokinase (Stebbins et al., 1996) transcription factors of *Saccharomyces cerevisiae* (Murray et al., 1993), the cI repressor of bacteriophage λ (Sices, H. J., and T. M. Kristie, 1998) and are conducted mainly in yeast or bacterial cells and thus do not provide the appropriate environment for screening HIV-1 PR inhibitors. While several mammalian cell based assays to detect HIV-1 PR activity have the limitation of not being suitable for a high throughput screening set up. In this context, our assay system is suitable for both monitoring the protease activity and its inhibitor in an appropriate cellular environment as well as is suitable for a high throughput screening format.

The most important aspect of our work relates to the analysis of drug resistant HIV-1 protease variants and identification of novel inhibitors. Treatment with protease inhibitor results in accumulation of multiple mutations not only in the active site of the protease but also in regions located distant from the active sites. Phenotypic assays are currently the only way to directly determine resistance and give a therapeutic adjustment, since they measure susceptibility of the actual viral strains to antiretrovirals (Nijhuis et al., 1997). In this situation of rapidly mutating HIV-1 strains, a simple addition of a membrane-diffusible and non-toxic substrate to the cells is highly useful as compared to

generation of stable cell lines harboring the cleavage sequences. Specifically without a major redesign, by making use of the genetically engineered protein module the cleavage sequences can be easily changed to the mutated sequences as found in the drug resistant variants and can be used to detect the cleavage efficiency of the protease. Moreover, with the use of the plasmid expressing the HIV-1 protease, it can be easily envisioned to do the mutagenesis of the wild type protease to mimic the drug resistant strains and then several permutation and combination of substrate and protease can be carried out for screening novel inhibitors. Thus, the QD-based FRET assay system represents a step toward the development of a rapid, convenient and sensitive system for analysis of viral resistance in AIDS patients. We therefore anticipate that the QD-based FRET assay system could become a major tool in the identification of candidate HIV-1 PR inhibitors.

It seems reasonable to assume that the strategy of putting a protease cleavage sequence between a QD and Alexa dye could be applied to other viral proteases as the protease cleavage sequence can be easily changed according to the specific target protease under study. Thus, the QD based FRET assay system can be easily adapted to screen inhibitors for other viral proteases. Further, this new approach can be extended to screen inhibitors for proteases which get overexpressed in certain disease conditions like cancers and require monitoring the inhibitory effects of drugs in human cells.

Acknowledgement

The following reagent was obtained through the NIH AIDS Research and Reference Reagent Program, Division of AIDS, NIAID, NIH: pNL4-3.HSA.R-E- from Dr. Nathaniel Landau.

References

Baum, E. Z., G. A. Bebernitz, and Y. Gluzman. 1990. b-Galactosidase containing a human immunodeficiency virus protease cleavage site is cleaved and inactivated by human immunodeficiency virus protease. Proc. Natl. Acad. Sci. USA **87:**10023–10027

Berkhout, B. 1999. HIV-1 evolution under pressure of protease inhibitors: climbing the stairs of viral fitness. J. Biomed. Sci. **6**:298-305.

Block, T. M., and R. H. Grafstrom. 1990. Novel bacteriological assay for detection of potential antiviral agents. Antimicrob. Agents Chemother. **34:**2337–2341.

Clapp, A.R., Goldman, E.R., Mattoussi, H. 2006. Capping of CdSe-ZnS quantum dots with DHLA and subsequent conjugation with proteins. Nature Protocols 1: 1258-1266.

Connor RI, Chen BK, Choe S, Landau NR. 1995. Vpr is required for efficient replication of human immunodeficiency virus type-1 in mononuclear phagocytes. *Virology* **206**:935-944.

for rapid phenotyping of HIV. Curr. Opin. Infect. Dis. **10:**475–479.

Gupta, B., Levchenko, T.S., Torchilin, V.P. 2005. Intracellular delivery of large molecules and small particles by cell-penetrating proteins and peptides. Advanced Drug Delivery Reviews **57**: 637– 651.

He J, Choe S, Walker R, Di Marzio P, Morgan DO, Landau NR. 1995. Human immunodeficiency virus type 1 viral protein R (Vpr) arrests cells in the G2 phase of the cell cycle by inhibiting p34cdc2 activity. *J Virol* **69**:6705-6711.

Heim, R., Tsien, R.Y. 1996. Engineering green fluorescent protein for improved brightness, longer wavelengths and fluorescence resonance energy transfer. Curr. Biol. **6**: 178-182.

Kim J.-Y., S. O'Malley, A. Mulchandani and W. Chen. 2005**.** Genetically engineered elastin-protein A fusion as a universal platform for homogeneous, phase-separation immunoassay**.** Analytical Chemistry**.77**:2318-2322

Kupiec, J. J., S. Hazebrouck, T. Leste-Lasserre, and P. Sonigo. 1996. Conversion of thymidylate synthase into an HIV protease substrate. J. Biol. Chem. **271:**18465–18470.

Lao, U.L., Chen, A., Matsumoto, M.R., Mulchandani, A., Chen, W. 2007. Cadmium removal from contaminant soil by thermally responsive elastin (ELPEC20) Biopolymers. Biotechnol. Bioeng. **98**: 349-355

Lewin, M., Carlesso, N., Tung, C., Tang, X., Cory, D., Scadden, D.T., Weissleder, R. 2000**.** Tat peptide-derivatized magnetic nanoparticles allow in vivo tracking and recovery of progenitor cells. Nature Biotechnology **18:** 410-414.

Massodi, I., Bidwell, G.L. III, Raucher, D. 2005. Evaluation of cell penetrating peptides fused to elastin-like polypeptide for drug delivery. J. Control. Release 108: 396-408.

Medintz, I.G., Clapp, A.R., Brunel, F.M., Tiefenbrunn, T., Uyeda, H.T., Chang, E.L., Deschamps, J.R., Dawson, P.E., Mattoussi, H. 2006. Proteolytic activity monitored by fluorescence resonance energy transfer through quantum-dot–peptide conjugates. Nature Materials **5**: 581-589.

Murray, M. G., W. Hung, I. Sadowski, and B. Das Mahapatra. 1993. Inactivation of a yeast transactivator by the fused HIV-1 proteinase: a simple assay for inhibitors of the viral enzyme activity. Gene **134:**123–128

Neurath, H. 1999. Proteolytic enzymes, past and future. Proc Natl Acad Sci USA.**96**:10962-10963.

Nijhuis, M., R. Schuurman, and C. A. B. Boucher. 1997. Homologous recombination for rapid phenotyping of HIV. Curr. Opin. Infect. Dis. **10:**475-479

Patick, A and K. Potts. 1998. Protease inhibitor as antiviral agents. Clinical Microbiol. Rev.**11**:614-627.

Sices, H. J., and T. M. Kristie. 1998. A genetic screen for the isolation and characterization of site-specific proteases. Proc. Natl. Acad. Sci. USA **95:**2828–2833.

Stebbins, J., I. C. Deckman, S. B. Richardson, and C. Debouck. 1996. A heterologous substrate assay for the HIV-1 protease engineered in *Escherichia coli*. Anal. Biochem. **242:**90–94.

Urry, D.W. 1997. Physical Chemistry of biological free energy transduction as demonstrated by elastic protein-based polymers. Journal of Physical Chemistry B. **101**:11007-11028

Vickrey, J., B. Logsdon, G. Proteasa, S. Plamer, M. Winters, T. Merigan, and L. Kovari. 2003. HIV-1 protease variants from 100-fold drug resistant clinical isolates: expression, purification, and crystallization. Protein Expression and Purification. 28:165-172.

Vihinen, P., Ala-Aho,R, Kahari, V.M .2005. Matrix metalloproteinases as therapeutic targets in Cancer. Curr. Cancer Drug Targets. **5**:203-220.

Zhang, B. 2004. Design of FRET-based GFP probes for detection of protease inhibitors Biochemical and Biophysical Research Communications **323**: 674-678.

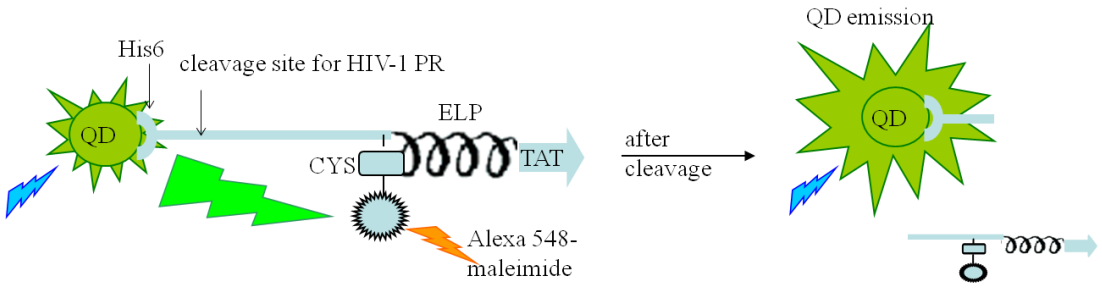

Scheme 3.1: Schematic representation of the self assembled QD-peptide nanoprobe harboring engineered protein module H- MA/CA-ET. H- MA/CA-ET contains hexahistidine, HIV-1 PR cleavage sequence (MA/CA), cysteine residue for dye incorporation, ELP for thermal purification and cell penetrating TAT peptide. Dye labelled modular peptides containing appropriate cleavage sequences are self-assembled onto the QDs. In this design, the QD photoluminescence (PL) is quenched by the fluorescent dye due to fluorescence resonance energy transfer (FRET). Presence of active proteases disrupts FRET resulting in an increased QD PL thus enabling a simple activity assay.

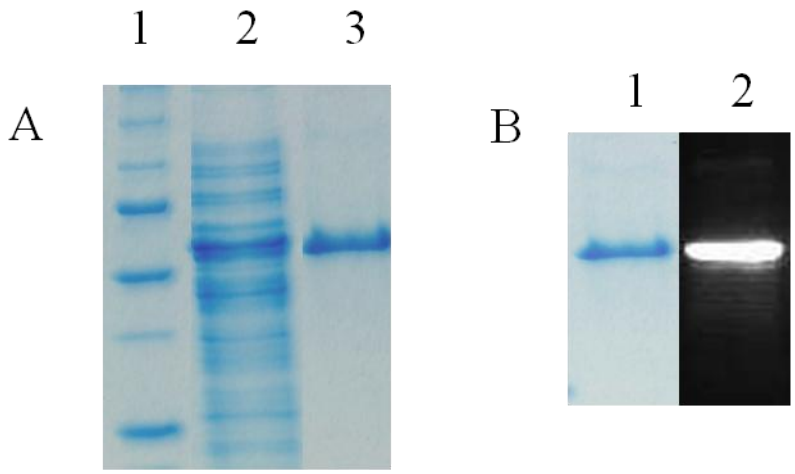

Figure 3.1: (A) SDS-PAGE analysis of purified protein module. Lane 1: protein size marker, Lane 2: cell lysate, Lane 3: purified protein module. **(B)** Conjugation of protein module with Alexa 568 maleimide. Lane 1: Protein module conjugated with Alexa Lane 2: Protein module conjugated with Alexa visualized under UV-lamp

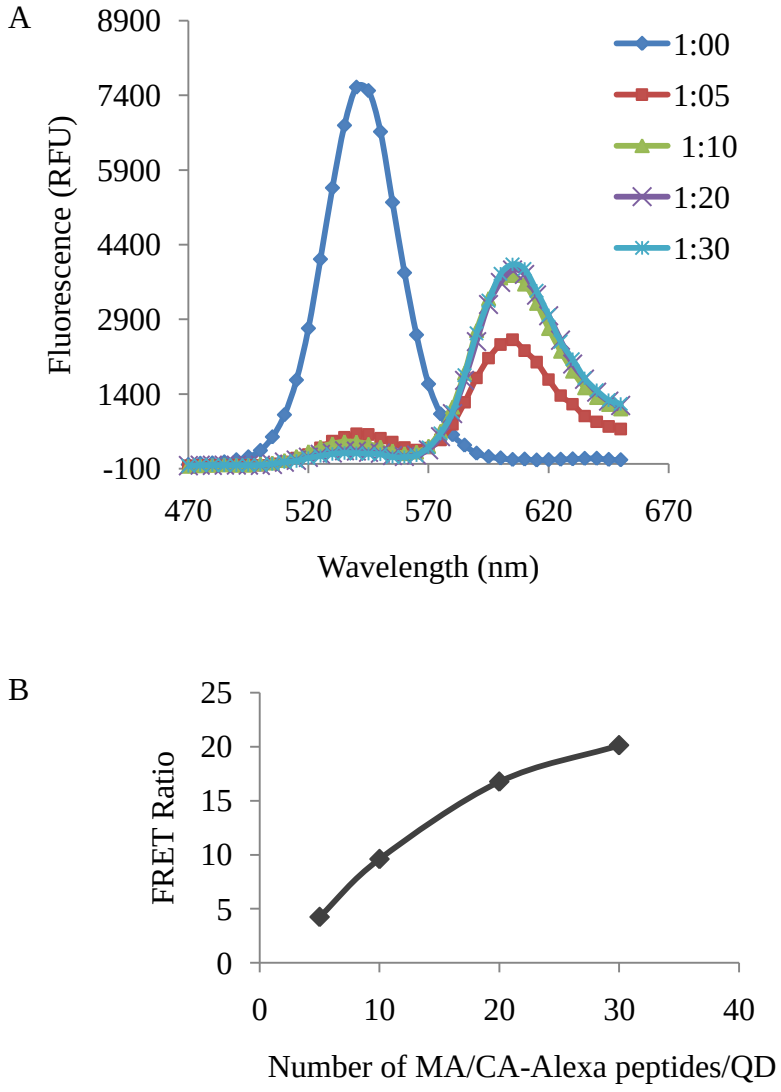

Figure 3.2 A: Fluorescence emission spectra of QD-MA/CA-Alexa assembly at the various QD: Alexa ratios. Excitation is 435 nm. **(B).** FRET efficiency of the different QD-MA/CA-Alexa ratio conjugates

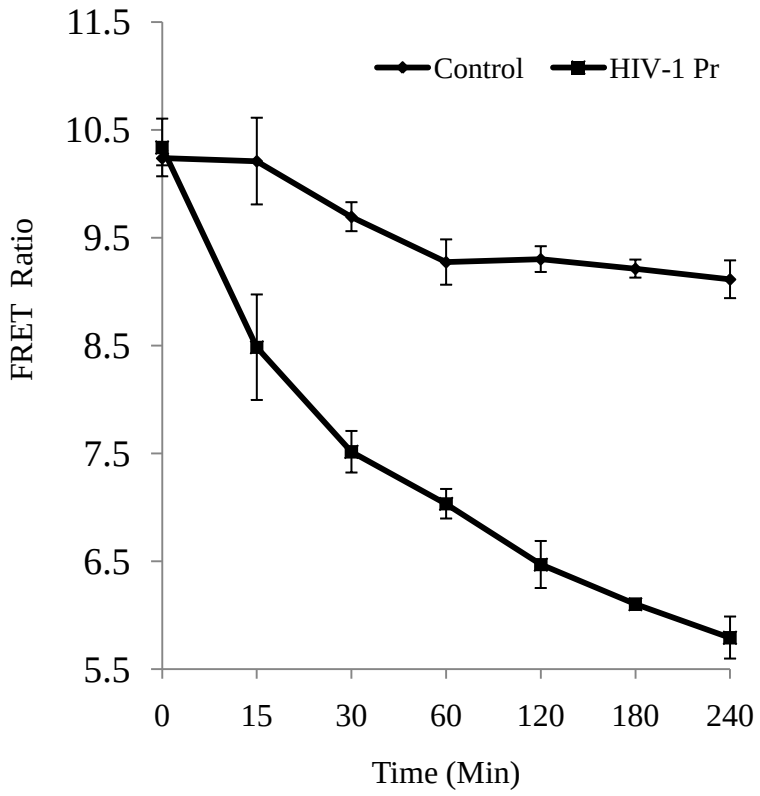

Figure 3.3: Detection of HIV-1 PR activity by nanoprobe QD-MA/CA-Alexa. Time dependent measurements of the changes in Fa/Fd ratio of QD-MA/CA-Alexa based probes in the presence and absence of 500 nM of HIV-1 PR was plotted. The decrease in Fa/Fd ratio with time in the presence of HIV-1 PR indicates proteolytic cleavage of MA/CA by HIV-1 PR. The error bars indicate the standard deviation from 3 independent experiments.

QD FILTER EX 435 EM 535

FRET FILTER EX 435 EM 610

MERGED IMAGE

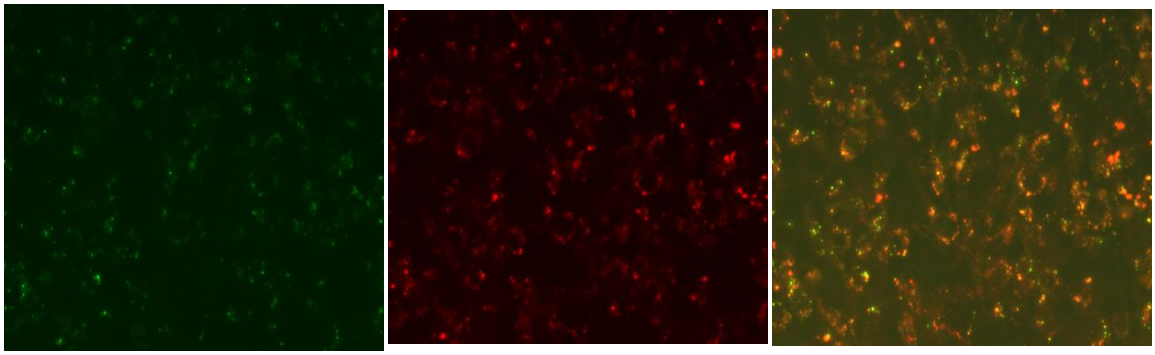

DIC

MERGED COMPOSITE

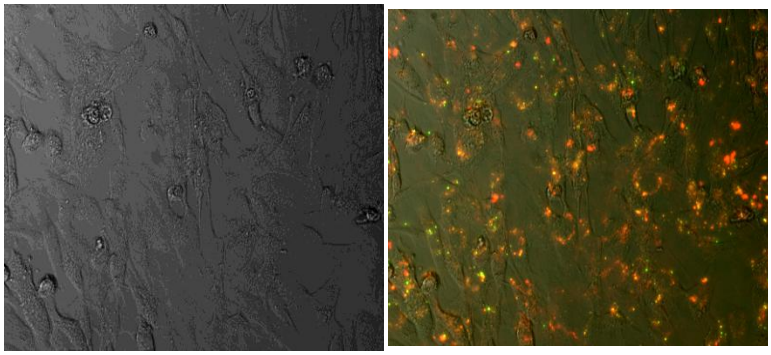

Figure 3.4: Cellular uptake of QD-MA/CA-Alexa probes. Representative images of HeLa cells incubated for 2 hour with 150 nM of self assembled QD-MA/CA-Alexa probes. The cells were visualized with a fluorescence microscope at 435 ex/ 535 em for QD and 435 ex/ 610 em for FRET. The images obtained using QD filter and FRET filter sets were merged. The cells were also observed with DIC filter. The DIC images were merged with merged fluorescent image to obtain corresponding merged composite fluorescent images.

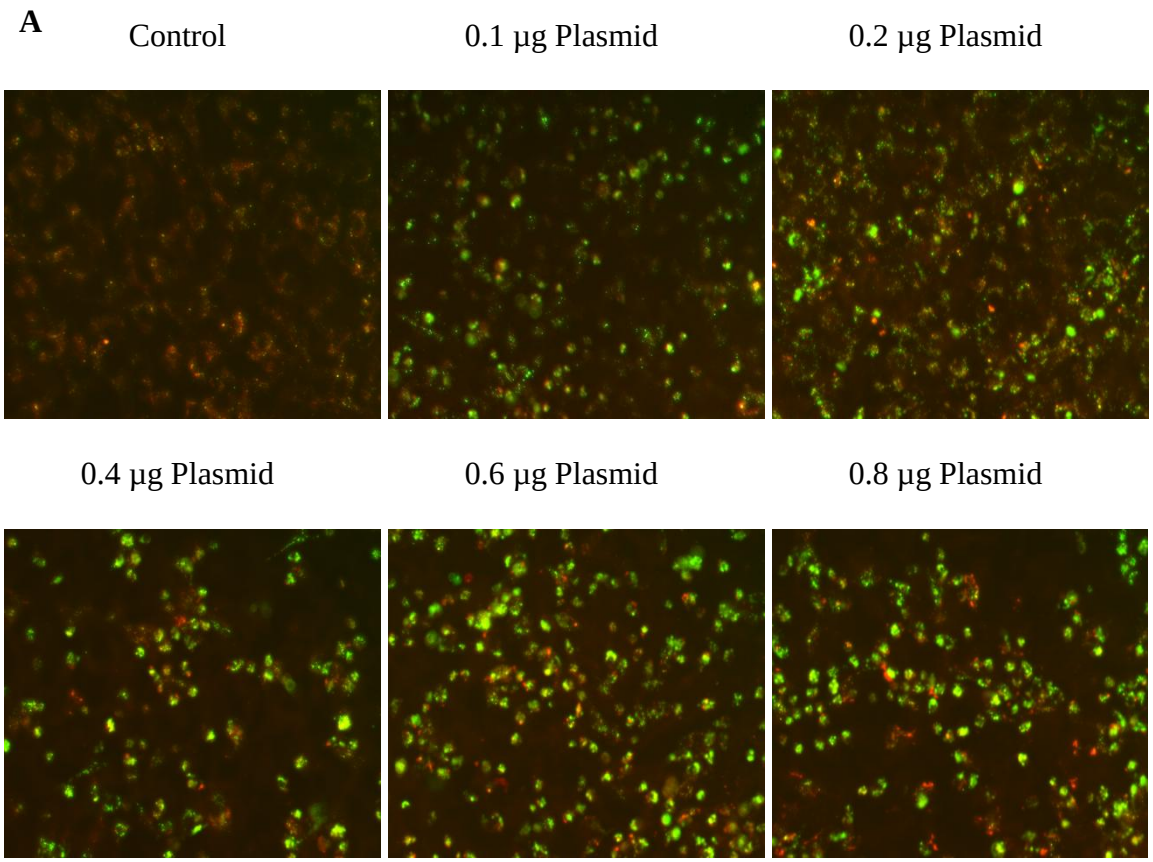

Figure 3.5 (A): Detection of HIV-1 PR activity in HeLa cells using QD based FRET assay system. QD-MA/CA-Alexa probes were delivered in HeLa cells. HeLa cells containing the probes were transfected with increasing concentration of plasmid pNL4.3 HSA R^-E^- expressing the HIV-Provirus. 18 hours post-transfection cells were observed under fluorescence microscope at 435 ex/ 535 em for QD and 435 ex/ 610 em for FRET. The images obtained using QD filter and FRET filter sets were merged. Only merged representative fluorescent images are shown for control (untransfected) and each dosage of plasmid. The increased QD fluorescence in the transfected cells was attributed to proteolytic cleavage of the MA/CA peptides by HIV-1 PR, which resulted in marked reduction in FRET efficiency between QD and Alexa dye. The increase in number of cells showing increased QD fluorescence correlates well with the plasmid dosages.

B

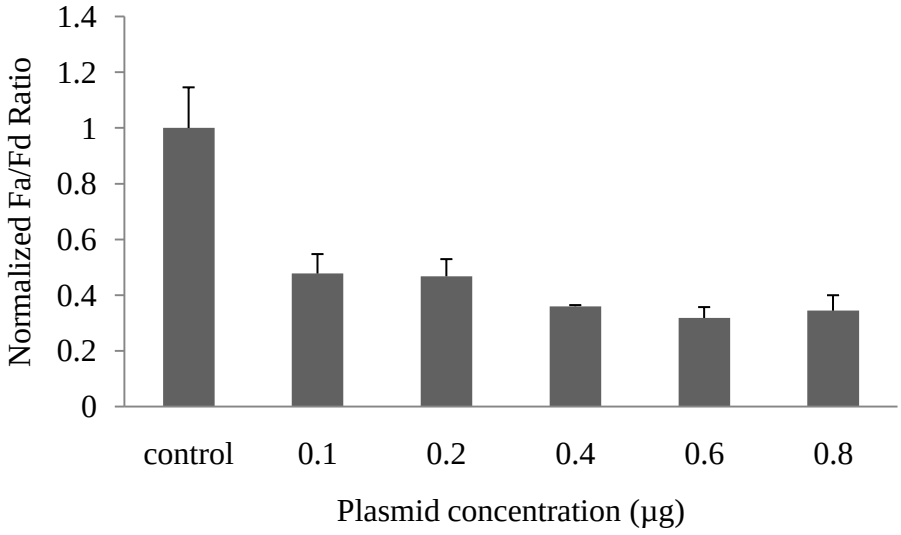

Figure 3.5 (**B**): Quantitative Analysis of the images. The total fluorescence intensity of images obtained using QD filter (Fd) and FRET filter (Fa) for control (untransfected), transfected and with the different dosages of plasmid were quantified using Image-Pro PLUS software. The Fa/Fd for each set of images were then normalized to $(Fa/Fd)_0$, which is the value of Fa/Fd in the control cells. Data are means ± standard deviation from three experiments.

A

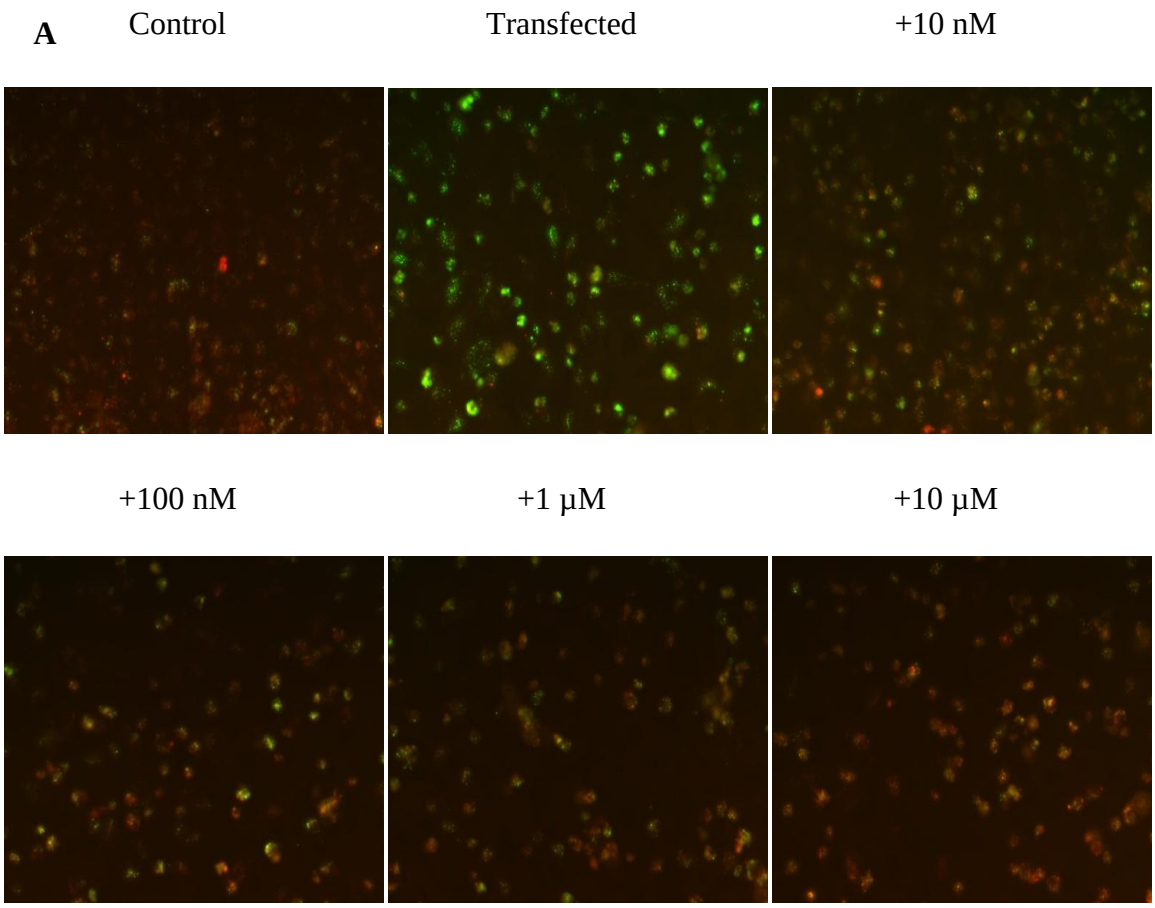

Continued

B

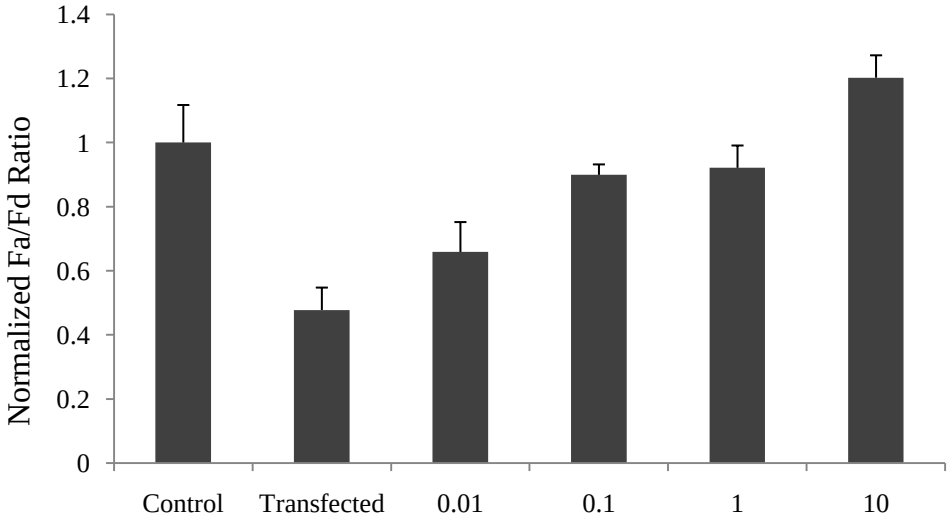

Figure 3.6: (**A**) Monitoring the inhibition efficiency of HIV-1 protease inhibitor-Saquinavir using the QD-MA/CA-Alexa based assay system. QD-MA/CA-Alexa probes were delivered in HeLa cells. HeLa cells containing the probes were transfected with plasmid pNL4.3-HSA-R^-E^- expressing the HIV-Provirus and were treated with increasing concentration (0.01-10 μM) of Saquinavir. 18 hours post-transfection cells were observed under fluorescence microscope at 435 ex/ 535 em for QD and 435 ex/ 610 em for FRET. The images obtained using QD filter and FRET filter sets were merged. Only merged representative fluorescent images are shown for each dosage of Saquinavir. (**B**) Quantitative Analysis of the images. The total fluorescence intensity of images obtained using QD filter (Fd) and FRET filter (Fa) for control (untransfected), transfected and with the different dosages of Saquinavir were quantified using Image-Pro PLUS software. The Fa/Fd for each set of images were then normalized to $(Fa/Fd)_0$, which is the value of Fa/Fd in the control cells. Data are means ± standard deviation from three experiments.

A

Control Transfected +10 nM

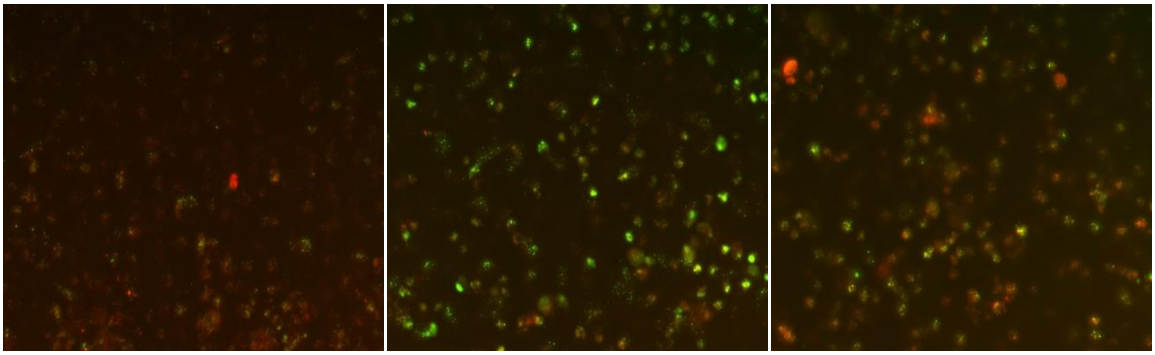

+100 nM +1 µM

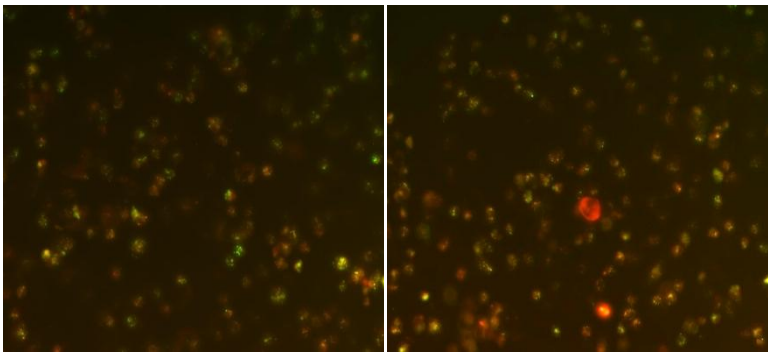

Continued

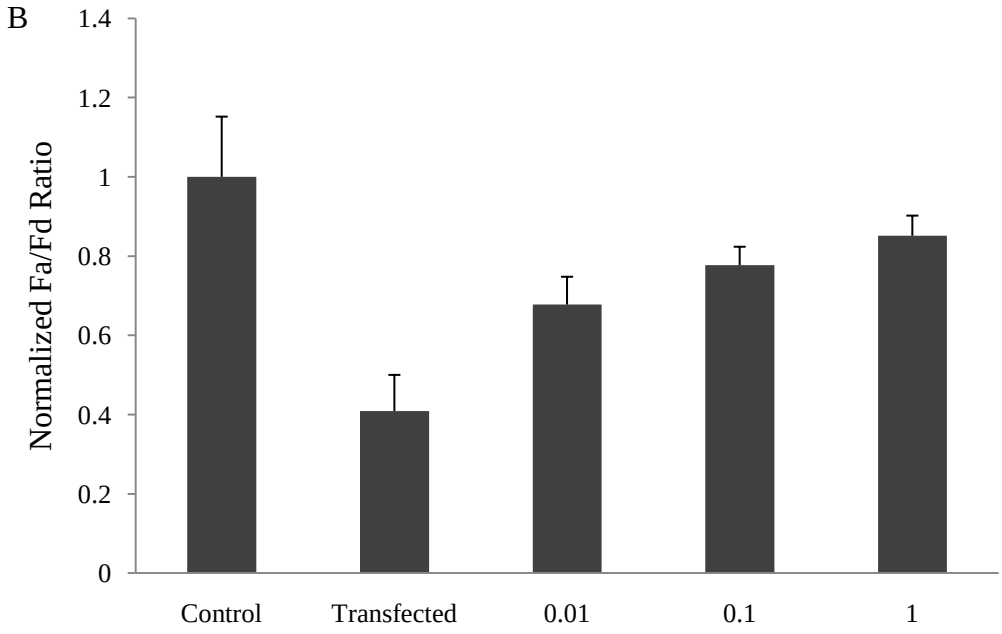

Figure 3.7: (**A**) Monitoring the inhibition efficiency of HIV-1 protease inhibitor-Nelfinavir using the QD-MA/CA-Alexa based assay system. QD-MA/CA-Alexa probes were delivered in HeLa cells. HeLa cells containing the probes were transfected with plasmid pNL4.3-HSA-R$^-$E$^-$ expressing the HIV-Provirus and were treated with increasing concentration (0.01-10 µM) of Nelfinavir. 18 hours post-transfection cells were observed under fluorescence microscope at 435 ex/ 535 em for QD and 435 ex/ 610 em for FRET. The images obtained using QD filter and FRET filter sets were merged. Only merged representative fluorescent images are shown for each dosage of Nelfinavir. (**B**) Quantitative Analysis of the images. The total fluorescence intensity of images obtained using QD filter (Fd) and FRET filter (Fa) for control (untransfected), transfected and with the different dosages of Nelfinavir were quantified using Image-Pro PLUS software. The Fa/Fd for each set of images were then normalized to $(Fa/Fd)_0$, which is the value of Fa/Fd in the control cells. Data are means ± standard deviation from three experiments.

A

Control Transfected +10 nM

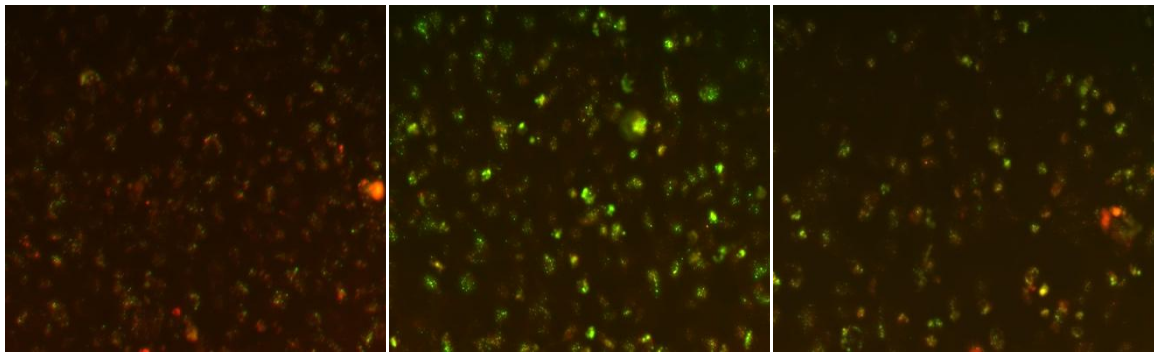

+100 nM +1 µM

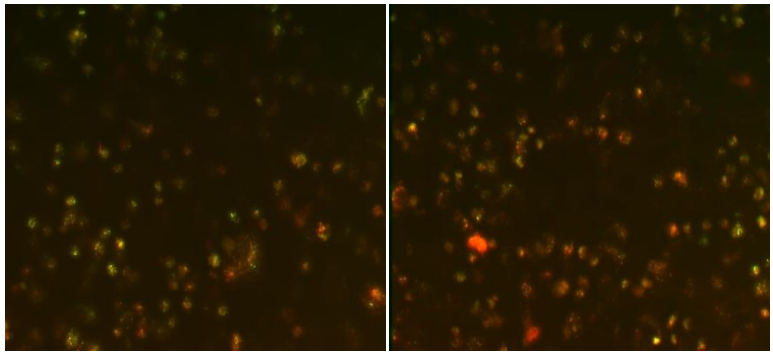

Continued

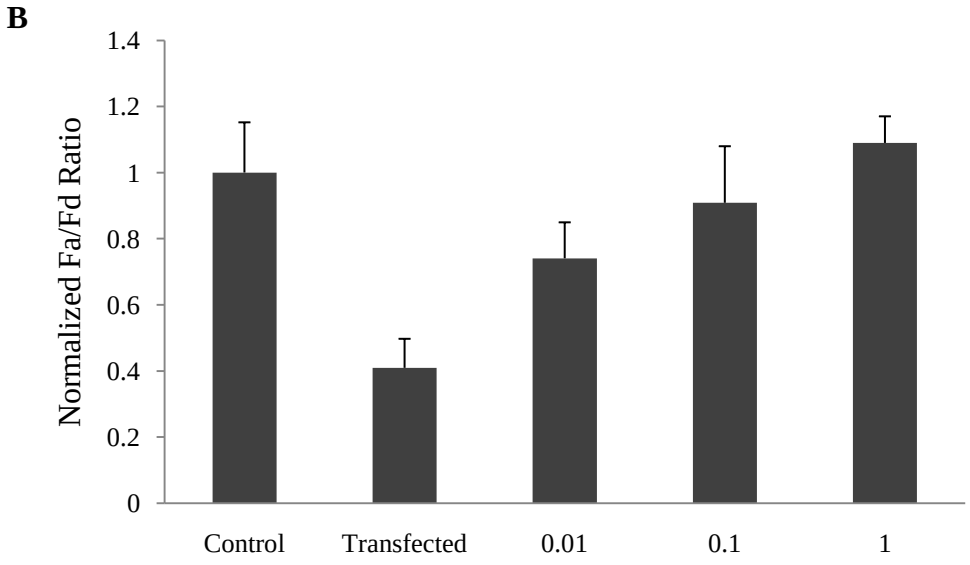

Figure 3.8: (**A**) Monitoring the inhibition efficiency of HIV-1 protease inhibitor-Atazanavir sulfate (AZT) using the QD-MA/CA-Alexa based assay system. QD-MA/CA-Alexa probes were delivered in HeLa cells. HeLa cells containing the probes were transfected with plasmid pNL4.3-HSA-R$^-$E$^-$ expressing the HIV-Provirus and were treated with increasing concentration (0.01-10 µM) of AZT. 18 hours post-transfection cells were observed under fluorescence microscope at 435 ex/ 535 em for QD and 435 ex/ 610 em for FRET. The images obtained using QD filter and FRET filter sets were merged. Only merged representative fluorescent images are shown for each dosage of AZT. (**B**) Quantitative Analysis of the images. The total fluorescence intensity of images obtained using QD filter (Fd) and FRET filter (Fa) for control (untransfected), transfected and with the different dosages of AZT were quantified using Image-Pro PLUS software. The Fa/Fd for each set of images were then normalized to $(Fa/Fd)_0$, which is the value of Fa/Fd in the control cells. Data are means ± standard deviation from three experiments.

A

Control | Transfected | +10 nM

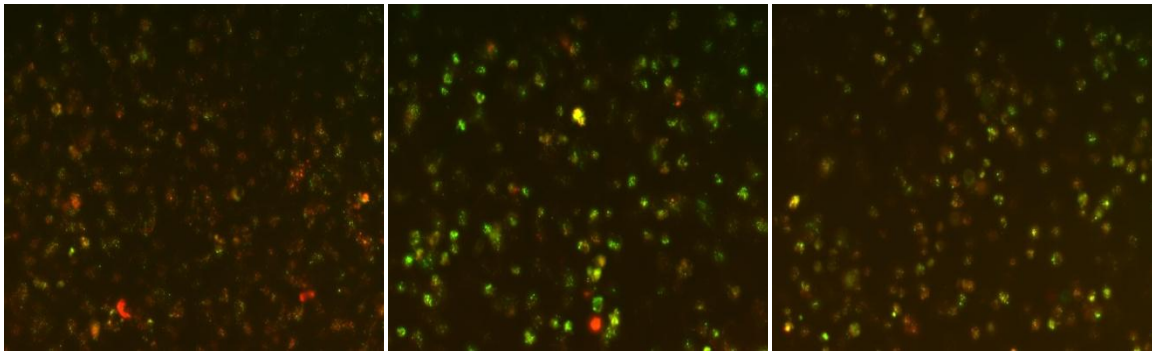

+100 nM | +1 µM | +10 µM

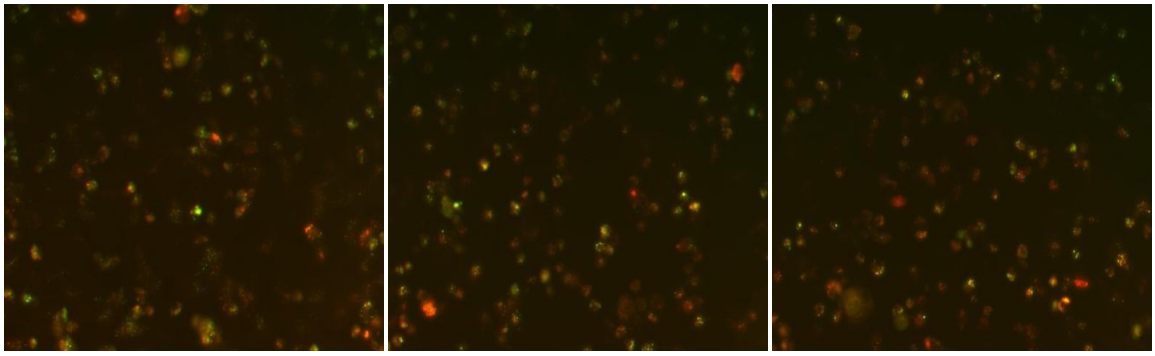

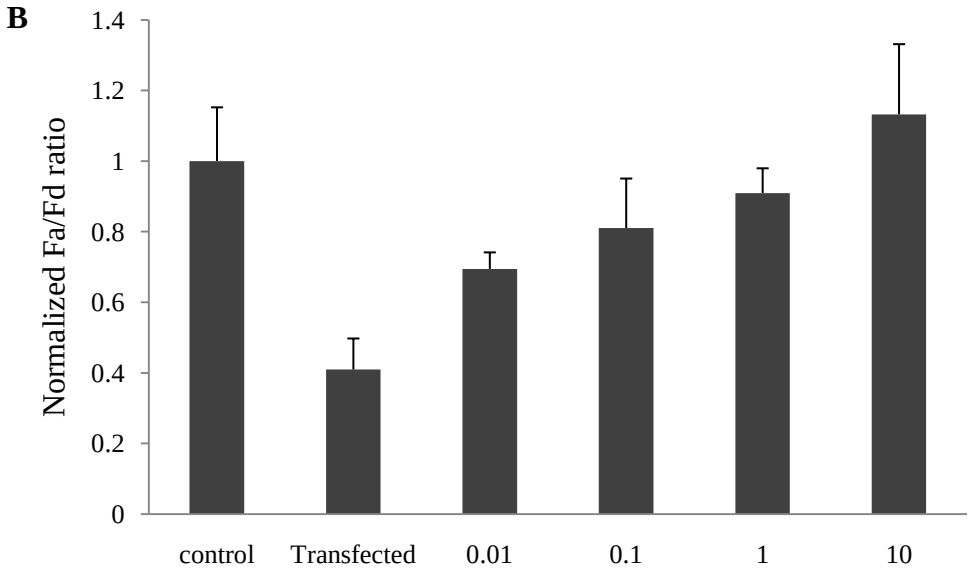

Figure 3.9: (**A**) Monitoring the inhibition efficiency of HIV-1 protease inhibitor-Amprenavir using the QD-MA/CA-Alexa based assay system. QD-MA/CA-Alexa probes were delivered in HeLa cells. HeLa cells containing the probes were transfected with plasmid pNL4.3-HSA-R^-E^- expressing the HIV-Provirus and were treated with increasing concentration (0.01-10 µM) of Amprenavir. 18 hours post-transfection cells were observed under fluorescence microscope at 435 ex/ 535 em for QD and 435 ex/ 610 em for FRET. The images obtained using QD filter and FRET filter sets were merged. Only merged representative fluorescent images are shown for each dosage of Amprenavir. (**B**) Quantitative Analysis of the images. The total fluorescence intensity of images obtained using QD filter (Fd) and FRET filter (Fa) for control (untransfected), transfected and with the different dosages of Amprenavir were quantified using Image-Pro PLUS software. The Fa/Fd for each set of images were then normalized to $(Fa/Fd)_0$, which is the value of Fa/Fd in the control cells. Data are means ± standard deviation from three experiments.

A

Control | Transfected | +10 nM

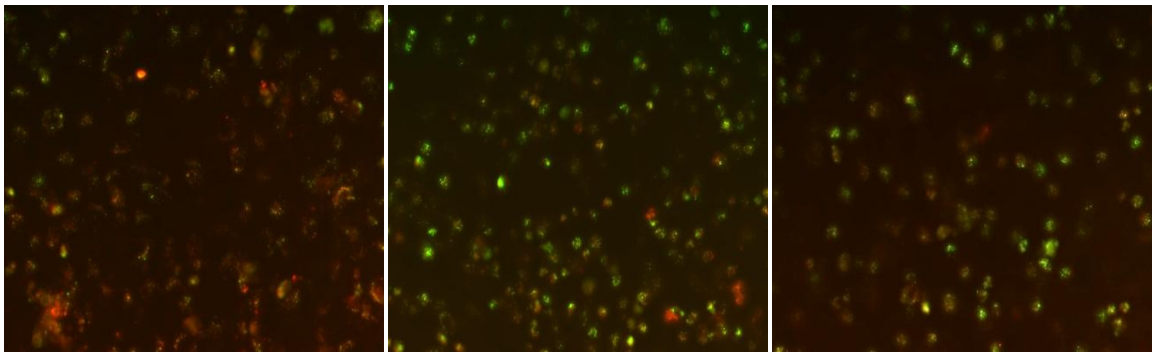

+100 nM | +1 µM | +10 µM

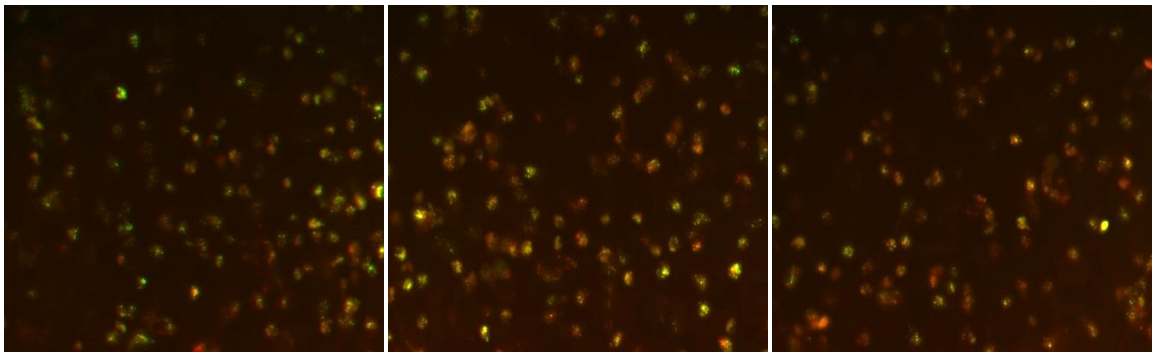

Continued

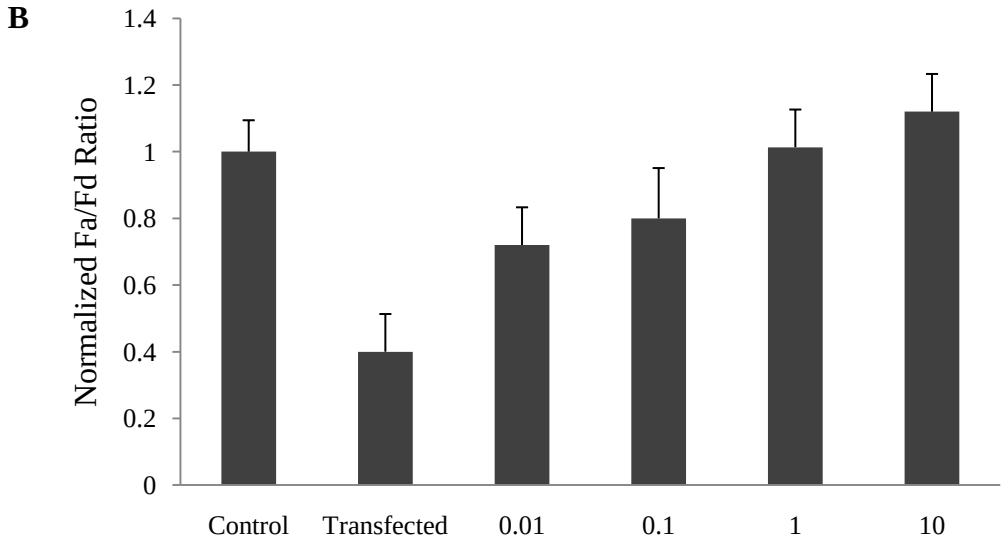

Figure 3.10: (**A**) Monitoring the inhibition efficiency of HIV-1 protease inhibitor-Ritonavir using the QD-MA/CA-Alexa based assay system. QD-MA/CA-Alexa probes were delivered in HeLa cells. HeLa cells containing the probes were transfected with plasmid pNL4.3-HSA-R^-E^- expressing the HIV-Provirus and were treated with increasing concentration (0.01-10 µM) of Ritonavir. 18 hours post-transfection cells were observed under fluorescence microscope at 435 ex/ 535 em for QD and 435 ex/ 610 em for FRET. The images obtained using QD filter and FRET filter sets were merged. Only merged representative fluorescent images are shown for each dosage of Ritonavir. (**B**) Quantitative Analysis of the images. The total fluorescence intensity of images obtained using QD filter (Fd) and FRET filter (Fa) for control (untransfected), transfected and with the different dosages of Ritonavir were quantified using Image-Pro PLUS software. The Fa/Fd for each set of images were then normalized to $(Fa/Fd)_0$, which is the value of Fa/Fd in the control cells. Data are means ± standard deviation from three experiments.

.

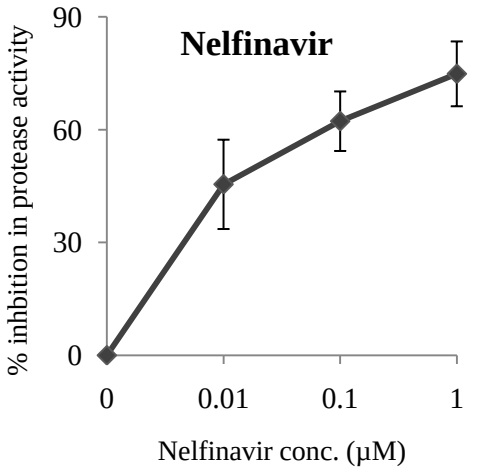
Nelfinavir
% inhbition in protease activity
90
60
30
0
0
0.01
0.1
1
Nelfinavir conc. (µM)

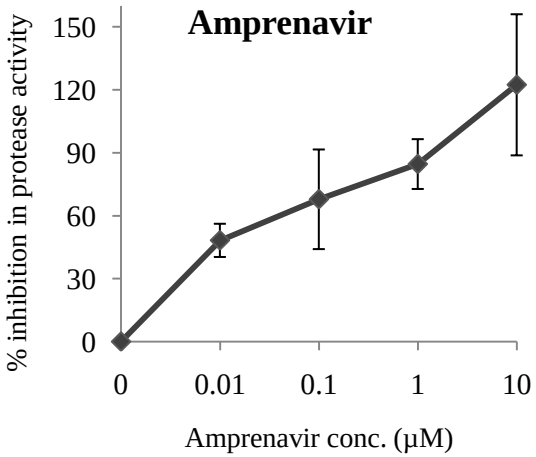
Amprenavir
% inhibition in protease activity
150
120
90
60
30
0
0
0.01
0.1
1
10
Amprenavir conc. (µM)

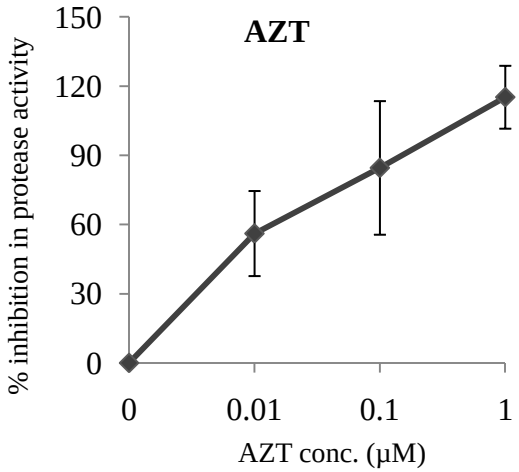
AZT
% inhibition in protease activity
150
120
90
60
30
0
0
0.01
0.1
1
AZT conc. (µM)

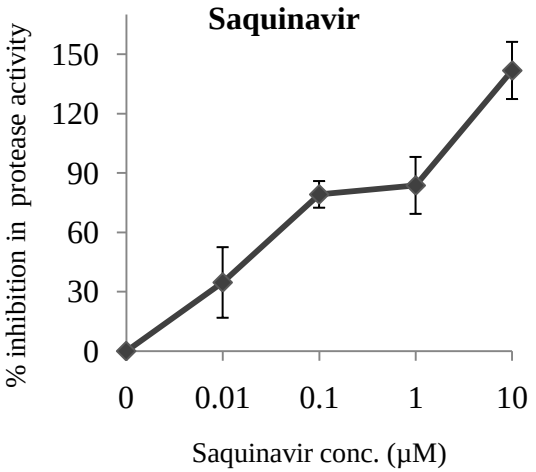
Saquinavir
% inhibition in protease activity
150
120
90
60
30
0
0
0.01
0.1
1
10
Saquinavir conc. (µM)

Continued

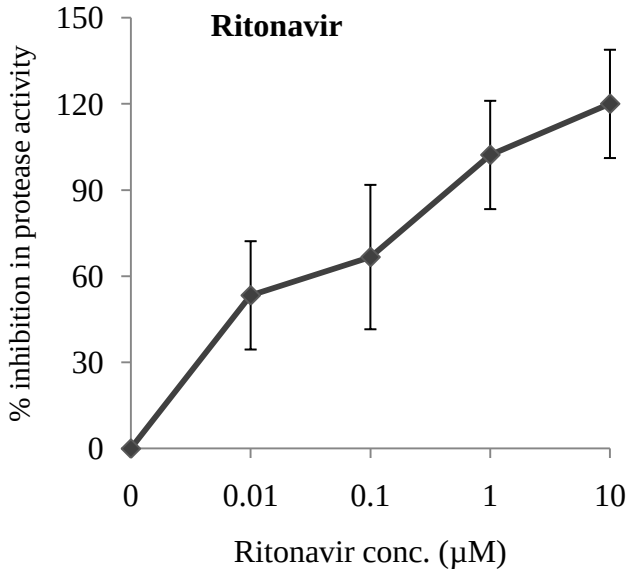

Figure 3.11: Percent inhibition in HIV-1 protease activity with different HIV-1PR inhibitors based on the QD-MA/CA-Alexa assay system. The Fa/Fd ratio of each sample was used to calculate the percent inhibition in protease activity by using the equation; (Inhibitor treated- Untreated)/ (Untransfected- Untreated)*100. Data are means ± standard deviations from three experiments.

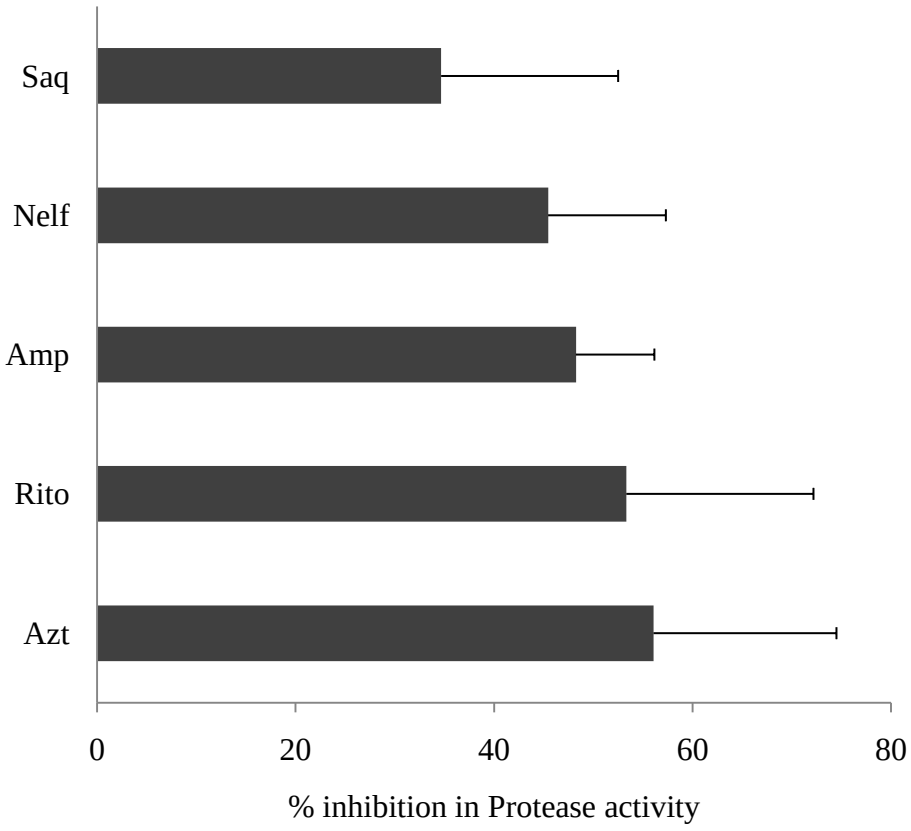

Figure 3.12: Comparative analysis of inhibition efficiency of different HIV-1 protease inhibitors at a concentration of 10 nM. Data are means ± standard deviations from three experiments.

Chapter 4

Novel QD- based bioassay for HIV protease cleavage site specific inhibitor screening using a genetically programmable protein module

Abstract

Human immunodeficiency virus type 1 protease (HIV-1 PR) plays a key role in viral maturation and production of infectious virus particles. It recognizes and cleaves up to 12 different sites in the Gag and Gag-Pol precursor polypeptides, and is thus a major target for anti-HIV agents. However, current problem with antiviral therapy is the acquirement of amino acid substitutions at the different cleavage sites leading to emergence of drug resistant viruses. At present, there are no assays available to identify inhibitors that could block HIV-1 PR activity by selectively inhibiting cleavage at a particular site. Thus, we developed a simple and rapid assay system to screen inhibitors specific to cleavage sites. In order to do so, we have developed a genetically engineered protein module that is designed with: 1) a Quantum Dot (QD) binding moiety containing poly-histidine, 2) a cysteine site for fluorescent dye incorporation based on cysteine-thiol interaction, 3) HIV-1 PR cleavage site, 4) an ELP domain for thermal purification and 5) a flanking TAT peptide sequence for cell penetration. The modular nature of the protein module was exploited for designing two probes containing two different HIV-1 PR cleavage sites. In this design, the QD fluorescence (FL) is quenched by the fluorescent dye due to fluorescence resonance energy transfer (FRET). Cleavage of the sequences by HIV-1 PR resulted in separation of the FRET pair with subsequent increase in QD FL. However, presence of inhibitors specific to the cleavage sites prevented FRET disruption and a reduced QD FL was detected. Thus, the genetically programmable protein module enabled rapid and easy production of different QD-based FRET substrates, to be used for high throughput screening of inhibitors specific to the different cleavage sites.

Introduction

In the human immunodeficiency virus type 1 (HIV-1) structural and enzymatic components are expressed as polyprotein precursors, i.e., Gag ($p55^{gag}$) and Gag-Pol ($p160^{gag\text{-}pol}$) (Wills and craven, 1991), respectively, which assemble into immature virions on the cytoplasmic side of the cell membrane (Go¨ttlinger et al., 1989). The protease encoded by the virus (HIV-1 PR) is part of the $p160^{gag\text{-}pol}$ polyprotein precursor and plays an essential role in the retroviral life cycle for conformational rearrangement of the immature virion and production of infectious virus paticles (Lindsten et al., 2001). The HIV-1 PR belongs to the class of aspartyl PRs (Pearl et al., 1987). During the viral assembly process the HIV-1PR monomer dimerizes to form an active homodimer and catalyzes its own release (Debouck et al,. 1987). For the production of infectious virions, during and after virion budding from the cell membrane, the HIV-1 PR recognizes and cleaves up to 12 sites, each with a different amino acid sequence in the $p55^{gag}$ and $p160^{gag\text{-}pol}$ polyprotein precursors (Pettit et al., 1993) leading to mature Gag (MA, CA and NC; for nomenclature see reference Leis et al., 1988) and Pol (PR, RT, IN, and RNaseH) proteins and condensation of the retroviral core (Kohl et al., 1988 and Peng et al., 1989). Due to the essential role of the HIV-1 PR, it has become an attractive target for development of antiviral agents to treat AIDS. Several potent HIV-1 PR inhibitors have been developed, which are currently in clinical use (Patick et al., 1998 and Deeks et al., 1997). However, one of the emerging problems with antiviral therapy is the emergence of drug resistant variants. Protease inhibitor (PI) –resistant or cross resistant isolates (Bodel et al., 1998 and Condra et al., 1995) with impaired replication or Gag and Gag-Pol

processing ((Mammano et al., 1998 and Zennou et al., 1998) can partially compensate by acquiring amino acid substitutions at Gag cleavage sites in HIV culture (Carrillo et al., 1998 and Doyon et al., 1996) and in vivo (Zhang et al., 1997). In fact, studies have shown that mutations in the HIV-1 PR and at Gag cleavage sites are specifically selected during PI therapy (Côté et al., 2001). Furthermore, small molecule compounds have been identified recently that act on selective HIV-1 protease sites to delay maturation of the precursor Gag protein (Zhou et al., 2004). 3-*O*-{3',3'-dimethylsuccinyl}-betulinic acid (DSB) has been shown to act late in the HIV-1 life cycle to specifically retard cleavage at the CA-p2 junction of Gag by the viral PR without affecting processing at other sites in the Gag (Zhou et al., 2004). Thus, it will be interesting to not only identify antiviral compounds that target PR itself, but to identify small molecules that could block PR cleavage by selectively inhibiting cleavage at a particular site.

The majority of assays available today are based on trans- or autocatalytic cleavage of reporter proteins in bacteria, in yeasts, or in vitro (Baum et al., 1990; Deo et al., 2000; Murray et al., 1993 and Stebbins et al., 1996**)** or on the in vitro hydrolysis of synthetic peptides encompassing the scissile bonds in $p55^{Gag}$ and $p160^{Gag\text{-}Pol}$ (Billich et al., 1990; Matayoshi et al., 1990 and Stebbins et al., 1997). These systems are very sensitive; however, none of them allows probing all the native HIV-1 PR function sites under physiological conditions. To overcome the limitations of determining HIV-1 protease activity in-vitro and to facilitate the drug screening process (Hu et al., 2005), cell-based reporter systems have been developed. A green fluorescent protein (GFP)-PR chimera was developed that can be expressed in mammalian cells, causing minimal toxicity until

autocatalytic cleavage occurs (Lindsten et al., 2001 and Fuse et al., 2006). The reporter becomes toxic upon autocatalytic cleavage of the protease resulting in disappearance of fluorescence providing a simple means of quantifying protease activity. Despite their potential applications, there are inherent difficulties and inconsistency associated with transient transfections. Moreover, in the context of rapidly mutating HIV-1 strains, generating stable cell lines containing the different cleavage site is a time consuming and formidable task. In this context, assay systems that can allow probing of all the native HIV-1 protease cleavage sites to screen for cleavage site specific inhibitors, under physiologic conditions in a high throughput setting is urgently needed.

Thus, in this paper we demonstrate the development of an assay system that can be used to probe all the different cleavage sites of HIV-1 PR and screen inhibitors specific to the cleavage sites in a high throughput way. The goal was achieved by generating a genetically programmable protein module containing the protease cleavage sites as a linker between a donor fluorophore [Quantum dot (QD)] and an acceptor fluorophore (Alexa 568 dye). In this design, the QD photoluminescence is quenched by the fluorescent dye due to fluorescence resonance energy transfer (FRET). However, in the presence of the protease, the cleavage sequence is cleaved resulting in separation of the FRET pair with subsequent increase in QD fluorescence. Thus, the activity of the protease can be detected by measuring the changes in the fluorescence of QD and Alexa dye. Further, this assay system can be used to screen potent cleavage site specific inhibitors. Intracellular delivery of the substrates was facilitated by the use of a flanking TAT peptide (Gupta et al.,2005; Lewin et al., 2000) and the site-specific incorporation of

an acceptor dye was accomplished using a unique cysteine residue. Presence of an elastin domain at the C-terminus of the module enabled the simple purification of the FRET substrate by thermally triggered precipitation (Urry D.W., 1997). Using the two different cleavage sites MA/CA and p6/PR (Leis et al., 1988) of HIV-1 PR as a target, we demonstrate that the new QD FRET probes can be used for probing the different cleavage sites as well as quantitative assessment of site specific inhibitors.

Materials and Methods

Design of constructs

To construct an expression vector for His6-MA/CA-Cys-ELP105K-Tat (H-MA/CA- ET), plasmid p08-ELP105K-EC20 described by Lao et al (Lao 2007) was digested with *Sma*I and *Hin*dIII and a DNA fragment encoding Tat peptide (amino acid sequence: GGTKTGRRRQRRKKRGY) was inserted between the same restriction sites. The resulting plasmid p08-ELP105K-Tat was cut with *Bam*HI and *Nde*I and 1.7 kb fragment was ligated to plasmid pET14 (Novagen, Madison, WI) treated with same enzymes to generate pET-ELP105K-Tat. An artificial gene for hexa-histidines, MA/CA peptide with cysteine was prepared by heating and annealing two oligonucleotides, CATGGGCCATCACCATCACCATCACTCCCAGGTCAGCCAAAATTACCCTATA GTGCAGAACCTGCAGTTCTGCCA and TATGGCAGAA CTGCAGGTTCTGCACTATAGGGTAATTTTGGCTGACCTGGGAGTGATGGTGAT GGTGATGGCC and ligated to the 6.3kb fragment obtained from pET-ELP105K-Tat by digesting with *Nco*I and *Nde*I to create pET-H-MA/CA-ET. The expression vector for His6-p6/PR-Cys-ELP105K-Tat (H- p6/PR-ET) was prepared the same way by using the oligonucleotides CATGGGCCATCATCATCATCATCATGGAACT GTATCCTTTAGCTTCCCTCAGATCACTCTTTGGCAGCGATGCCA and TATGGCATCGCTGCCAAAGAGTGATCTGAGGGAAGCTAAAGGATACAGTTCC ATGATGATGATGATGATGGCC

Expression and purification of peptides

For protein expression, *E.coli* BL-21 (DE3) (Novagen, Madison, WI) transformed with plasmid pET-H-MA/CA-ET or pET- p6/PR -ET was grown in terrific broth media containing 100 μg/ml ampicillin at 37^{o}C until optical density (O.D.) at 600 nm reached 0.5. The flasks were then transferred to 30^{o}C for protein expression. When the O.D. at 600 nm reached 5, cells were harvested by centrifugation, resuspended in 50mM Tris/HCl (pH 8.0) with 0.1M NaCl and 1 mg/ml of lysozyme, and lysed by sonication. Cell debris was removed by centrifugation at 16,000 g for 30 min. Proteins were purified by repeated temperature transition cycle as described previously (Kim et al., 2005). Briefly, for each cycle, NaCl was added to the sample at a final concentration of 2M and the sample was heated to 37^{o}C and centrifuged at 16,000 g at 30^{o}C for 15 min. The pellet containing the proteins were resuspended in ice-cold 50mM Tris/HCl (pH 8.0) with 0.1M NaCl and centrifuged at 16,000 g at 4^{o}C for 15 min to remove undissolved proteins. This temperature transition cycle was repeated once more, and the pellet containing either H-MA/CA-ET or H- p6/PR-ET was finally resuspended in ice cold 50mM Tris/HCl (pH 8.0) with 0.1M NaCl. The purity of the protein was determined by SDS-PAGE electrophoresis.

Conjugation of peptides with fluorescent dye

The labeling of the proteins with thiol reactive dye was performed by modifying the procedure of Massodi *et al*. (Massodi 2005). Purified proteins were resuspended in 50mM potassium phosphate buffer (pH 7) at a final concentration of 40 uM. Tris-(2-

carboxyethyl) phosphine (TCEP) and Alexa 568 maleimide (Invitrogen, Carlsbad, CA), thiol reactive dye, were added to a 10-fold and 2-fold molar excess, respectively. The mixture was incubated with end-over-end rotation for 2hr at room temperature in the dark. The reaction was stopped and the unreacted dyes were removed by two or three thermal precipitation cycles as described in the protein purification procedure. The degree of labeling of the protein was calculated using the following formula:

$$\frac{A_x}{\epsilon} \times \frac{\text{MW of protein}}{\text{mg protein/mL}} = \frac{\text{moles of dye}}{\text{moles of protein}}$$

Where Ax is the absorbance value of the dye at the absorption maximum wavelength and Ɛ is the molar extinction coefficient of the dye.

Assembly and characterization of QD-protein-dye conjugates

The conjugation of QDs to fluorophore-labeled protein module to complete the FRET pair was adapted from Clapp et al., 2006. To start with, the TOPO-capped CdSe/ZnS QDs with 545 nm of emission maximum (Evident Tech. Inc) were made water-soluble QDs, by doing a cap exchange with dihydrolipoic acid (DHLA) according to the protocol by Clapp et al., 2006. 300 nM of DHLA-capped QDs were added to Alexa568-labeled proteins, resuspended in 10mM HEPES buffer (pH 8.2) at 1:3 to 1:10 ratio of QDs to protein module. The samples were mixed thoroughly and incubated at room temperature for overnight. After conjugation, the FRET efficiency was measured

using a fluorometer by exciting at 430 nm and the spectrum was recorded from 475 nm to 650 nm.

Cell culture

HeLa cells obtained from American Type Culture Collection were grown in 400 mL of 1× autoclavable minimum essential medium (AMEM; Irvine Scientific) containing 1% of 7.5% $NaHCO_3$, 2% of 1 M Hepes, 1% of nonessential amino acids (NEAA; HyClone, Thermo Scientific), 100 µg/mL of penicillin and 100 U/mL of streptomycin (HyClone, Thermo Scientific), 1% of 200 mM L-glutamine in 0.85% NaCl (HyClone, Thermo Scientific), and 10% of FBS (Sigma–Aldrich) at 37°C in a 5% CO_2 atmosphere.

Intracellular delivery of probes, Transfection and Titration of inhibitors

HeLa cells were seeded into 96 well clear bottom black wall side plates (Nunc Scientific) at 37°C in 5% CO_2 in air and cultured to >90% confluence. After removing the incubation medium, the cell monolayer was washed twice with 1× PBS. Cells were then incubated at 37°C in the dark with 1× Leibovitz L-15 medium (Invitrogen) containing QD- MA/CA- Alexa 568 at QD concentrations of 150 nM. 2 hrs after incubation with the probes, the cells were washed with PBS and observed under Zeiss Axiovert 40 CFL inverted fluorescence microscope. To introduce the HIV-1 PR, HeLa cells containing the probes were transfected using Lipofectamine^{TM} 2000 transfection reagent (Invitrogen) with the plasmid pNL4-3.HSA.R$^-$E$^-$ (Connor et al., 1995; He et al., 1995) expressing the entire HIV-1 genome. After 6 h, the medium was changed to the normal growth medium and cells were propagated for another 18 hrs and were then

observed under fluorescent microscope. In order to test the activity of the HIV-1 PR inhibitors, after removal of the transfection reagent, the cells were incubated with the growth medium containing an increasing concentration (0.01-10 μM) of the inhibitor Indinavir sulfate (NIH).

Fluorescence Microscopy and image processing

Cell imaging was performed on a Zeiss Axiovert 40 CFL inverted microscope equipped with a 12-V, 35-W halogen lamp (for the phase-contrast images) and an HBO 50 W/AC mercury lamp (for the fluorescence images). The objectives used were a 5×/0.12 A-Plan, a 10×/0.25 A-Plan, a 20×/0.50 EC Plan-NEOFLUAR, and a 40×/0.50 LD A-Plan (Zeiss). Fluorescent probes were detected by using two different filter sets; QD filter consisting of a D436-nm exciter, a D535/50-nm emitter, and a 475 nm-dichroic long pass beam splitter (Chroma Technology) and FRET filter consisting of a D436-nm exciter, a D610/50-nm emitter, and a 475 nm-dichroic long pass beam splitter. Images were acquired by using a ProgRes MFscan Monochrome CCD camera (Jenoptik). Both phase-contrast and fluorescence images were analyzed by using Image-Pro PLUS analysis software (Media Cybernetics). All settings for image processing were kept constant, and the exposure time for image capture was adjusted, if necessary, to maintain output levels similar to those observed under the fluorescence microscope. The intracellular distribution of the QD- based probes were analyzed by merging the bright field images with the fluorescence images. Composite merged images were produced by superimposing the fluorescence images from the QD filter and from the FRET filter**.**

Quantification of Fluorescent Signals

The QD fluorescence intensity and Alexa fluorescence intensity for each well was quantified by randomly choosing four to five fields within each well of untreated or treated samples using Image-Pro PLUS analysis software.

Results

Protein module design and peptide synthesis

For the production of peptides containing either the MA/CA or the p6/PR cleavage sites, a genetically programmable protein module was rationally designed to have several functional domains in a linear N to C terminal configuration (scheme 4.1) including: (i) an N terminal hexahistidine (His_6) for QD attachment, (ii) an exposed protease recognition/cleavage sequence, (iii) a unique cysteine residue for site-specific conjugation with a fluorescent dye, (iv) an ELP domain for thermal purification and (v) a flanking TAT peptide sequence for cell penetration. By taking advantage of the genetically programmable protein module the two different peptides were produced by altering the cleavage site sequence, while keeping rest of the domains same. This led to a significant reduction on the cost of protein synthesis. In addition, the multifunctional modular peptide provided rapid production and purification of the protein. The proteins were produced uniformly in E. coli BL-21 Gold (DE3) and purified by taking advantage of the temperature-responsive properties of ELP. SDS-PAGE analysis indicated the expected molecular weight of 48 kDa (Figure 4.1 A), corresponding to the composition of the proteins (scheme 4.1).

Assembly and characterization of the QD-peptide-dye conjugates

The peptides were labeled with a thiol-reactive fluorescent dye - Alexa 568 maleimide through the formation of a thioether bond with a unique cysteine residue after the protease cleavage sequence. The conjugation of the dye to the protein module was evaluated using SDS-PAGE (Figure 4.1 A). A strong fluorescent band corresponding to the protein module was detected under UV light, indicating the successful conjugation to Alexa 568 maleimide. The fluorescently labeled peptides were then self assembled on the DHLA capped QDs 545 through the metal affinity of His to the ZnS shell of the QDs. Figure 4.1 B shows the spectra for QDs 545 self-assembled with either MA/CA Alexa 568 or p6/PR-Alexa 568. Binding of protein-Alexa to QDs showed a loss in QD photoluminescence (PL) along with a concomitant increase in acceptor PL. Monitoring the relative QD donor and fluorescent protein acceptor emissions at different acceptor ratios (data not shown) allowed us to choose an optimal conjugation ratio of 10 protein-Alexa dyes per QD. Moreover, our previous results have shown that with 1:10 conjugation ratio (Figure 3.5. Chapter 3), HIV-1PR could effectively cleave the probe and resulted in a large, detectable change in the FRET/QD signal.

Cellular uptake of QD-MA/CA-alexa and QD-p6/PR alexa probes

To determine that QD-MA/CA-alexa and QD-p6/PR alexa probes could be translocated across the plasma membrane with the help of the TAT peptide, the HeLa cells were incubated with the probes for 2 hrs and then washed with PBS and subsequently imaged using a fluorescent microscope. Figure 4.2 shows images collected

for HeLa cells incubated with the indicated QD bioconjugates. First row of panel shows 510 nm emitting QDs (green), Alexa 568 (red), merged fluorescent images and second row of panel shows representative DIC and merged fluorescent composite images. The composite image clearly shows the localization of the probes inside the cells in a homogenous manner, indicating the successful translocation of the probes by TAT peptide mediated delivery. In contrast, incubation of QDs without any conjugation resulted in no substantial uptake within the same duration, confirming that the TAT sequence presented on the protein module is fully functional and is solely responsible for the intracellular uptake (data not shown). Interestingly it was found that red fluorescent signal from Alexa 568 was brighter in nearly 100% of cells, while only a weak green fluorescent signal was detected for the QD. Moreover, in the merged image the fluorescent signal from Alexa 568 was prominent over the QD signal, indicating that the energy was transferred from the QD to Alexa 568. Thus, FRET between QD and Alexa 568 could be monitored not only in solution but also inside the HeLa cells. The fluorescent intensity was constant for up to 48 hr, indicating that the probes were retained inside the cells after delivery and were resistant to intracellular degradation.

Proteolytic cleavage of the different probes by HIV-1 PR

Cleavage of Gag occurs in a temporally regulated manner; however individual cleavage sites on the HIV Gag and Gag-Pol polyproteins are processed at different rates which can be reproduced in in vitro reactions (Erickson et al., 1989). Thus, we examined the proteolytic activity of HIV-1PR towards its two different cleavage sites. HeLa cells

carrying either the QD-MA/CA-Alexa or QD-p6/PR-Alexa were transfected with the plasmid pNL4.3 R^-E^- expressing the HIV-1 genome. One of the major advantages of using this plasmid is that due to a deletion in the envelope gene, the viruses produced are non-infectious. In addition, they undergo only one round of replication. 18 hr post transfection, the transfected cells were analysed by using fluorescence microscope. In the transfected cells, a significant increase in QD signal with a reduction in the FRET signal was observed, thus causing a shift in the merged fluorescent image from red to green. It was evident in both QD-MA/CA-Alexa and QD-p6/PR-Alexa probes containing cells (Figure 4.3 A & B). In contrast no appreciable FRET abrogation was seen in non-transfected cells, clearly indicating that the increase in QD signal with a concomitant decrease in FRET signal was due to the proteolytic cleavage of MA/CA and p6/PR by HIV-1 PR. In addition, the transfected cells also showed characteristic CPE as compared to non-transfected cells, which further supports that HIV-1 PR was expressed in these cells and abrogation in FRET was protease dependent.

We next did a quantitative analysis of the QD and FRET signals by randomly choosing four to five fields within each well of non-transfected and transfected cells using Image-Pro PLUS analysis software. As shown in Figure 4.3 C, when we plotted Fa/Fd ratio, in the untransfected cells containing the MA/CA probes the ratio was 4.8due to the energy transfer from QD to Alexa 568 dye, while in the transfected cells this ratio came down to 1.76 due to the disruption in FRET by the HIV-1 PR mediated proteolytic cleavage of the MA/CA sequences. Similarly, Fa/Fd ratio in the untransfected cells containing the p6/PR probes, was 6.8, while in the transfected cells this ratio came down

to 2.7 which reflects the proteolytic cleavage of the p6/PR site by HIV-1 PR. Thus, by using the QD-based FRET assay system we can quantitatively measure the proteolytic activity of the specific proteases in-vivo. Although the cleavage efficiency of the p6/PR site by HIV-1 PR is 9 fold lower than the MA/CA site, the fact that similar cleavage efficiency was observed in both cases in-vivo was because, we provided sufficient time after transfecting the cells with the plasmid for complete cleavage of the substrates by HIV-1 PR.

Screening cleavage site specific inhibitors

We next determined the efficacy of our assay system in screening HIV-1 PR cleavage site specific inhibitors. Indinavir sulfate (IDV) is a selective, competitive inhibitor of HIV-1 protease. Moreover, it is a structural analogue of the HIV *Phe-Pro* protease cleavage site. Since the p6/PR cleavage site is the *Phe-Pro* protease cleavage site, we hypothesized that presence of IDV would inhibit the HIV-1 PR mediated cleavage of p6/PR, while it would have little or no effect towards the cleavage of MA/CA by HIV-1 PR. For screening the cleavage site inhibitor, the HeLa cells containing the QD-p6/PR-Alexa probes were pretreated with increasing concentration (10 nM- 10 µM) of IDV and then transfected with the plasmid pNL4.3 R^-E^-. It was found that with the increase in concentration of IDV, there was a progressive decline in the number of cells showing an increase in the QD signal (Figure 4.4 A). Furthermore there was a concomitant increase in the FRET signal in the transfected cells, indicating that IDV inhibited the activity of HIV-1 PR by acting as a competitive inhibitor and thus FRET

was retained in these cells. We next quantified the effects of IDV by measuring the total QD fluorescence (Fd) intensity and Alexa fluorescence (Fa) intensity within each well of control (untransfected), transfected and with the different dosages of Indinavir using Image-Pro PLUS analysis software. The Fa/Fd for each set of images were then normalized to $(Fa/Fd)_0$, which is the value of Fa/Fd in the control cells. As shown in Figure 4.4 B, when the Fa/Fd ratio was plotted, in the untransfected cells the ratio was 1 due to the energy transfer from QD to Alexa 568 dye, while in the transfected cells this ratio came down to 0.39. However, in case of the inhibitor treated cells a dose dependent increase in Fa/Fd ratio was found. This increase in Fa/Fd ratio evidently reflects the inhibitory action of IDV. On the other hand, when the HeLa cells containing the QD-MA/CA-Alexa probes were pretreated with increasing concentration (10 nM- 10 µM) of IDV and then transfected with the plasmid pNL4.3 R^-E^-, very little inhibition was monitored at lower dosages of IDV (Figure 4.5 A). The effects of IDV were further quantified. As shown in Figure 4.5 B at the lower dosages of IDV, the Fa/Fd ratio increased marginally. This clearly signified that IDV acts as a cleavage site specific inhibitor. However, at a concentration of 10 µM of IDV, the HIV-1PR mediated cleavage of MA/CA was completely abolished, which is in agreement with the drug's structure which binds to the active site of HIV-1 PR and prevents HIV-1 PR mediated proteolytic cleavage.

The Fa/Fd ratio of each sample was further used to calculate the percent inhibition in protease activity by using the equation; (Inhibitor treated- Untreated)/ (Untransfected-Untreated)*100. A dramatic difference was found in the inhibition efficacy of IDV for

the p6/PR and MA/CA site. As shown in Figure 4.6, the IC_{50} of IDV for the p6/PR site was 10 nM while it was 0.1- 1 µM for the MA/CA site. IDV completely inhibited the HIV-1 PR mediated cleavage of p6/PR at a concentration of 1 µM, while for MA/CA the complete inhibition was achieved at a 10 fold higher concentration. These results taken together further signified that the QD-FRET based bioassay could be used for screening HIV-1 PR cleavage site specific inhibitors and would prove useful in high throughput screening assays.

Discussion

Here we present a novel method to probe the different native cleavage sites of HIV-1 PR under physiologic condition. The system is easy to design as it is based on a genetically engineered protein module. By the engineered protein module the cleavage sites can be easily changed without redesigning the entire module. The protein module containing the cleavage site can be easily labeled with a fluorescent dye and finally conjugated to QDs. The cleavage site acts as a linker between the QD and fluorescent dye and enables the transfer of energy from QD to fluorescent dye. The presence of protease causes proteolytic cleavage of its substrate thereby disrupting FRET. However, the presence of a cleavage site specific inhibitor acts as a competitive inhibitor for the active site of the protease and prevents proteolytic cleavage of the substrate. By using Indinavir sulfate which is a structural analogue of the p6/PR cleavage site of HIV-1 PR we demonstrated that our assay system can be used to screen inhibitors specific to the cleavage sites. Several studies have demonstrated that even subtle alterations in Gag precursor processing can lead to severe defects in the assembly of infectious virus particles. Furthermore, mutations in the HIV-1 p2 spacer peptide, which alters ordered Gag precursor cleavage, results in defective virus particle production (Krausslich et al., 1995). Thus, it appears that by blocking the access of PR towards its cleavage sites, the assembly and release of infectious virions can be blocked. Moreover, results indicate that p6 is not required for efficient particle production from constructs expressing only the Gag precursor protein but rather is required in the context of the complete viral genome when PR is present. This observation reconciles the finding that p6 deletion does not

affect the production of HIV-1 and HIV-2 Gag-only particles (Luo et al., 1995; Hoshikawa et al., 1991) with results demonstrating that p6 is critical for virion production from full-length HIV-1 molecular clones (Go¨ttlinger et al., 1989; Huang et al., 1995). Results also indicate that data obtained with subgenomic Gag expression systems may not apply to systems using full-length, infectious molecular clones. Hence, our assay system can be used to not only screen for new blockers but at the same time can be used to check the effect of the blocker on the virion assembly and release. Moreover, this assay system can be used to screen inhibitors specific to cleavage sites in a high-throughput way. Thus, this assay system holds potential for finding inhibitors for patients infected with a HIV strain with particular mutations in the cleavage sites. The sites observed to mutate most frequently flank the nucleocapsid protein (NC) (Cote et al., 2001). The NC/p1 and NC/TFP are cleaved most slowly within the Gag and Gag-Pol precursors (Pettit et al., 1993; Wondrak et al., 1993). These sites may therefore evolve relatively quickly under small selective pressures.

It seems reasonable to assume that the strategy of putting a protease cleavage sequence between a QD and Alexa dye could be applied to other viral proteases that work on different cleavage sites as the protease cleavage sequences can be easily changed according to the specific target protease under study. Thus, the QD based FRET assay system can be easily adapted to screen inhibitors for other viral proteases specific cleavage sites. Further, this new approach can be extended to screen inhibitors for proteases which get overexpressed in certain disease conditions like cancers and require monitoring the inhibitory effects of drugs in human cells.

Acknowledgement

The following reagent was obtained through the NIH AIDS Research and Reference Reagent Program, Division of AIDS, NIAID, NIH: pNL4-3.HSA.R-E- from Dr. Nathaniel Landau.

References

Baum, E. Z., G. A. Bebernitz, and Y. Gluzman. 1990. β-Galactosidase containing a human immunodeficiency virus protease cleavage site is cleaved and inactivated by human immunodeficiency virus protease. Proc. Natl. Acad. Sci. USA **87:**10023–10027.

Billich, A., and G. Winkler. 1990. Colorimetric assay of HIV-1 proteinase suitable for high-capacity screening. Pept. Res. **3:**274–276.

Boden, D. and M. Markowitz. 1998. Resistance to human immunodeficiency virus type 1 protease inhibitors. Antimicrob. Agents Chemother. **42:**2775–2783.

Carrillo, A., K. D. Stewart, H. L. Sham, D. W. Norbeck, W. E. Kohlbrenner, J. M. Leonard, D. J. Kempf, and A. Molla. 1998. In vitro selection and characterization of human immunodeficiency virus type 1 variants with increased resistance to ABT-378, a novel protease inhibitor. J. Virol. **72:**7532–7541.

Clapp, A.R., Goldman, E.R., Mattoussi, H. 2006. Capping of CdSe-ZnS quantum dots with DHLA and subsequent conjugation with proteins. Nature Protocols **1**: 1258-1266.

Condra, J. H., W. A. Schleif, O. M. Blahy, L. J. Gabryelski, D. J. Graham, J. C. Quintero, A. Rhodes, H. L. Robbins, A. Rothy, M. Shivaprakash, D. Titus, T. Yang, H. Teppler, K. E. Squires, P. J. Deutsch, and E. A. Emini. 1995. In vivo emergence of HIV-1 variants resistant to multiple protease inhibitors. Nature **374:**569–571.

Connor RI, Chen BK, Choe S, Landau NR. 1995. Vpr is required for efficient replication of human immunodeficiency virus type-1 in mononuclear phagocytes. Virology **206**:935-944.

Côté, H. C., Z. L. Brumme, and P. R. Harrigan. 2001. Human immunodeficiency virus type 1 protease cleavage site mutations associated with protease inhibitor cross-resistance selected by indinavir, ritonavir, and/or saquinavir. J. Virol. **75:**589-594.

Debouck, C., J. G. Gorniak, J. E. Strickler, T. D. Meek, B. W. Metcalf, and M. Rosenberg. 1987. Human immunodeficiency virus protease expressed in *Escherichia coli* exhibits autoprocessing and specific maturation of the gag precursor. Proc. Natl. Acad. Sci. USA **84:**8903–8906

Deeks SG, Smith M, Holodniy M, Kahn JO. 1997. HIV-1 protease inhibitors **:**A review for clinicians. JAMA**. 277:** 145 -153**.**

Deo, S. K., J. C. Lewis, and S. Daunert. 2000. Bioluminescence detection of proteolytic bond cleavage by using recombinant aequorin. Anal. Biochem. **281:**87–94.

Doyon, L., G. Croteau, D. Thibeault, F. Poulin, L. Pilote, and D. Lamarre. 1996. Second locus involved in human immunodeficiency virus type 1 resistance to protease inhibitors. J. Virol. **70:**3763–3769.

Erickson-Viitanen, S., J. Manfredi, P. Viitanen, D. E. Tribe, R. Tritch, C. A. Hutchison III, D. D. Loeb, and R. Swanstrom. 1989. Cleavage of HIV-1 *gag*

polyprotein synthesized in vitro: sequential cleavage by the viral protease. AIDS Res. Hum. Retroviruses **5:**577-591

Fuse T., K. Watanabe, K. Kitazato and N. Kobayashi. 2006. Establishment of a new cell line inducibly expressing HIV-1 protease for performing safe and highly sensitive screening of HIV protease inhibitors, Microbes Infect. **8**: 1783–1789

Go¨ttlinger, H. G., J. G. Sodroski, and W. A. Haseltine. 1989. Role of capsid precursor processing and myristoylation in morphogenesis and infectivity of human immunodeficiency virus type 1. Proc. Natl. Acad. Sci. USA **86:**5781–5785.

Gupta, B., Levchenko, T.S., Torchilin, V.P. 2005. Intracellular delivery of large molecules and small particles by cell-penetrating proteins and peptides. Advanced Drug Delivery Reviews **57**: 637– 651.

He J, Choe S, Walker R, Di Marzio P, Morgan DO, Landau NR. 1995. Human immunodeficiency virus type 1 viral protein R (Vpr) arrests cells in the G2 phase of the cell cycle by inhibiting p34cdc2 activity. J Virol **69**:6705-6711.

Hoshikawa, N., A. Kojima, A. Yasuda, E. Takayashiki, S. Masuko, J. Chiba,T. Sata, and T. Kurayta. 1991. Role of the *gag* and *pol* genes of human immunodeficiency virus in morphogenesis and maturation of retrovirus-like particles expressed by recombinant vaccinia virus: an ultrastructural study. J.Gen. Virol. **72**:2509–2517.

Hu, K., J. Clément, L. Abrahamyan, K. Strebel, M. Bouvier, L. Kleiman, and A. Mouland. 2005. A human immunodeficiency virus type 1 protease biosensor assay using bioluminescence resonance energy transfer. J. Virol. Methods. **128**:93-103

Huang, M., J. M. Orenstein, M. A. Martin, and E. O. Freed. 1995. p6 Gag is required for particle production from full-length human immunodeficiency virus type 1 molecular clones expressing protease. J. Virol. **69:**6810-6818

Kim J.-Y., S. O'Malley, A. Mulchandani and W. Chen. 2005**.** Genetically engineered elastin-protein A fusion as a universal platform for homogeneous, phase-separation immunoassay**.** Analytical Chemistry**.77**:2318-2322

Kohl, N. E., E. A. Emini, W. A. Schleif, L. J. Davis, J. C. Heimbach, R. A. F. Dixon, E. M. Scolnick, and I. S. Sigal. 1988. Active human immunodeficiency virus type 1 protease is required for viral infectivity. Proc. Natl. Acad. Sci.USA **85:**4686–4690.

Krausslich, H.-G., M. Facke, A.-M. Heuser, J. Konvalinka, and H. Zentgraf. 1995. The spacer peptide between human immunodeficiency virus capsid and nucleocapsid proteins is essential for ordered assembly and viral infectivity. J. Virol. **69:**3407–3419

Lao, U.L., Chen, A., Matsumoto, M.R., Mulchandani, A., Chen, W. 2007. Cadmium removal from contaminant soil by thermally responsive elastin (ELPEC20) Biopolymers. Biotechnol. Bioeng. **98**: 349-355

Leis, J., D. Baltimore, J. M. Bishop, J. Coffin, E. Fleissner, S. P. Goff, S. Oroszlan, H. Robinson, A. M. Skalka, H. M. Temin, and V. Vogt. 1988. Standardized and simplified nomenclature for proteins common to all retroviruses. J. Virol. **62:**1808–1809

Lewin, M., Carlesso, N., Tung, C., Tang, X., Cory, D., Scadden, D.T., Weissleder, R. 2000**.** Tat peptide-derivatized magnetic nanoparticles allow in vivo tracking and recovery of progenitor cells. Nature Biotechnology **18:** 410-414.

Lindsten, K., T. Uhlikov, J. Konvalinka, M. Masucci, and N. Dantuma. 2001. Cell-based fluorescence assay for human immunodeficiency virus type 1 protease activity. Antimicrob. Agents Chemother. **45**:2616-2622.

Luo, L., Y. Li, S. Dales, and C. Y. Kang. 1994. Mapping of functional domains for HIV-1 *gag* assembly into virus-like particles. Virology **205**:496–502.

Mammano, F., C. Petit, and F. Clavel. 1998. Resistance-associated loss of viral fitness in human immunodeficiency virus type 1: phenotypic analysis of protease and *gag* coevolution in protease inhibitor-treated patients. J. Virol. **72:**7632–7637.

Massodi, I., Bidwell, G.L. III, Raucher, D. 2005. Evaluation of cell penetrating peptides fused to elastin-like polypeptide for drug delivery. J. Control. Release **108**: 396-408.

Matayoshi, E. D., G. T. Wang, G. A. Krafft, and J. Erickson. 1990. Novel fluorogenic substrates for assaying retroviral proteases by resonance energy transfer. Science **247:**954–958

Murray, M. G., W. Hung, I. Sadowski, and B. Das Mahapatra. 1993. Inactivation of a yeast transactivator by the fused HIV-1 proteinase: a simple assay for inhibitors of the viral enzyme activity. Gene **134:**123–128.

Patick, A and K. Potts. 1998. Protease inhibitor as antiviral agents. Clinical Microbiol. Rev.**11**:614-627.

Pearl, L. H. and W. R. Taylor. 1987. A structural model for the retroviral proteases. Nature (London) **329:**351–354

Peng, C., B. K. Ho, T. W. Chang, and N. T. Chang. 1989. Role of human immunodeficiency virus type 1-specific protease in core protein maturation and viral infectivity. J. Virol. **63:**2550–2556

Pettit, S. C., S. F. Michael, and R. Swanstrom. 1993. The specificity of the HIV-1 protease. Perspect. Drug Discov. Des. **1:**69–83.

Stebbins, J., and C. Debouck. 1997. A microtiter colorimetric assay for the HIV-1 protease. Anal. Biochem. **248:**246–250

Stebbins, J., I. C. Deckman, S. B. Richardson, and C. Debouck. 1996. A heterologous substrate assay for the HIV-1 protease engineered in *Escherichia coli*. Anal. Biochem. **242:**90–94.

Urry, D.W. 1997. Physical Chemistry of biological free energy transduction as demonstrated by elastic protein-based polymers. Journal of Physical Chemistry B**.** **101:**11007-11028

Wiegers, K., G. Rutter, H. Kottler, U. Tessmer, H. Hohenberg, and H. G. Krausslich. 1998. Sequential steps in human immunodeficiency virus particle maturation revealed by alterations of individual Gag polyprotein cleavage sites. J. Virol. **72:**2846-2854

Wills, J. W. and R. C. Craven. 1991. Form, function, and use of retroviral gag proteins. AIDS **5:**639–654.

Wondrak, E. M., J. M. Louis, H. de Rocquigny, J. C. Chermann, and B. P.Roques. 1993. The Gag precursor contains a specific HIV-1 protease cleavage site between the NC (p7) and p1 proteins. FEBS Lett. **333:**21–24.

Zennou, V., F. Mammano, S. Paulous, D. Mathez, and F. Clavel. 1998. Loss of viral fitness associated with multiple Gag and Gag-Pol processing defects in human immunodeficiency virus type 1 variants selected for resistance to protease inhibitors in vivo. J. Virol. **72:**3300–3306.

Zhang, Y. M., H. Imamichi, T. Imamichi, H. C. Lane, J. Falloon, M. B. Vasudevachari, and N. P. Salzman. 1997. Drug resistance during indinavir therapy is caused by mutations in the protease gene and in its Gag substrate cleavage sites. J. Virol. **71:**6662–6670.

Zhou J., X. Yuan, D. Dismuke, B. M. Forshey, C. Lundquist, K. H. Lee, C. Aiken, and C. H. Chen. 2004**.** Small-molecule inhibition of human immunodeficiency virus type 1 replication by specific targeting of the final step of virion maturation. J. Virol**.** **78**:922-929

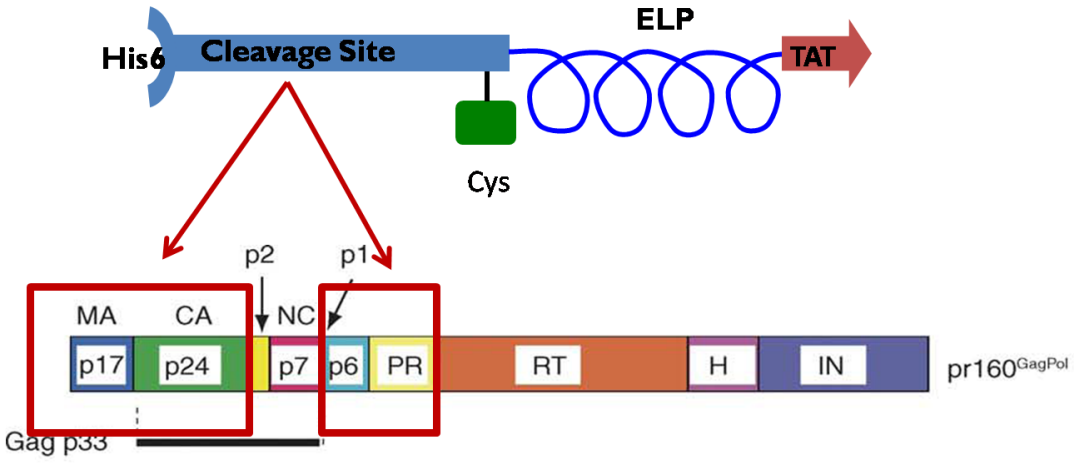

Scheme 4.1: Schematic representation of the self assembled QD-peptide nanoprobes harboring engineered protein modules H-MA/CA-ET or H- p6/PR-ET. H-MA/CA-ET contains hexahistidine, HIV-1 PR cleavage sequence (MA/CA), cysteine residue for dye incorporation, ELP for thermal purification and TAT peptide for cellular delivery. In H-p6/PR-ET only the cleavage sequence is changed to another HIV-1 PR cleavage sequence (p6/PR), keeping the other modules same. Dye labelled modular peptides containing appropriate cleavage sequences are self-assembled onto the QDs. In this design, the QD photoluminescence (PL) is quenched by the fluorescent dye due to fluorescence resonance energy transfer (FRET). Presence of active proteases disrupts FRET resulting in an increased QD PL thus enabling a simple activity assay.

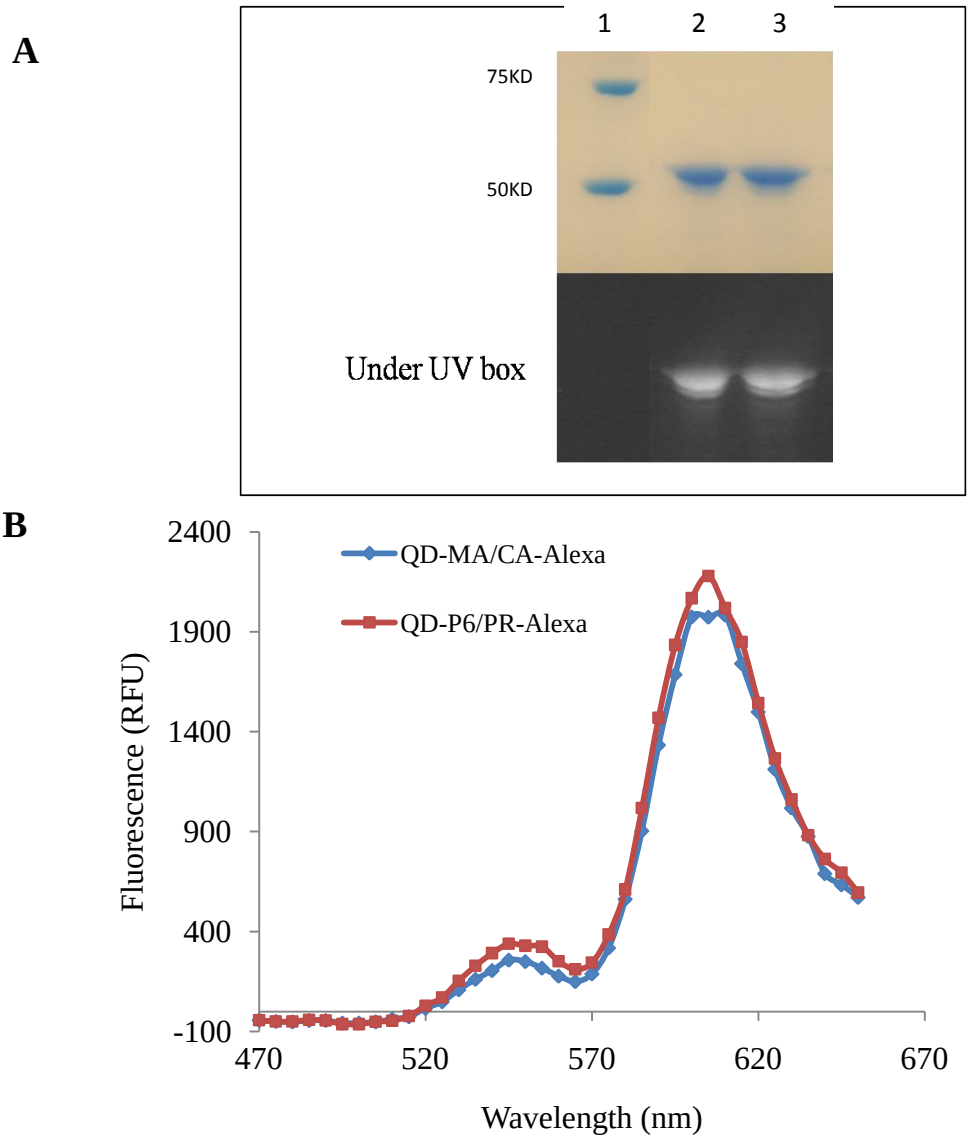

Figure 4.1: (**A**) SDS-PAGE analysis of H-MA/CA-ET and H-p6/PR-ET. Upper Panel; Lane 1: protein size marker, Lane 2: purified protein module H-MA/CA-ET, Lane 3: purified protein module H-p6/PR-ET. Lower Panel; H-MA/CA-ET and H-p6/PR-ET conjugated with Alexa 568 maleimide, observed under UV lamp. (**B**) Fluorescence emission spectra of QD-MA/CA-Alexa and QD-p6/PR-Alexa assembly at QD: Alexa ratio of 1:10. Excitation is 435 nm

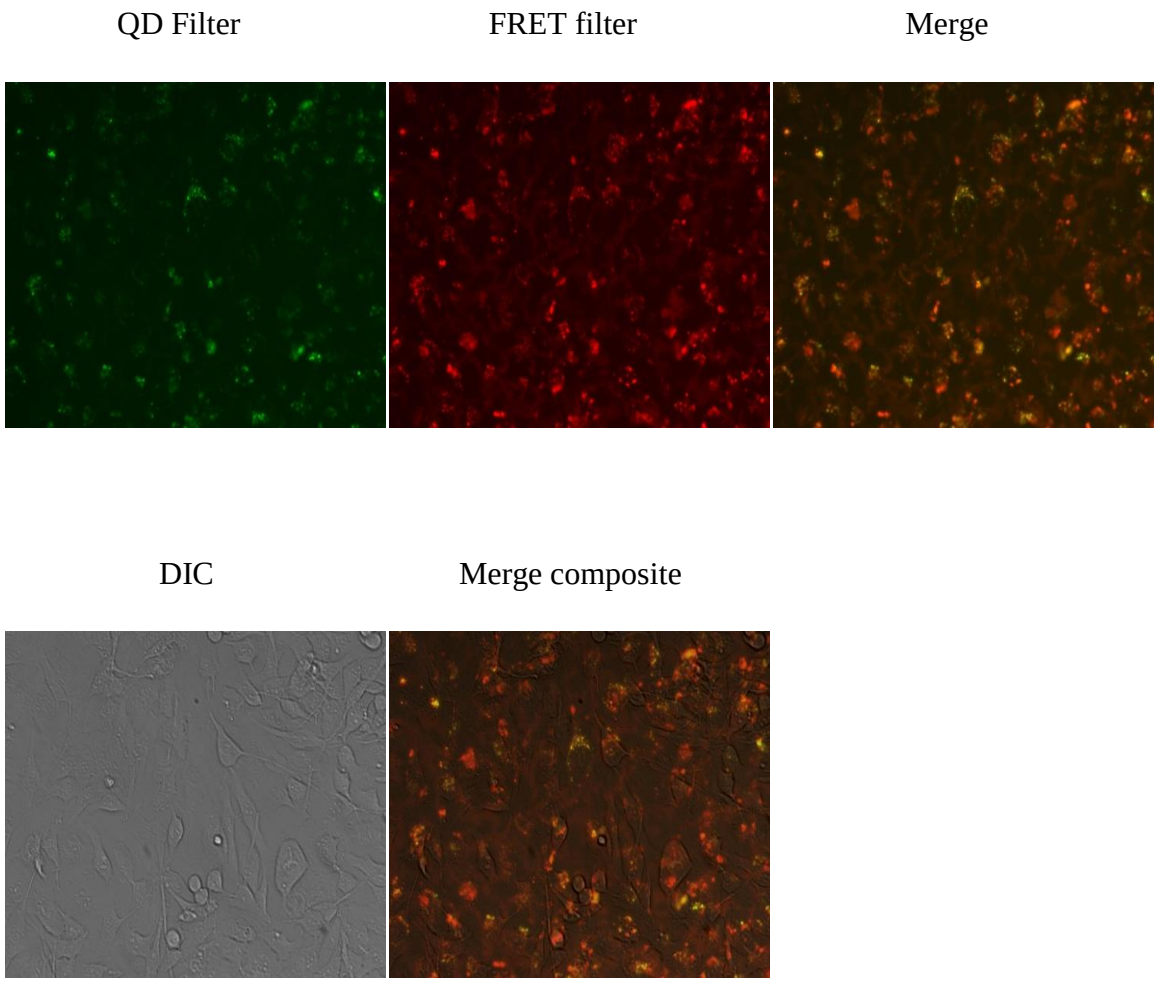

Figure 4.2: Cellular uptake of QD-p6/PR-Alexa probes. Representative images of HeLa cells incubated for 2 hour with 150 nM of self assembled QD-p6/PR-Alexa probes. The cells were visualized with a fluorescence microscope at 435 ex/ 535 em for QD and 435 ex/ 610 em for FRET. The images obtained using QD filter and FRET filter sets were merged. The cells were also observed with DIC filter. The DIC images were merged with merged fluorescent image to obtain corresponding merged composite fluorescent images.

Control Transfected

A

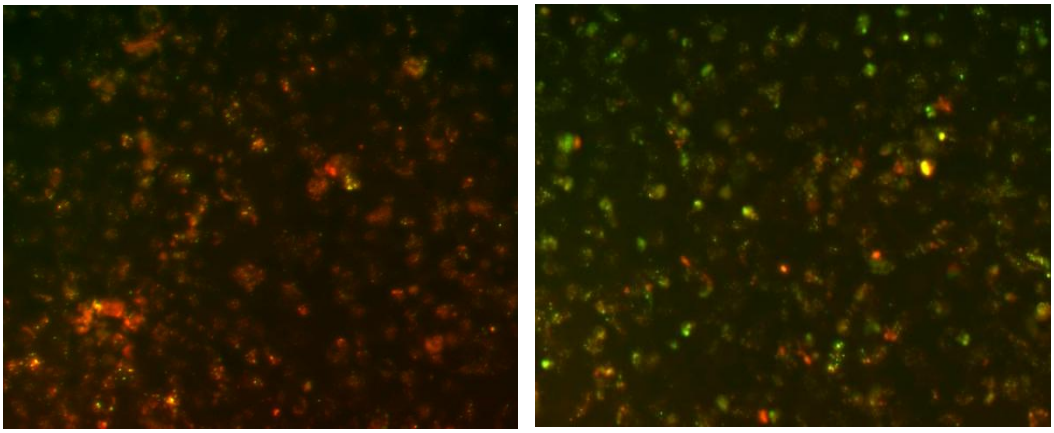

Control Transfected

B

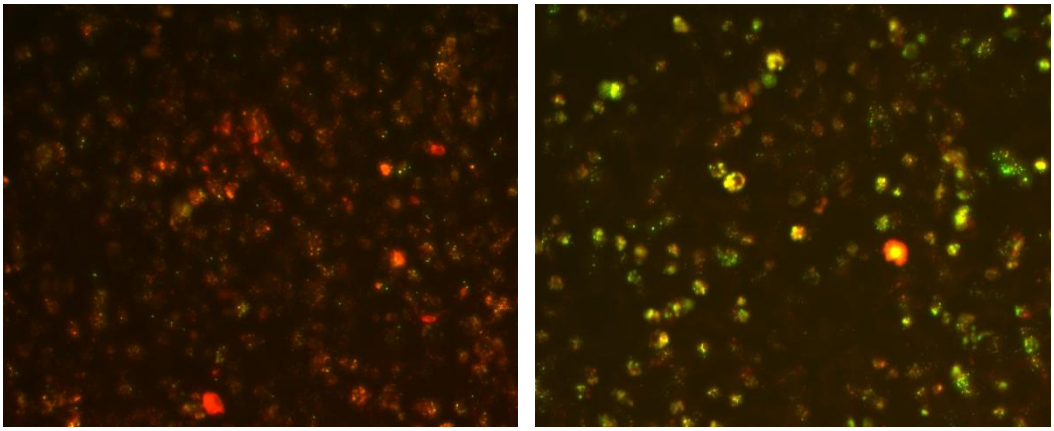

Continued

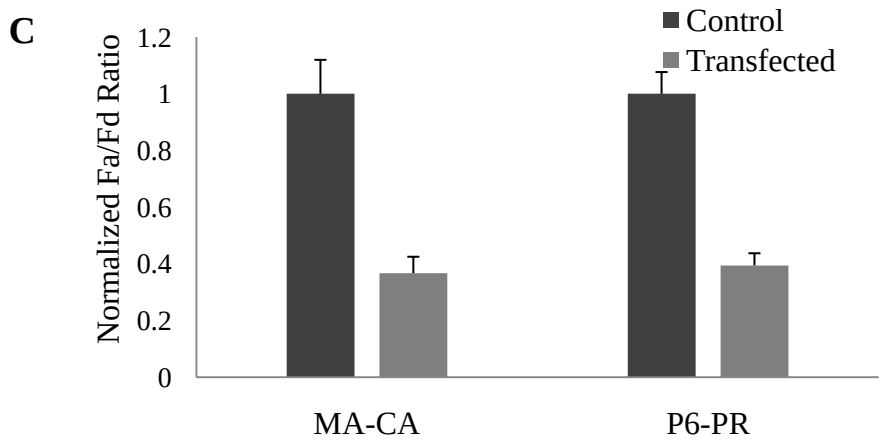

Figure 4.3: **A & B** Proteolytic activity of HIV-1 PR on its two different cleavage sites. QD-MA/CA-Alexa and QD-p6/PR-Alexa probes were delivered in HeLa cells. HeLa cells containing the probes were transfected with plasmid pNL4.3 HSA R^-E^- expressing the HIV-Provirus. 18 hours post-transfection cells were observed under fluorescence microscope at 435 ex/ 535 em for QD and 435 ex/ 610 em for FRET. The images obtained using QD filter and FRET filter sets were merged. Only merged representative fluorescent images are shown for control (untransfected) and transfected cells. The increased QD fluorescence in the transfected cells was attributed to proteolytic cleavage of the MA/CA peptides and p6/PR by HIV-1 PR, which resulted in marked reduction in FRET efficiency between QD and Alexa dye. (**C**) Quantitative Analysis of the images. The total fluorescence intensity of images obtained using QD filter (Fd) and FRET filter (Fa) for control (untransfected) and transfected were quantified using Image-Pro PLUS software. The Fa/Fd of transfected cells were then normalized to $(Fa/Fd)_0$, which is the value of Fa/Fd in the control cells. Data are means ± standard deviation from three experiments.

A

Control | Transfected | +10 nM IDV

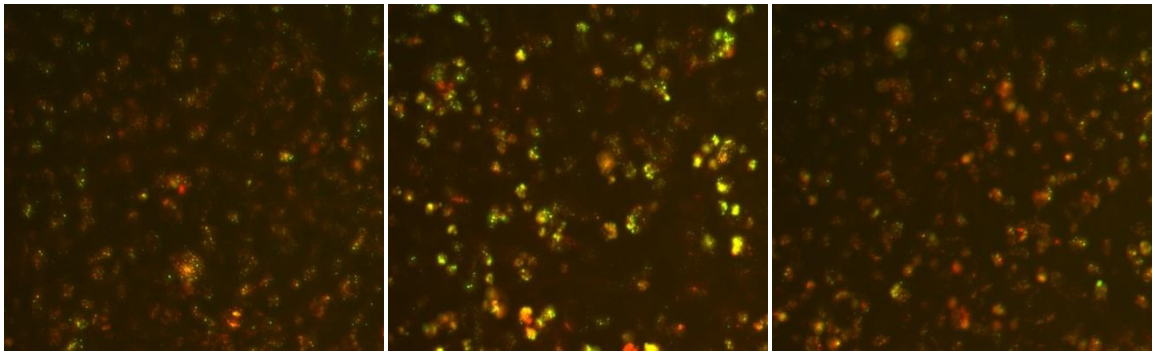

+100 nM IDV | +1 µM IDV | +10 µM IDV

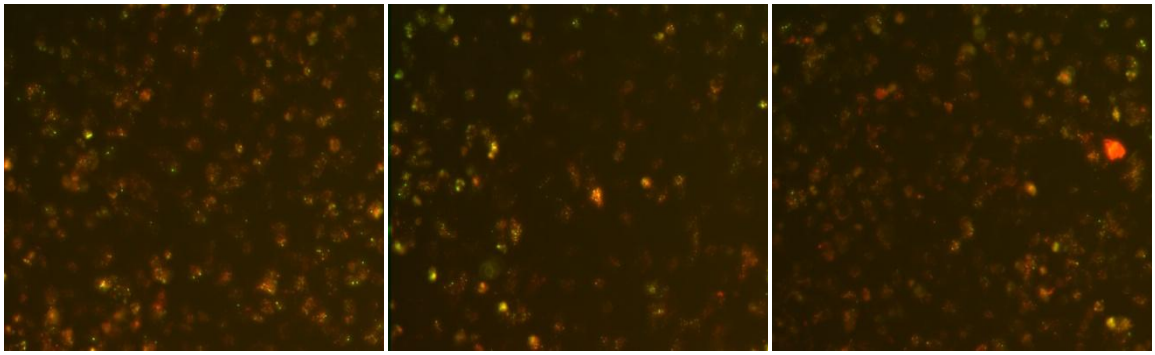

Continued

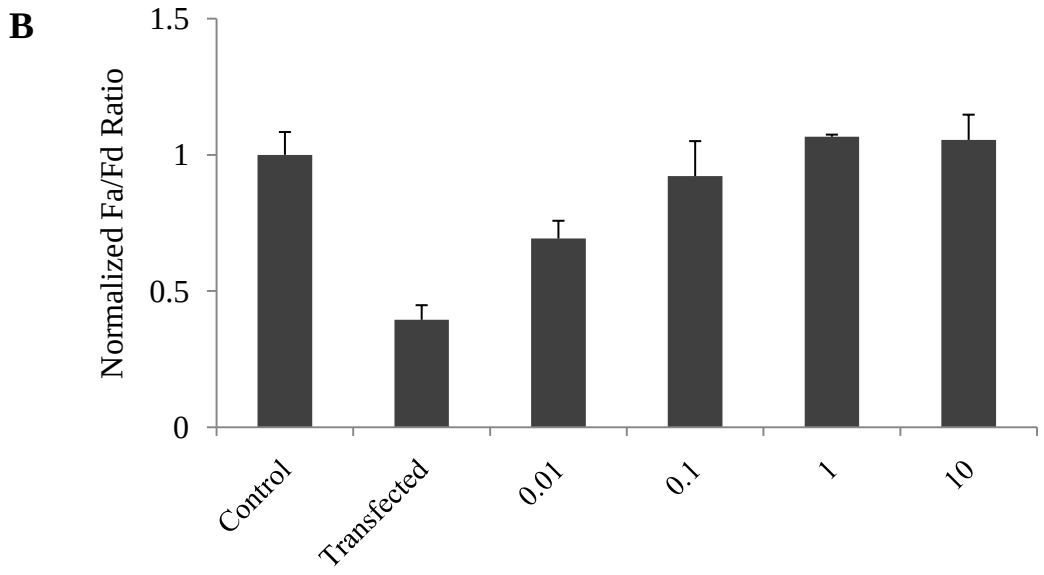

Figure 4.4: (**A**) Monitoring the inhibition efficiency of Indinavir for p6/PR cleavage site. QD-p6/PR-Alexa probes were delivered in HeLa cells. HeLa cells containing the probes were transfected with plasmid pNL4.3-HSA-R$^-$E$^-$ expressing the HIV-Provirus and were treated with increasing concentration (0.01-10 µM) of Indinavir. 18 hours post-transfection cells were observed under fluorescence microscope at 435 ex/ 535 em for QD and 435 ex/ 610 em for FRET. The images obtained using QD filter and FRET filter sets were merged. Only merged representative fluorescent images are shown for each dosage of Indinavir. (**B**) Quantitative Analysis of the images. The total fluorescence intensity of images obtained using QD filter (Fd) and FRET filter (Fa) for control (untransfected), transfected and with the different dosages of Indinavir were quantified using Image-Pro PLUS software. The Fa/Fd for each set of images were then normalized to $(Fa/Fd)_0$, which is the value of Fa/Fd in the control cells. Data are means ± standard deviation from three experiments.

A

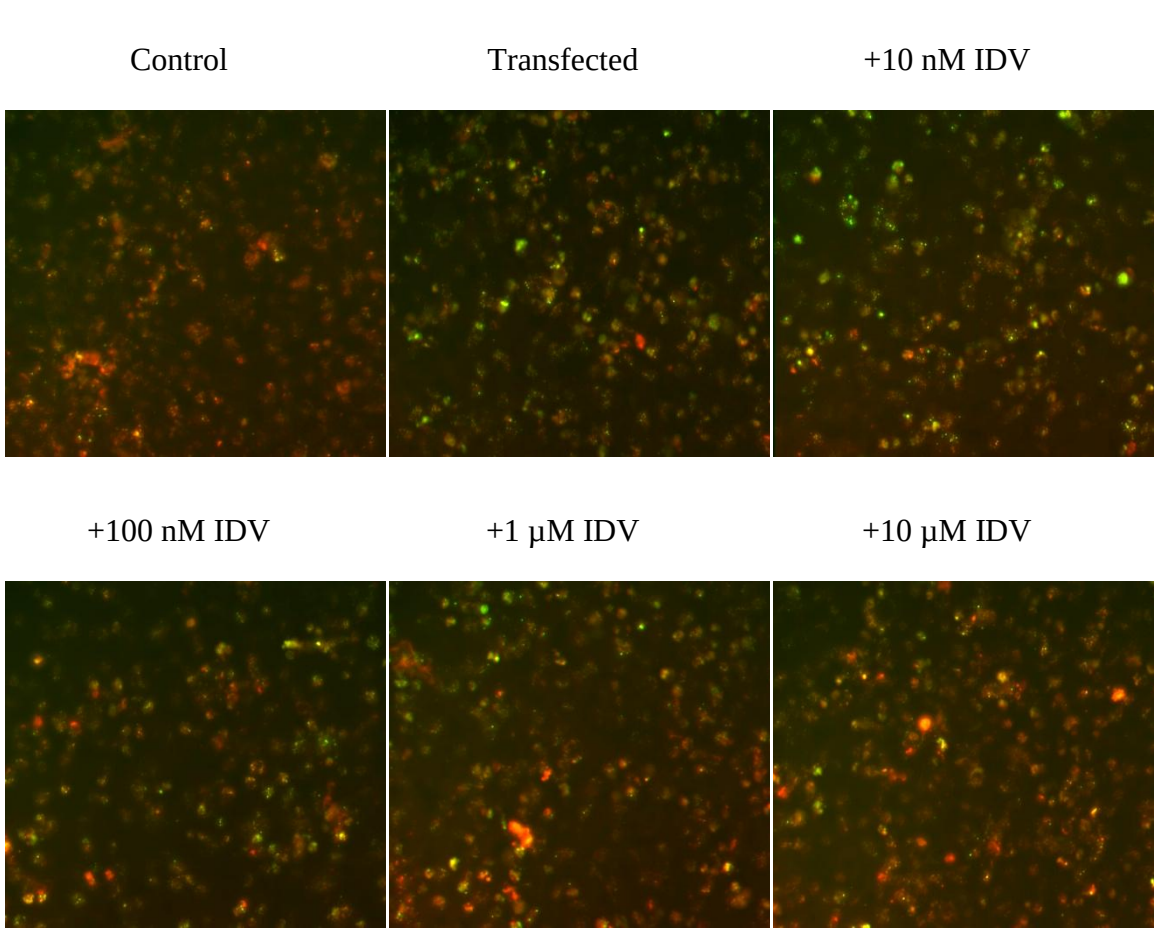

Continued

B

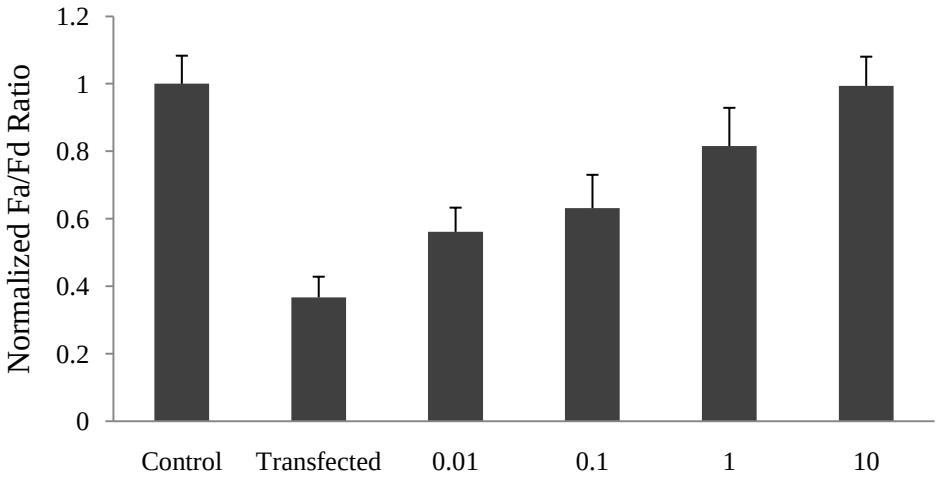

Figure 4.5: (**A**) Monitoring the inhibition efficiency of Indinavir for MA/CA cleavage site. QD-MA/CA-Alexa probes were delivered in HeLa cells. HeLa cells containing the probes were transfected with plasmid pNL4.3-HSA-R^-E^- expressing the HIV-Provirus and were treated with increasing concentration (0.01-10 μM) of Indinavir. 18 hours post-transfection cells were observed under fluorescence microscope at 435 ex/ 535 em for QD and 435 ex/ 610 em for FRET. The images obtained using QD filter and FRET filter sets were merged. Only merged representative fluorescent images are shown for each dosage of Indinavir. (**B**) Quantitative Analysis of the images. The total fluorescence intensity of images obtained using QD filter (Fd) and FRET filter (Fa) for control (untransfected), transfected and with the different dosages of Indinavir were quantified using Image-Pro PLUS software. The Fa/Fd for each set of images were then normalized to $(Fa/Fd)_0$, which is the value of Fa/Fd in the control cells. Data are means ± standard deviation from three experiments.

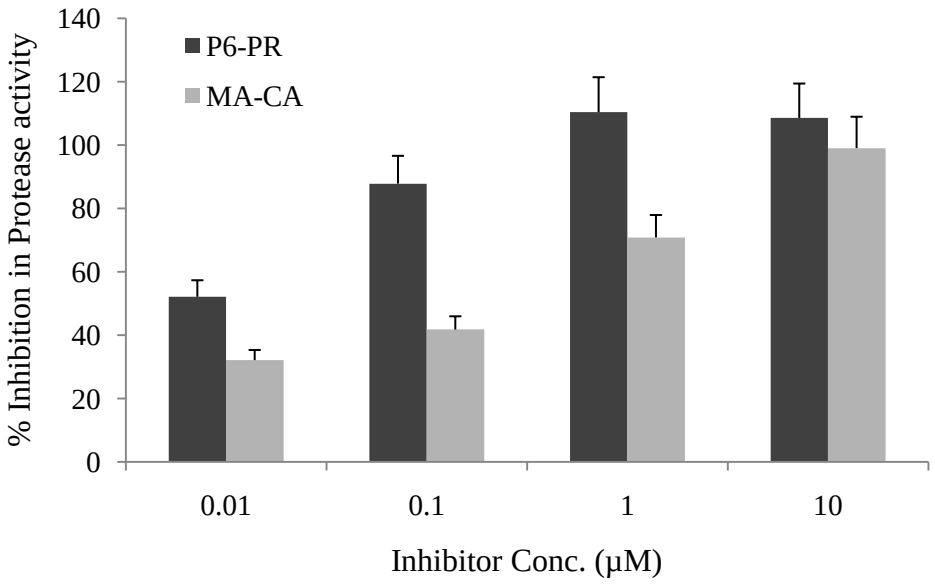

Figure 4.6: Inhibition efficiency of Indinavir for p6/PR and MA/CA cleavage sites using the QD based FRET assay system. The Fa/Fd ratio of each sample was used to calculate the percent inhibition in protease activity by using the equation; (Inhibitor treated- Untreated)/ (Untransfected- Untreated)*100. Data are means ± standard deviations from three experiments.

Chapter 5

Conclusion

Conclusions and Future Directions

In this thesis protein modules were engineered and applied for conducting different bioassays like detecting viral protease activity in-vitro and in-vivo, detecting cancer markers and for screening protease inhibitors. A series of genetically engineered protein modules as QD based FRET -substrates were designed to work as nanoprobes for sensing protease activity. The use of programmable protein module for developing nanoprobes is a novel approach and offers several distinct advantages as compared to synthetic peptides for the purpose. The in-house production of peptides caused a significant reduction on the cost of peptide synthesis. This method enabled rapid production and easy purification of peptides and thus helped to escape the tedious and time consuming protein purification procedures. Furthermore, by using this method, the peptides could be easily labeled with fluorescent dyes and finally conjugated to QDs to form functional nanoprobes. As the labeling of fluorescent dyes uses the thiol-maleimide chemistry, several different dyes can be used for labeling and thus QDs of different emission can be used for conjugation. Hence, this method has the potential to generate several different FRET pairs which can be used for multiplex assays.

Most importantly, with the modular design of the protein module there was no need for major redesign when targeting a new protease. Peptide specificity could be varied by altering only the recognition sequence without significantly modifying other modules**.** The flexibility of the approach was demonstrated by generating nanoprobes for rapid and sensitive detection of the cancer-specific matrix metalloprotease (MMP-7) and the West Nile virus protease (NS3). The developed nanoprobes were able to detect

protease activity with the sensitivity to a few nanograms per milliliter. Besides, the limit of detection of West Nile Virus protease is the lowest reported in literature. These nanoprobes were also able to measure the activity of protease inhibitors and thus can be used for high-throughput anti-protease drug screening.

The most important feature of these nanoprobes is the TAT peptide sequence by which the nanoprobes were efficiently delivered inside mammalian cells in a non-invasive way. The delivery of sensors took as low as 2 hrs and the probes were homogenously distributed inside the cells. Moreover, the fluorescent signal from the QD and fluorescent dye was intact for atleast 48 hrs. Through this research, we successfully generated QD-based biosensors capable of detecting protease activity inside living cells. By far, this is the first report of a sensor that can be used to detect protease activity in-vivo in a rapid, sensitive and facile way. Moreover, the protease activity could be monitored in response to different inhibitors making it a low-cost and tunable approach for protease inhibitor discovery. In addition, cell based assay aids in monitoring the cytotoxicity and transport efficiency of potential drugs. With the development of high-throughput fluorescence microscopy and its associated image analysis system, it is reasonable to assume that this QD based FRET assay system can be an ideal platform adaptable for high-throughput screening of inhibitors for proteases which require monitoring the inhibitory effects of drugs in human cells. Also in the context of rapidly mutating viruses like HIV-1, a rapid, sensitive and convenient assay system to screen protease inhibitors is an invaluable tool. Thus, we anticipate that our QD based FRET assay system will find applications in the diagnostic and pharmaceutical fields for the

diagnosis of protease related diseases and screening of potential drugs with high sensitivity in a high throughput manner.